



Nanoparticules pour l'administration orale de l'amphotéricine B pour le traitement de la leishmaniose

Antonio Lipa Castro

► To cite this version:

Antonio Lipa Castro. Nanoparticules pour l'administration orale de l'amphotéricine B pour le traitement de la leishmaniose. Sciences pharmaceutiques. Université Paris-Saclay, 2021. Français. NNT : 2021UPASQ019 . tel-03373170

HAL Id: tel-03373170

<https://theses.hal.science/tel-03373170>

Submitted on 11 Oct 2021

HAL is a multi-disciplinary open access archive for the deposit and dissemination of scientific research documents, whether they are published or not. The documents may come from teaching and research institutions in France or abroad, or from public or private research centers.

L'archive ouverte pluridisciplinaire **HAL**, est destinée au dépôt et à la diffusion de documents scientifiques de niveau recherche, publiés ou non, émanant des établissements d'enseignement et de recherche français ou étrangers, des laboratoires publics ou privés.

**Nanoparticules pour l'administration orale
de l'amphotéricine B pour le traitement
de la Leishmaniose**

*Nanoparticles for the oral administration of
amphotericin B for leishmaniasis treatment*

Thèse de doctorat de l'université Paris-Saclay

École doctorale n°569

Innovation thérapeutique : du fondamental à l'appliqué (ITFA)

Spécialité de doctorat : Pharmacotechnie et Biopharmacie

Unité de recherche : Université Paris-Saclay, CNRS, Institut Galien Paris-Saclay, 92296,

Châtenay-Malabry, France

Référent : Faculté de pharmacie

**Thèse présentée et soutenue à Paris-Saclay
le 25 mai 2021, par**

Antonio LIPA CASTRO

Composition du Jury

Philippe LOISEAU

Professeur, Chimiothérapie antiparasitaire
UMR 8076 CNRS BioCIS

Président

Karine ANDRIEUX

Professeure, Equipe VICT, UTCBS, UMR CNRS 8258,
Inserm U1267, Université de Paris Descartes
Faculté de Pharmacie de Paris Descartes

Rapporteure & Examinatrice

Frédéric LAGARCE

Professeur – Praticien Hospitalier, Université d'Angers
CHU Angers, INSERM MINT 1066

Rapporteur & Examinateur

Maud CANSELL

Professeure, Université de Bordeaux

Examinatrice

Direction de la thèse

Gillian BARRATT

Directrice de Recherche CNRS, Université Paris-Saclay
Institut Galien Paris-Sud, UMR CNRS 8612

Directrice de thèse

REMERCIEMENTS

Je tiens à remercier toutes les personnes qui ont contribué au succès de mon doctorat et qui m'ont aidé lors de la rédaction de ce rapport.

Tout d'abord, j'adresse mes remerciements à ma directrice de thèse Gillian BARRATT pour son accueil, le temps passé ensemble et le partage de son expertise au quotidien. Grâce aussi à sa confiance j'ai pu accomplir mes missions.

Je remercie aussi Frédéric LAGARCE, professeur à l'Université d'Angers, pour la gentillesse d'avoir accepté d'être dans mon jury comme rapporteur.

J'adresse aussi mes remerciements à Karine ANDRIEUX, professeure à l'université de Paris Descartes, pour la gentillesse d'avoir accepté d'être dans mon jury comme rapporteure.

Tous mes remerciements à Maud CANSELL, consultante indépendante à Bordeaux, qui a accepté d'être dans mon jury de thèse en qualité d'examinatrice.

J'adresse mes remerciements à Philippe LOISEAU, professeur à Paris Saclay, qui m'a honoré en acceptant d'être le président du jury.

Je voudrais aussi remercier Valérie NICOLAS pour l'encadrement et les heures passées en microscopie confocale.

Je remercie très spécialement Vincent FAIVRE pour son aide constante dans la partie extrêmement galénique et aussi pour la bonne humeur.

Je tiens à remercier à Angelina ANGELOVA pour l'aide, le conseil et le support lors de l'analyse de mes formulations.

Je remercie énormément Ghislène MEKHOUI pour son accueil et le temps investi sur mon projet.

Je tiens à remercier vivement Claudie BOURGAUX pour l'aide toujours très chaleureuse.

J'adresse mes remerciements à Francois-Xavier LEGRAND pour le support constant dans la rédaction, l'expérimentation et la présentation de mon projet.

Je voudrais remercier David CHAPRON et Jean-Jacques VACHON avec qui grâce à leur support technique, j'ai pu plusieurs fois me débrouiller au laboratoire.

J'adresse ici tous mes remerciements à Sébastien POMEL pour son aide constante lors de l'évaluation *in vivo* des formulations.

Je voudrais remercier Indira DENNEMONT pour son aide spéciale lors du traitement des échantillons, merci énormément.

Je voudrais remercier Audrey SOLGADI et Bastien PROST pour leur support chaleureux lors de l'analyse de mes échantillons.

Je remercie infiniment mes camarades et amis de travail Louis BRONSTEIN, Islam ZMERLI, Eloísa BERBEL MANAIA, Baptiste ROBIN et Hichème HADJI pour leur esprit d'équipe et leur accompagnement constant et également de m'avoir beaucoup supporté au cours de ces trois ans. Je vais me souvenir de vous tout le temps.

Enfin, mes remerciements vont aussi vers tout le personnel du service de mise au point galénique et les différentes doctorants et stagiaires qui ont contribué à mon projet, Maryème BARENDJI, Zhiqiangw WANG (Matis), Laura MONTAGNAC, Wafa NASRAOUI, Omar MERTINS.

Je voudrais enfin remercier et dédié mon travail à tout ma famille pour m'avoir soutenu de manière constante aux cours de ces années: mes parents Eulogia et Benito, mes frères Carlos, Gonzalo et Linda et mes neveux Lia, Bianca et Franchesco.

SOMMAIRE

1. INTRODUCTION GENERALE.....	10
1.1 La Leishmaniose.....	10
1.2 Types de Leishmanioses	11
1.2.1 Leishmaniose cutanée (LC).....	11
1.2.2 Leishmaniose cutanéo-muqueuse (LCM)	12
1.2.3 Leishmaniose viscérale (LV).....	12
1.3 Aspects épidémiologiques.....	13
1.4 Prophylaxie	15
1.5 Traitement	15
1.5.1 Dérivés pentavalents de l'antimoine.....	17
1.5.2 Amphotéricine B (AmB).....	17
1.5.3 Pentamidine	18
1.5.4 Miltéfosine.....	18
1.5.5 Paromomycine.....	18
1.6 Systèmes d'administration de l'AmB.....	19
1.6.1 Formulations lipidiques d'AmB	22
1.6.2 Nouveaux systèmes d'administration par voie orale.....	23
1.7 Perspectives actuelles des systèmes d'administration de l'AmB.....	27
1.8 Caractérisation des cochléates (revue)	28
1.8.1 Introduction.....	30
1.8.2 Cochleates: physicochemical description.....	31
1.8.3 Raw materials	34
1.8.4 Advantages of cochleates as a drug delivery system	39
1.8.5 Methods for cochlate preparation	41
1.8.6 Characterization techniques for cochleates.....	43
1.8.7 Interaction with biological systems.....	58
1.8.8 Other studies related to cochleates	58
1.8.9 Conclusion	59

2. TRAVAUX EXPERIMENTAUX.....	66
Objectif du travail.....	66
2.1 Chapitre 1 : AmB-cochléates à base de lipides d'origine synthétique	67
2.1.1 Matériels.....	68
2.1.2 Méthodologie	68
2.1.3 Résultat et discussion	75
2.1.4 Conclusion	79
2.2 Chapitre 2 : AmB-Cochléates d'origine naturelle (article).....	80
2.2.1 Introduction.....	83
2.2.2 Material	84
2.2.3 Method	85
2.2.4 Result and Discussion	95
2.2.5 Conclusion	112
2.3 Chapitre 3 : Etudes <i>in vivo</i> des cochléates à base de phospholipides naturels chargés en AmB (article).....	119
2.3.1 Introduction.....	122
2.3.2 Material	123
2.3.3 Method	123
2.3.4 Result and discussion	129
2.3.5 Conclusion and perspectives	136
3. DISCUSION	139
4. CONCLUSION ET PERSPECTIVE	145
5. REFERENCES.....	146
6. ANNEXES	152

ABREVIATIONS

AmB: amphotericin B

CD: circular dichroism

Cho: cholesterol

DLS: dynamic light scattering

DOPS: dioleoyl phosphatidylserine

DSC: differential scanning calorimetry

EDTA: ethylenediaminetetraacetic

FASSIF: fasted-state simulated intestinal

FESSIF: fed-state simulated intestinal

FT-IR: Fourier transform infrared spectroscopy

HBSS: Hanks' Balanced Salt Solution

LC: leismaniose cutanée

LCM: leishmaniose cutanéo-muqueuse

LV: leishmaniose viscérale

MLV: multilamellar vesicles

NMR: nuclear magnetic resonance

OA: oral administration

PA: phosphatidic acid

PC: phosphatidylcholine

PdI: Polydispersity index

PE: phosphatidylethanolamine

PG: phosphatidylglycerol

PI: phosphatidylinositol

POPS: palmitoyl-oleoyl phosphatidylserine

PS: phosphatidylserine

SAXS: small angle X-ray scattering

Sb^v: dérivés pentavalents de l'antimoine

SFG: simulated gastric fluid

TEER: transepithelial electrical resistance

WAXS: wide-angle X-ray scattering

LISTE DE FIGURES

Introduction

Figure 1. Cycle de développement de <i>Leishmania spp.</i>	10
Figure 2. Leishmaniose cutanée: A gauche LCL et à droit LCD (Mischler, 2017).....	11
Figure 3. Leishmaniose cutanéo-muqueuse (Torres-Guerrero et al., 2017)	12
Figure 4. Leishmaniose viscérale (splénomégalie)	12
Figure 5. Distribution géographique de la leishmaniose viscérale.....	14
Figure 6. Distribution géographique de la leishmaniose cutanée.....	14
Figure 7. Principales molécules actuellement utilisées dans le traitement de la leishmaniose	16
Figure 8. Interaction de l'AmB avec la membrane cellulaire fongique (formation de pores hydrophiles). L'interaction électrostatique entre la mycosamine et les hydroxyles de l'ergostérol est mis en évidence et ainsi que les groupes pharmacophores impliqués des phospholipides (A), de l'ergostérol (B), de la mycosamine (C) et de l'hydroxyle (D) (Ketllyn et al., 2016).	20
Figure 9. Effets de l'interaction AmB-membrane cellulaire (A): l'AmB (B) dans une cellule fongique et (C) dans une cellule de mammifère (Cavassin et al., 2021)	20
Figure 10. Structures monomère et dimère d'AmB par liaison aminoalkyle (Hirano et al., 2011)	21
Figure 11. Structure des cochléates	26
Figure 12. Internal structure of cochleates.....	31
Figure 13. Intermediate structures after the addition of calcium ions that give the cochleates as a final product (adapted from Nagarsekar et al., 2016).	32
Figure 14. Arrangements of the drugs loaded as cochleates (adapted from Zarif, 2005).	33
Figure 15. Structure of phospholipids used in obtaining cochleates (adapted from Li et al., 2015).	35
Figure 16. Schematic of the interaction of cochlate particles when the dehydrated bilayers approach a membrane cell resulting cochlate fusion with cell membrane (reproduced with permission from Lipa-Castro et al. 2021)..	40
Figure 17. SEM image of optimized DOPS cochlate composites obtained from the NanoAssemblerTM microfluidic device (reproduced from Nagarsekar et al., 2017, with permission).....	43
Figure 18. Images of cochleates by optical microscopy (A) and transmission electron microscopy (B). Black arrows indicate larger cochleates not detected by transmission electron microscopy (reproduced with permission from Lipa-Castro et al. 2021).	47
Figure 19. Structural formula of laurdan.....	49
Figure 20. Normalized excitation and emission spectra of laurdan in SUV corresponding to liquid-crystalline phase (green line), cochlate phase (blue line) and gel phase (red line) (adapted with permission from Ramani & Balasubramanian, 2003).	50
Figure 21. Small-angle X-ray scattering (SAXS) patterns of MLV (A) and cochlates (B) formed from soy phosphatidylserine. (Reproduced with permission from Lipa-Castro et al. 2021).	53
Figure 22. Electron density patterns from cochleates formed from dioleoylphosphatidylserine with and without incorporated amphotericin B. (Lipa, Bourgaux, Legrand, Barratt, unpublished results).	54
Figure 23. FT-IR attenuated total reflectance spectrum of hydrated film of DMPS (addapted from Manrique-Moreno et al., 2016).	55

Chapitre I

Figure 24. Technique de film lipidique	69
Figure 25. Schéma de la méthode hydrogel.....	70
Figure 26. Images de microscopie électronique (A) et optique (B) des AmB-cochléates obtenus à partir du phospholipide synthétique DOPS.....	75
Figure 27. Résultats de viabilité des formulations d'AmB-cochléates à base de DOPS	76

Figure 28. Activité antileishmanienne <i>in vivo</i> d'AmB-cochléates. Test non paramétrique de Kruskal Wallis suivi d'un Dunn's test non corrigé. La significativité a été établie pour une valeur * $p < 0.05$ et *** $p < 0.0001$ par rapport au contrôle.....	78
Figure 29. AmB-Lipoid PSP70 cochléates observed by transmission electron (1) and optical microscopy (2). Formulation compositions are given in Materials and Methods. A: F0.5; B: F1; C: F2; D: F3.	98

Chapitre II

Figure 30. SAXS spectra of Lipoid PSP70 in various formulations (molar proportions).	100
Figure 31. UV spectra ($\epsilon \text{ M}^{-1} \text{ cm}^{-1}$) (A) and CD spectra ($\Delta\epsilon \text{ M}^{-1} \text{ cm}^{-1}$) (B) of AmB-loaded cochléate formulations treated with 0.05M EDTA.....	103
Figure 32. Release profiles of AmB from different formulations in FASSIF and FeSSIF media. The initial AmB concentration was 10 $\mu\text{g}/\text{mL}$. Values are expressed as mean \pm SD (n=3).....	106
Figure 33. Cytotoxic effects of AmB-loaded cochléates on Caco-2 cell monolayers after 24h as a function of concentration, determined by MTT reduction. Values are expressed as percentages of untreated controls, mean \pm SD of three experiments. * $P < 0.05$ for comparison with untreated control, # $P < 0.05$ for comparison with Fungizone at the same concentration, Student's unpaired two-tailed t test.	107
Figure 34. Confocal microscopy images of Caco2 cells taken at the cell surface (A and B) and in the cell interior (C and D). Fluorescein emission (1) and Rhodamine emission (2) after exposure for 2h to Rhodamine-PE micelles (A and C) and Rhodamine-PE cocheates (B and D). On the left, 3D images showing the possible absorption and fusion of the cochléates on the cell membrane: Fluorescein emission (A3), Rhodamine emission (B3) and overlay (C3).	109
Figure 35. Schematic representation of the interaction of cochléate particles with the cell membrane.	112

Chapitre III

Figure 36. Pharmacokinetic profiles after oral administration of AmB-cochléate formulations and AmBisome® at a dose of 7.5mg/kg (mean \pm S.D. , n=6)	130
Figure 37. Pharmacokinetic profile of AmBisome® after intravenous administration at a dose of 1mg/kg (mean \pm S.D. , n=6).....	131
Figure 38. AmB biodistribution after intravenous administration AmBisome® at a dose of 1mg/kg (mean \pm S.D. , n=5)	132
Figure 39. AmB biodistribution after oral administration of AmB-Cochléate formulations and AmBisome® at a dose of 7.5mg/kg (mean \pm S.D. , n=5).	133
Figure 40. <i>In-vivo evaluation</i> of AmB formulations against visceral leishmaniasis. There was significant difference in comparison to control * $p < 0.05$, *** $p < 0.001$, **** $p < 0.0001$, n=7).	134
Figure 41. Schéma de mécanismes d'absorption proposés	144

LISTE DES TABLEAUX

Tableau 1. Les manifestations cliniques de la leishmaniose suivant l'espèce de <i>Leishmania</i>	13
Tableau 2. Examples of active molecules reported to have been incorporated into cochleates. NSAIDs: non-steroidal anti-inflammatory drugs, CVS: cardiovascular system, CNS: central nervous system, BCS: biopharmaceutical classification system.....	37
Tableau 3. Main experimental techniques used for cochlate characterization	44
Tableau 4. Composition de milieu intestinal FASSIF (Pham et al., 2014)	74
Tableau 5. Pourcentage de récupération d'AmB après 3H d'incubation sur Caco2	77
Tableau 6. Phosphatidylserine species composition of Lipoid PSP70 identified by MS ² mass spectrometry. Where PS (AC1 / AC2) denotes that AC1 is on one of the sn-1 carbon and AC2 is on the sn-2 carbon while PS (AC1-AC2) denotes that the position of the two acyl chains is unknown.....	95
Tableau 7. Physical and chemical characterization of AmB-loaded liposomes and cochleates.Values expressed as mean ± SD (n=3). Formulation compositions are defined in Material and Methods. D _h : Equivalent hydrodynamic diameter; Pdi: Polydispersity index.....	96
Tableau 8. AmB stability in SGF medium. Formulation compositions are defined in Material and Methods. Values are the percentage of intact AmB recovered, mean ± SD for 3 determinations.	105
Tableau 9. Transepithelial electrical resistance (TEER) of Caco2 monolayers cultivated on inserts for at least 21 days after 4h of incubation with 100 µg/mL Amphotericine B in different formulations. Values are expressed as mean ± SD of measurements from 3 inserts.	108
Tableau 10. Uptake of AmB into Caco-2 cell monolayers grown on inserts and passage to the lower compartment. Inserts were incubated for 6h with 100 µg/mL AmB in various cochlate formulations added to the upper compartment. Results are expressed as the percentage of added AmB found into cell monolayer and in the lower compartment as the mean ± SD of 3 inserts.	111
Tableau 11. Biochemical parameters in mice infected with <i>Leishmania</i> and treated with AmB formulations (n=4).	135

1. INTRODUCTION GENERALE

Le présent manuscrit sera divisé en deux parties. Dans la première partie, nous allons présenter les travaux antérieurs à notre projet notamment la description de la maladie, des traitements et des avancées obtenues à l'aide des nouvelles technologies. La deuxième partie concerne les résultats expérimentaux obtenus durant cette thèse et est divisée en 3 chapitres.

1.1 La Leishmaniose

La leishmaniose est une maladie tropicale et subtropicale provoquée par des parasites intracellulaires du genre *Leishmania* (Torres-Guerrero et al., 2017). Il existe plus de 20 espèces du parasite *Leishmania* responsable de la maladie (Georgiadou et al., 2015). La figure 1 présente le cycle du parasite, qui se développe à l'intérieur des cellules du système des phagocytes mononucléés des mammifères, et est transmis aux humains et aux animaux (rongeurs, canidés, édentés, marsupiaux, procyonidés, ongulés primitifs et primates) par la piqûre de l'insecte vecteur infecté : *Phlebotomus* (dans l'ancien monde) ou *Lutzomyia* dans le nouveau monde (Bañuls et al., 2007).

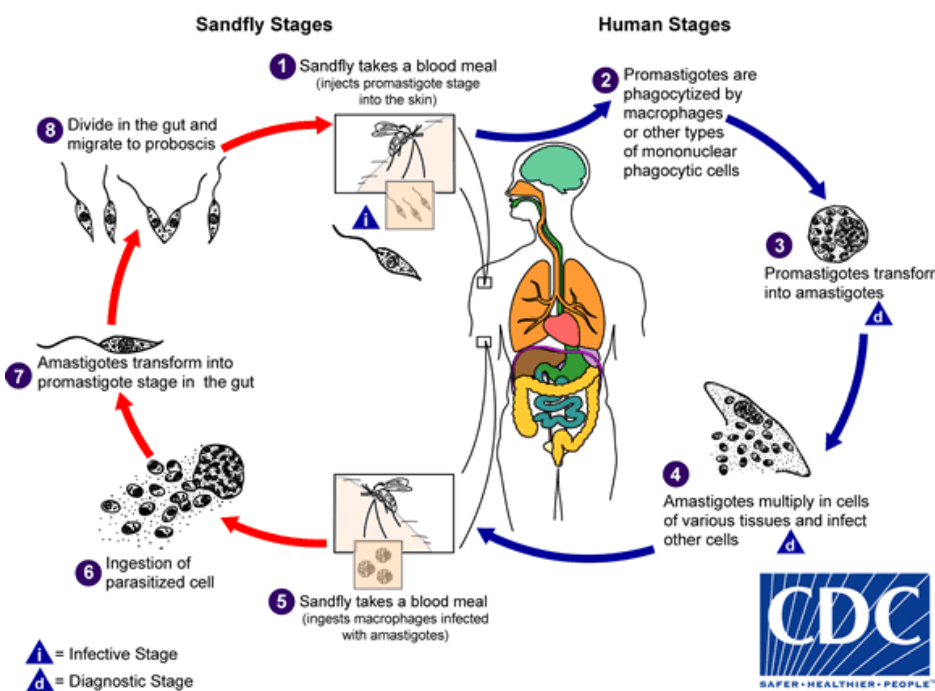


Figure 1. Cycle de développement de *Leishmania* spp.

(<http://www.cdc.gov/parasites/leishmaniasis/>)

1.2 Types de Leishmanioses

La leishmaniose regroupe un ensemble de maladies qui peuvent provoquer différentes manifestations cliniques. Sur la base de la symptomatologie clinique la leishmaniose peut être classifiée en trois formes principales (Georgiadou et al., 2015).

1.2.1 Leishmaniose cutanée (LC)

La leishmaniose cutanée affecte les téguments de la peau d'une façon localisée ou diffuse (Torres-Guerrero et al., 2017). La leishmaniose cutanée localisée est la forme la plus courante de la leishmaniose, les parasites restent localisés dans les tissus cutanés et conduisent à des ulcères cutanés chroniques de guérison lente. Ces lésions (figure 2) sont indolores et peuvent s'auto-guérir sans traitement. Cependant, la guérison de la maladie peut prendre plusieurs mois et laisser des cicatrices disgracieuses (Scorza et al., 2017). Par contre, la leishmaniose cutanée diffuse est caractérisée par une dissémination à travers les voies tissulaires, lymphatiques et sanguines qui résulte de l'absence de réponse immunitaire cellulaire aux antigènes parasitaires (Torres-Guerrero et al., 2017). En effet l'immunité cellulaire déficiente permet au parasite de se diffuser dans les tissus sous-cutanés donc ce tableau clinique a été rapporté chez des patients porteurs du SIDA (Mischler, 2017). Les lésions se développent dans la majeure partie de la peau, sauf dans le cuir chevelu, et parfois atteignent également les muqueuses. Lorsque les muqueuses telles que l'oropharynx et le nasopharynx sont impliquées, des nodules douloureux peuvent entraîner une obstruction des voies respiratoires. Cette forme clinique ne se guérit pas spontanément (Torres-Guerrero et al., 2017).



Figure 2. Leishmaniose cutanée: A gauche LCL et à droit LCD (Mischler, 2017).

1.2.2 Leishmaniose cutanéo-muqueuse (LCM)

Les patients souffrent d'ulcérations graduellement destructives non cicatrisantes de la muqueuse avec des extensions allant du nez et de la bouche jusqu'au pharynx et larynx (figure 3). Ces lésions peuvent se présenter des mois ou des années après un premier épisode de leishmaniose cutanée à cause de l'invasion des macrophages de la muqueuse naso-oropharyngée (Chappuis et al., 2007).



Figure 3. Leishmaniose cutanéo-muqueuse (Torres-Guerrero et al., 2017).

1.2.3 Leishmaniose viscérale (LV)

C'est la plus grave des différentes formes de leishmaniose, mortelle sans traitement. La leishmaniose viscérale est caractérisée par une fièvre prolongée, une splénomégalie (figure 4), une hépatomégalie, une perte de poids importante, une anémie progressive, une pancytopenie et une hyperglobulinémie. Dans cette manifestation clinique, le parasite envahit et se multiplie dans les macrophages, affectant la rate, le foie, la moelle osseuse et le tissu lymphoïde (Kumar, 2013).



Figure 4. Leishmaniose viscérale (splénomégalie).

<https://www.cdc.gov/parasites/leishmaniasis/disease.html>

Le tableau 1 résume les espèces responsables de différentes manifestations cliniques.

Tableau 1. Les manifestations cliniques de la leishmaniose suivant l'espèce de *Leishmania* (Mekarnia, 2020)

ESPECES	TABLEAU CLINIQUE	LOCALISATION GEOGRAPHIQUE
<i>Leishmania infantum</i>	LV, LCL	Ancien et nouveau monde
<i>L. donovani</i>	LV, LCL	Asie, Afrique, Europe
<i>L. major</i>	LCL	Ancien monde
<i>L. tropica</i>	LCL	Ancien monde
<i>L. mexicana</i>	LCL	Nouveau monde
<i>L. peruviana</i>	LCL	Nouveau monde
<i>L. guyanensis</i>	LCL	Nouveau monde
<i>L. amazonensis</i>	LCL, LCD	Nouveau monde
<i>L. aethiopica</i>	LCL, LCD	Ancien monde
<i>L. braziliensis</i>	LCL, LCD, LCM	Nouveau monde
<i>L. panamensis</i>	LCL, LCM	Nouveau monde

LV : leishmaniose viscérale ; LCL : leishmaniose cutanée localisée
LCD : leishmaniose cutanée diffuse ; LCM : leishmaniose cutanéo-muqueuse.

1.3 Aspects épidémiologiques

La leishmaniose est largement répandue dans 98 pays tropicaux, subtropicaux et tempérés, touchant surtout les pays en voie de développement en Afrique, Asie et Amérique latine à cause de la malnutrition, la migration, les mauvaises conditions d'habitation, la fragilité du système immunitaire et le manque de ressources (Georgiadou et al., 2015). La leishmaniose représente un problème majeur de santé publique mondiale avec un chiffre de contamination en augmentation (Bañuls et al., 2007). Pour la LC le nombre de cas se situe entre 700 000 à 1,2 millions (ou plus) par année. Pour la LV les estimations de cas ont diminué jusqu'à 100 000 mais les chiffres précédents se situaiennt autour de 400 000 ou plus (CDC, 2020). Il est à noter que le 90% des cas de LV dans le monde se présentent dans six pays : le Bangladesh, le Brésil, l'Éthiopie, l'Inde, le Soudan du Sud et le Soudan. (Georgiadou et al., 2015). La figure 5 montre la distribution géographique de la leishmaniose viscérale dans le monde.

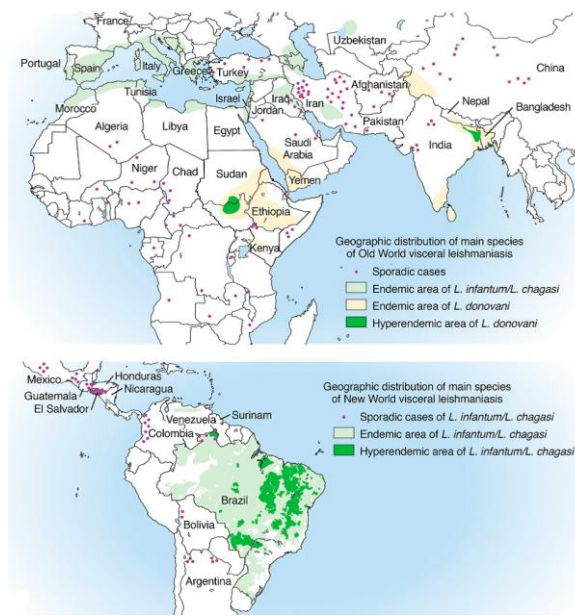


Figure 5. Distribution géographique de la leishmaniose viscérale
(Aronson et al., 2017).

En revanche, la figure 6 montre que la LC est plus largement distribuée en Amérique, dans le bassin méditerranéen et en Asie occidentale. Les 10 pays avec le plus grand nombre de cas de LC sont l'Afghanistan, l'Algérie, le Brésil, la Colombie, le Costa Rica, l'Éthiopie, l'Iran, le Pérou, le Nord-Soudan et la Syrie (Georgiadou et al., 2015).

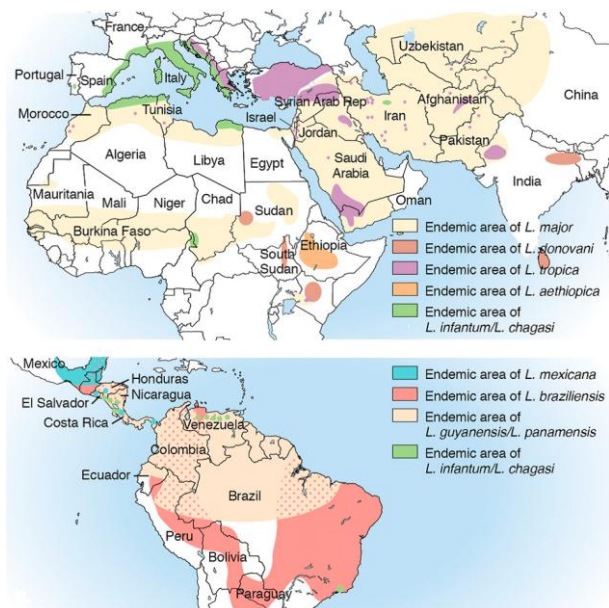


Figure 6. Distribution géographique de la leishmaniose cutanée
(Aronson et al., 2017).

1.4 Prophylaxie

L'utilisation du parasite atténué est une possibilité pour le développement d'un vaccin pour prévenir la maladie (Ismail et al., 2017) cependant le changement de la forme atténuee vers la forme virulente et la possibilité que la forme atténuee puisse causer la maladie chez un individu immunodéprimé présentent un risque (Palatnik-de-Sousa, 2008). Parmi d'autres candidats, comme le vaccin à base de protéine recombinante, le vaccin à base de sous-unités (fragments du parasite) et le vaccin à base d'ADN. Les vaccins obtenus à partir d'ADN représentent la meilleure approche à utiliser en thérapie et en prophylaxie contre la leishmaniose, car ils possèdent de nombreux avantages par rapport aux autres stratégies vaccinales comme un prix accessible, la facilité à les produire à grande échelle et surtout la protection à long terme vis-à-vis de plusieurs espèces de Leishmania mais ces vaccins sont encore en développement (Thakur et al., 2020). L'éradication des réservoirs, la lutte antivectorielle et le traitement de masse des individus ont montré du succès comme mesure de prévention cependant ils sont limités par la difficulté de coordination et des coûts importants (Mischler, 2017). En plus bien que l'efficacité de quelques agents biologiques et chimiques ait été démontrée au laboratoire, les sites de reproduction des phlébotomes sont généralement difficiles à identifier dans la nature. Ainsi les mesures de contrôle spécifique ne sont pas réalisables (Alexander & Maroli, 2003).

1.5 Traitement

Actuellement plusieurs principes actifs sont utilisés pour traiter les trois formes de leishmaniose (LV, LC et LCM) mais aucun d'entre eux n'est entièrement satisfaisant. Nous trouvons les dérivés pentavalents de l'antimoine (Sb^V), l'amphotéricine B, la pentamidine, la miltéfosine, la paromomycine (Padilla et al., 2019). Ils sont décrits dans les paragraphes suivants et leurs formules structurales sont présentées dans la figure 7.

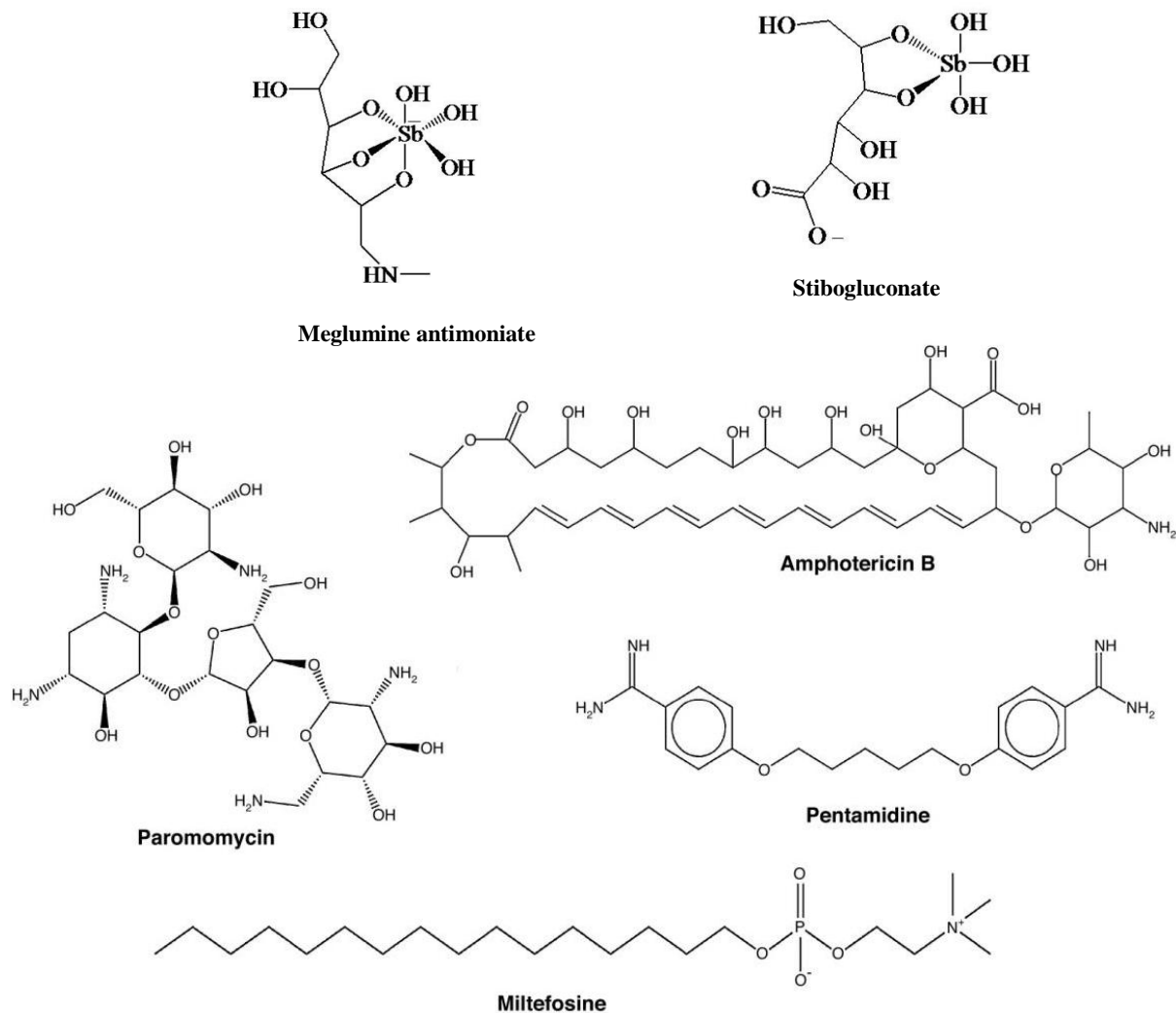


Figure 7. Principales molécules actuellement utilisées dans le traitement de la leishmaniose.

1.5.1 Dérivés pentavalents de l'antimoine

Ils sont considérés comme des pro-drogues, qui sont converties en dérivés trivalents de l'antimoine (Sb^{III}) dans les macrophages ou à l'intérieur du parasite (Singh et al., 2012). Ces médicaments inhibent l'activité des voies glycolytiques et oxydatives des acides gras chez les amastigotes du parasite (Goto, 2012) mais le mécanisme du passage de la molécule à l'intérieur du macrophage ou du parasite ainsi que leur mécanisme d'action exact reste encore peu documenté (Singh et al., 2012). Les effets secondaires les plus fréquents sont l'arthralgie, la myalgie, l'anorexie, les maux de tête, la fièvre, les vomissements et les étourdissements. De plus, à cause de leur toxicité au niveau du cœur, des reins, du foie et du pancréas, cette classe de médicament est déconseillée pour les femmes enceintes, les personnes âgées et les personnes souffrant de maladies cardiaque, rénale ou hépatique (Goto, 2012). Ils ont été utilisés dans le monde entier pour traiter les LV et LC pendant plus de six décennies ; cependant l'émergence de résistance au nord de Bihar en Inde a été reportée (Croft, Sundar, et al., 2006). Les dérivés pentavalents de l'antimoine (Sb^{V}) actuellement disponibles pour une utilisation clinique sont le stibogluconate de sodium (Pentostam) et l'antimoniate de méglumine (Glucantime). Tous les deux doivent être administrés par voie parentérale (intraveineuse ou intramusculaire) (Monzote, 2009).

1.5.2 Amphotéricine B (AmB)

L'Amphotéricine B est un antibiotique polyénique (Croft, Sundar, et al., 2006), composé d'un grand cycle de macrolide polyène et d'un monosaccharide aminé (mycosamine) (Borowski et al., 2020). L'AmB est utilisé comme deuxième ligne de traitement pour la leishmaniose. Cette molécule est également active sur les champignons ainsi que sur *Trypanosoma cruzi*. Son activité est due à la haute affinité de l'AmB pour l'ergostérol, qui est le stérol prédominant dans les membranes cellulaires de ces microorganismes (Croft, Sundar, et al., 2006). L'AmB devient la molécule de choix pour traiter la leishmaniose dans les régions endémiques présentant une résistance aux dérivés pentavalents de l'antimoine (Singh et al., 2012). Actuellement, quatre formulations de l'AmB sont autorisées pour l'utilisation clinique : AmB micellaire (Fungizone[®]), AmB liposomale (AmBisome[®]), AmB en dispersion colloïdale (Amphotericin B Lipid Complex, Abelcet[®]) et AmB en complexe lipidique (Abelcet[®]) (Monzote, 2009). Ces formulations sont détaillées ci-dessous (Section 1.6.1).

1.5.3 Pentamidine

La pentamidine est une diamine aromatique utilisée en deuxième ligne de traitement pour la leishmaniose, principalement utilisée pour traiter la LV (Singh et al., 2012). Elle interfère avec la synthèse de l'ADN agissant sur le kinétopaste et sur la membrane mitochondriale provoquant la mort du parasite (Goto, 2012). Malgré certains essais cliniques qui démontrent son efficacité sur certains types de leishmaniose, ce médicament n'est pas largement utilisé à cause de l'apparition de résistance (Croft, Sundar, et al., 2006). De plus la pentamidine présente une toxicité importante et comme principaux effets indésirables l'hypotension, l'hypoglycémie et la néphrotoxicité (Singh et al., 2012).

1.5.4 Miltéfosine

La miltéfosine est une alkylphosphocholine (hexadecylphosphocholine), développée en premier lieu comme agent anticancéreux (Singh et al., 2012). C'est le premier médicament par voie orale approuvé pour le traitement de la leishmaniose viscérale (Croft, Seifert, et al., 2006) et elle est aussi prescrite pour la leishmaniose cutanée. La miltéfosine étant un analogue des alkylphosphocholines, elle interfère dans la biosynthèse des phospholipides perturbant les voies de transduction intracellulaires (Taheri et al., 2019). Quelques effets indésirables comme la toxicité gastro-intestinale et rénale peuvent être observés mais ils sont de caractère réversible et ne constituent pas une source de préoccupation majeure. Cependant à cause de son effet tératogène, la miltéfosine est déconseillée chez les femmes enceintes (Monzote, 2009).

1.5.5 Paromomycine

La paromomycine est un antibiotique de la classe des aminoglycosides ayant à la fois une activité antileishmanienne et une activité antibactérienne (Singh et al., 2012). Son mécanisme d'action n'est pas totalement élucidé mais il a été constaté qu'elle modifie la synthèse des protéines du parasite (Monzote, 2009). Elle est très peu disponible par voie orale mais est rapidement absorbée après administration intramusculaire (Monzote, 2009). Cette molécule peut être utilisée pour traiter la LV mais s'avère plus efficace sur la LC. Ainsi, elle possède un grand potentiel contre la leishmaniose cutanée dû à la facilité et l'accessibilité de la thérapie topique (Singh et al., 2012). Un effet secondaire très fréquemment observé est l'ototoxicité, ainsi que des problèmes de la fonction hépatique. Chez les patients traités avec la formulation

sous forme de pommade, des éruptions cutanées et des prurits ont été rencontrés (Monzote, 2009).

1.6 Systèmes d'administration de l'AmB

Depuis les années 50, l'AmB a été employée pour le traitement des maladies fongiques (Serrano & Lalatsa, 2017) et depuis 1960 pour la leishmaniose (Ponte-Sucre et al., 2017). Maintenant, l'AmB est considérée comme le médicament de choix contre les pathogènes fongiques multirésistants et la leishmaniose viscérale (Faustino & Pinheiro, 2020). Cependant, un inconvénient important de l'AmB est sa toxicité substantielle pour les mammifères qui dérive de son mécanisme d'action (Borowski et al., 2020). La figure 8 montre le mécanisme d'action qui est basé sur l'interaction de l'AmB avec tous les stérols. Cette interaction AmB-membrane perturbe les phospholipides de la membrane fongique, suivie de la formation de canaux permettant l'afflux d'ions et de molécules provoquant un déséquilibre ionique et la mort cellulaire (Ketllyn et al., 2016).

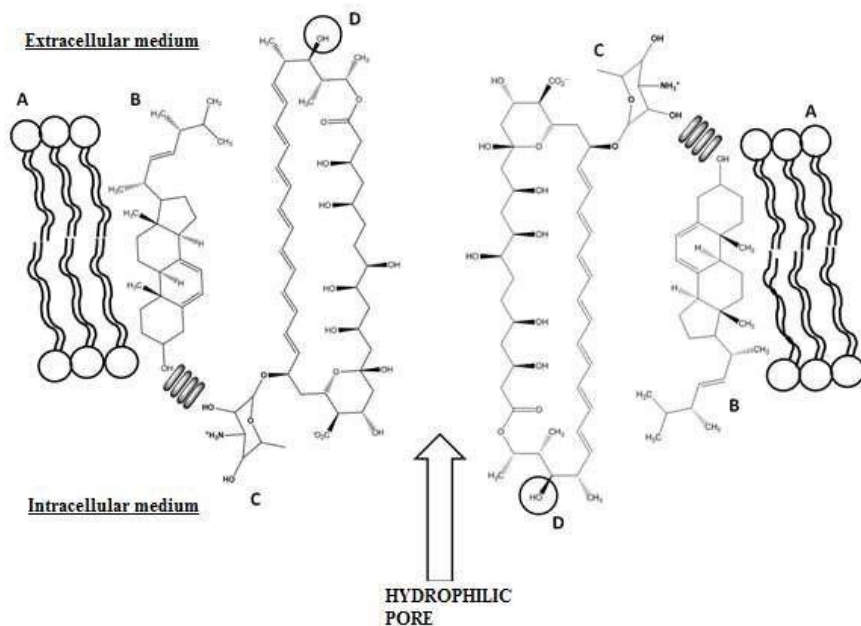


Figure 8. Interaction de l'AmB avec la membrane cellulaire fongique (formation de pores hydrophiles). L'interaction électrostatique entre la mycosamine et les hydroxyles de l'ergostérol est mis en évidence et ainsi que les groupes pharmacophores impliqués des phospholipides (A), de l'ergostérol (B), de la mycosamine (C) et de l'hydroxyle (D) (Ketllynn et al., 2016).

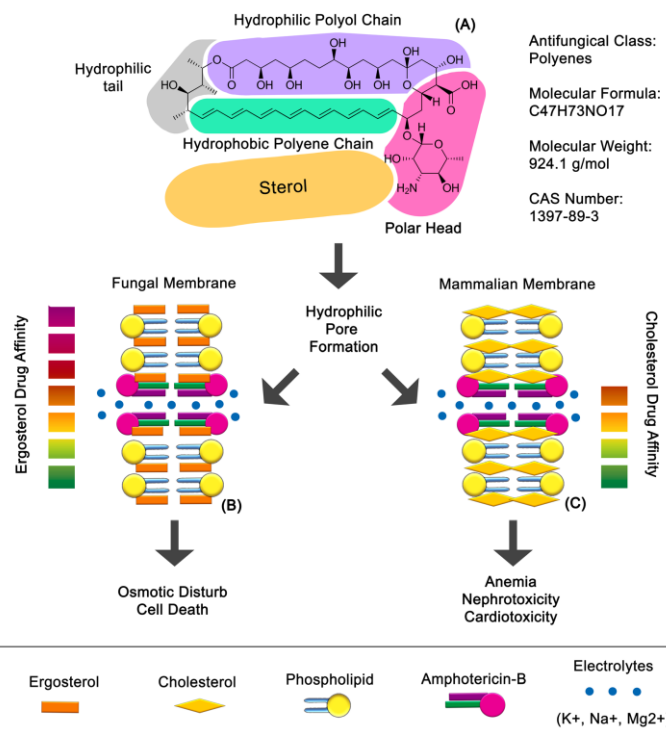


Figure 9. Effets de l'interaction AmB-membrane cellulaire (A): l'AmB (B) dans une cellule fongique et (C) dans une cellule de mammifère (Cavassin et al., 2021)

Comme le montre la figure 9, l'affinité de l'AmB pour l'ergostérol des membranes des microorganismes lui confère son activité sélective. Toutefois, cette sélectivité n'est que légèrement plus élevée comparativement au cholestérol des membranes cellulaires des mammifères, rendant sa fenêtre thérapeutique très étroite (Borowski et al., 2020).

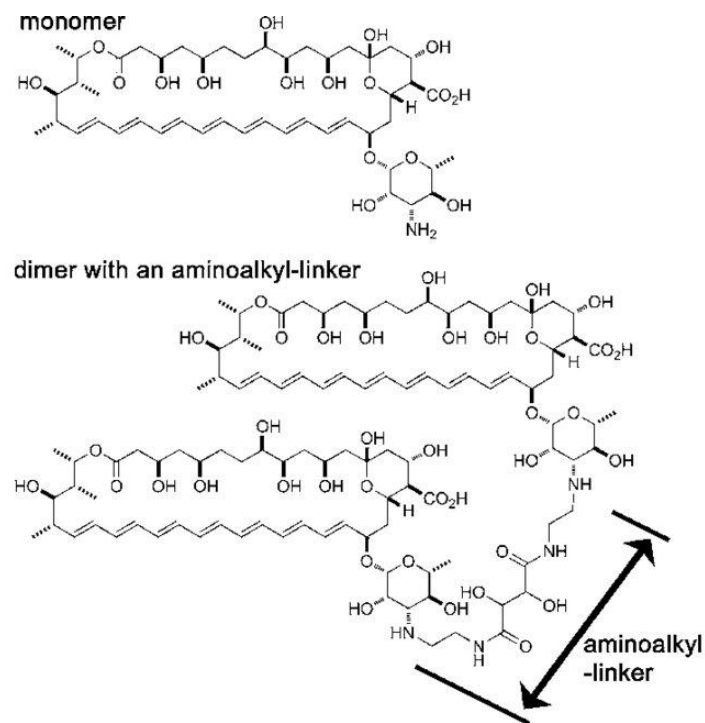


Figure 10. Structures monomère et dimère d'AmB par liaison aminoalkyle (Hirano et al., 2011)

Les dimères d'AmB (Figure 10) sont particulièrement toxiques pour les cellules eucaryotes (Ling Tan et al., 2019). Tandis que les formes polyagrégées et monomères présentent une toxicité réduite pour les cellules hôtes conservant en même temps une activité antiparasitaire (Faustino & Pinheiro, 2020)

Son utilisation clinique est aussi limitée par sa faible biodisponibilité par voie orale à cause de sa faible solubilité dans l'eau (< 0,001 mg/mL) (Zhou et al., 2017) ainsi que son poids moléculaire élevé (934 g/mol). L'AmB est également instable dans les milieux acides, sensible à la lumière et à la température, nécessitant un stockage entre 2 et 8°C (Faustino & Pinheiro, 2020).

La Fungizone® a été développée comme la première forme pharmaceutique d'AmB pour une administration parentérale. Il s'agit d'une dispersion micellaire d'AmB utilisant le désoxycholate de sodium (DOC) pour améliorer la solubilité de l'AmB (Zhou et al., 2017). Lors de la dilution dans le plasma après l'administration i.v., la Fungizone® libère rapidement l'AmB, principalement sous forme d'oligomères toxiques. La molécule s'accumule principalement dans le foie, la rate, les reins et les poumons, étant lentement excrétée sous forme inchangée par les voies urinaire et biliaire. Malgré son efficacité, l'AmB-DOC possède une fenêtre thérapeutique étroite en raison d'événements indésirables dose-dépendants (Faustino & Pinheiro, 2020). Les nombreux effets indésirables graves associés sont des nausées, vomissements, la fièvre, l'hypokaliémie, l'insuffisance rénale, l'anémie et des problèmes cardiaques. Surtout, la cardiotoxicité, la néphrotoxicité et l'hypokaliémie induites par cette formulation après administration intraveineuse limitent son utilisation en milieu hospitalier (Goto, 2012).

1.6.1 Formulations lipidiques d'AmB

Plusieurs formulations parentérales lipidiques ont été développées pour l'administration de l'AmB afin de contrôler la libération des oligomères toxiques, modifier sa biodistribution et faciliter son absorption préférentielle par les cellules réticuloendothéliales tout en évitant les tissus sensibles et ainsi réduisant sa toxicité (Monzote, 2009). Trois de ces formulations à base de lipides ont été mises sur le marché et restent autorisées dans de nombreux pays (Faustino & Pinheiro, 2020):

- Un complexe lipidique d'amphotéricine B (ABLC, Abelcet®), constitué de structures lipidiques microscopiques en forme de ruban.
- Une dispersion colloïdale d'amphotéricine B (ABCD, Amphotec® / Amphocil®), dans laquelle la molécule d'AmB forme des structures lipidiques en forme de disque avec le cholestéryl sulfate de sodium, un métabolite naturel du cholestérol.
- L'amphotéricine B liposomale (L-AmB, AmBisome®), dans laquelle la molécule d'AmB est intercalée dans la bicoche lipidique de liposomes contenant du cholestérol.

Ces formulations lipidiques montrent un profil favorable de sécurité (faible néphrotoxicité) permettant d'administrer des doses importantes par voie intraveineuse (5-10 mg/kg) par rapport à celles possibles avec la Fungizone® (0,5-1 mg/kg) (Serrano & Lalatsa, 2017). Le véhicule lipidique permet une libération sélective et contrôlée de la molécule vers les cellules

fongiques tout en empêchant son interaction avec le cholestérol membranaire des cellules hôtes, réduisant ainsi les effets secondaires. Parmi les formulations lipidiques, la L-AmB (AmBisome[®]) est associée à un taux de réactions liées à la perfusion et d'événements indésirables de néphrotoxicité moins nombreux et moins fréquents (Faustino & Pinheiro, 2020). Elle est par conséquent la forme la plus acceptée dans le traitement de la leishmaniose cutanée et viscérale (Monzote, 2009).

Malgré le fait d'avoir surmonté les inconvénients de la formulation classique (Fungizone[®]), les formulations lipidiques présentent un coût élevé qui limite leur accessibilité dans les pays en voie de développement (Borowski et al., 2020; Singh et al., 2012). De plus, les effets secondaires liés à la perfusion et la nécessité d'hospitalisation pour surveillance restent des inconvénients à surmonter (Serrano & Lalatsa, 2017).

Le développement d'une formulation d'AmB active par voie orale, capable de diminuer la toxicité systémique du médicament, d'éviter les événements indésirables liés à la perfusion, d'améliorer l'observance du patient et de réduire les coûts associés à l'administration intraveineuse des formulations commerciales d'AmB est une exigence urgente.

1.6.2 Nouveaux systèmes d'administration par voie orale

L'administration par voie orale est idéale pour diriger une molécule vers le foie et la moelle osseuse car après l'absorption la molécule peut atteindre le foie par la veine porte (Serrano & Lalatsa, 2017). Prenant en compte que *Leishmania* est un parasite intracellulaire affectant les organes du système réticuloendothélial (foie, rate, moelle osseuse), le transport de l'AmB vers ces organes peut conduire à un meilleur résultat thérapeutique (Serrano & Lalatsa, 2017). Cependant l'AmB présente une biodisponibilité orale très faible (0,2-0,9%) (Serrano & Lalatsa, 2017). D'autre part, les systèmes de nanoparticules (100 à 500 nm) administrés par voie orale sont un bon candidat pour l'absorption lymphatique via le système lymphatique gastro-intestinal (Khan et al., 2013) pouvant aussi cibler des molécules actives vers la moelle osseuse (Serrano & Lalatsa, 2017).

De nombreuses tentatives ont été réalisées pour obtenir des formes galéniques de l'AmB pour l'administration orale. Parmi ces systèmes se trouvent des conjugués lipidiques, micelles, liposomes, éthosomes et niosomes, nanoémulsions, cochleates, SEDDS (systèmes d'administration de médicaments auto-émulsifiants), cubosomes, nanodisques, SLN

(Nanoparticules lipidiques solides), hybrides lipide-polymère (Aigner & Lass-Flörl, 2020). Les plus prometteuses de ces formulations sont décrites dans les paragraphes qui suivent.

1.6.2.1 Conjugués lipidiques

Le développement d'une pro-drogue à base de lipides et d'AmB peut aider à réduire la toxicité et à résoudre les défis d'instabilité dans le milieu stomacal et la faible biodisponibilité orale de l'AmB. L'association de l'AmB avec l'acide oléique (OA) est possible via la formation d'une liaison amide avec le groupe amine de l'AmB pour obtenir le conjugué AmB-OA, destiné à l'administration orale. Cette association a bien amélioré la stabilité de l'AmB dans le milieu gastrique ainsi que son absorption dans un modèle cellulaire de Caco2 (Faustino & Pinheiro, 2020). L'administration orale d'AmB-OA (10 mg/kg) chez le rat a montré une augmentation significative de la Cmax et de l'ASC par rapport à l'AmB seule. De plus, des études *in vivo* chez des souris après administration orale d'AmB-OA (10 mg/kg dans du PBS) ne montrent aucune augmentation significative des niveaux de biomarqueurs de néphrotoxicité ou d'hépatotoxicité par rapport au contrôle non traité (Thanki et al., 2018).

1.6.2.2 Micelles

Des systèmes micellaires mixtes lipides-sels biliaires ont été utilisés pour améliorer la solubilité et la perméabilité membranaire de l'AmB afin d'améliorer la biodisponibilité orale de la molécule. Des micelles à base d'acides lipoaminés (LAA) et des micelles mixtes de LAA-sel bilaire comme systèmes d'administration d'AmB ont montré une activité antifongique *in vitro* contre *Candida albicans* comparable à celle de Fungizone® et la capacité de libérer l'AmB dans sa forme monomère (moins毒ique) (Faustino & Pinheiro, 2020).

1.6.2.3 Systèmes d'administration de médicaments auto-émulsifiants

Les systèmes d'administration de médicaments auto-émulsifiants (SEDDS) sont des mélanges isotropes d'huiles, de tensioactifs et de cosolvants ou de tensioactifs hydrophiles conçus pour améliorer la biodisponibilité orale de médicaments peu solubles dans l'eau (Joshi & Gawade, 2016). L'entreprise iCo Therapeutics a développé une formulation SEDDS pour améliorer la biodisponibilité orale de l'AmB qui est actuellement en essai clinique de phase I. La formulation AmB-SEDDS, dénommée iCo-010, est à base de monoglycérides, de diglycérides, de glycérides de polyéthylène glycol et de succinate de D- α -tocophéryl polyéthylène glycol (TPGS). Elle a montré une bonne efficacité dans le traitement des

infections fongiques chez le rat et la souris et dans le traitement de LV (modèles murins de LV) (Faustino & Pinheiro, 2020).

L'amélioration de la perméabilité et le ciblage vers le système de transport lymphatique sont les facteurs décisifs pour son efficacité prometteuse (Wasan et al., 2010). De plus, une accumulation d'AmB dans le foie, la rate, les reins et les poumons a été observée après administration orale de la formulation chez des souris sans induire de toxicité gastro-intestinale (Gershkovich et al., 2010).

1.6.2.4 Cubosomes

Les cubosomes, nanoparticules cristallines liquides cubiques à base de lipides, ont été étudiés comme système de libération pour améliorer la biodisponibilité orale de molécules peu solubles dans l'eau. Par exemple, le monooléate de glycérol (MO) et le phytantriol (PHY) sont des excipients huileux capables de former des nanostructures cristallines liquides dans un excès d'eau à température ambiante (Otte et al., 2018). Une formulation de cubosomes à base de MO et PHY a été développée pour l'administration orale de l'AmB. Des études *in vitro* ont montré une amélioration de la stabilité de l'AmB dans les fluides gastro-intestinaux et une augmentation de la perméabilité dans le modèle de cellules intestinales de Caco-2. Enfin, des formulations de cubosomes à base de MO et PHY ont permis un facteur d'augmentation significative de 4,2 et 5,1 de la biodisponibilité orale d'AmB (valeur d'AUC) comparé avec le médicament libre (dispersé dans l'eau) dans un modèle de rat (Jain et al., 2018).

1.6.2.5 Cochleates

Les cochléates (figure 11) sont des précipités stables de phospholipides anioniques en présence de cations divalents qui ont une structure de multicouches étroitement liées, formée par une seule bicouche lipidique continue, enroulée en spirale, sans espace aqueux interne (Nagarsekar et al., 2016; Santangelo et al., 2000). Ces structures cochléates peuvent être formées par l'interaction de liposomes négativement chargés avec des cations divalents (Syed et al., 2008). Le phospholipide le plus souvent utilisé est la phosphatidylsérine (PS) (Kay & Grinstein, 2011). La présence du cation formant un pont entre les têtes polaires de deux phospholipides déclenche une déshydratation et un processus d'auto-assemblage suivi d'un arrangement spontané pour former des systèmes plus complexes typiquement en forme de cigare (Nagarsekar et al., 2016).

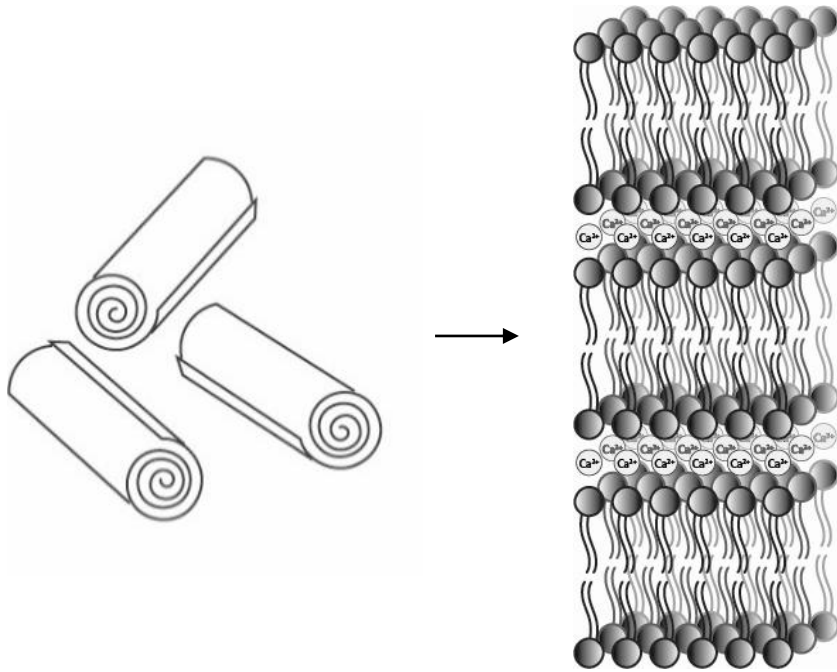


Figure 11. Structure des cochléates

Des molécules actives peuvent être facilement insérées dans ou entre les bicouches de PS où elles sont protégées contre des conditions agressives telles que des milieux gastro-intestinaux (Pham et al., 2014), ou des enzymes protéolytiques (Pathak & Thassu, 2016; Rao et al., 2007). En plus, en raison de leur structure déshydratée, les cochléates sont moins sensibles à l'oxydation à la fois des phospholipides et de la molécule encapsulée en comparaison avec les liposomes et à la différence des systèmes vésiculaires, ils conservent leur structure après lyophilisation sans qu'aucun cryoprotecteur ne soit nécessaire, augmentant ainsi considérablement leur durée de conservation (Pham et al., 2014). En particulier, les cochléates peuvent améliorer la biodisponibilité orale des médicaments hydrophiles et hydrophobes (Aigner & Lass-Flörl, 2020; Bhosale et al., 2013; Harkare et al., 2013; Vijeta & Vivek, 2011). Les molécules hydrophobes comme l'AmB peuvent être insérées dans les bicouches lipidiques déshydratées des cochléates et être ainsi efficacement protégées de l'environnement difficile comme le milieu acide et enzymatique du tractus gastro-intestinal (Faustino & Pinheiro, 2020). En outre, l'AmB contenue dans des cochléates a montré une activité *in vitro* contre *Leishmania chagasi* (Sesana et al., 2011). De plus, des cochléates contenant de l'AmB administrés par voie orale ont montré une efficacité *in vivo* chez la souris contre l'aspergillose (Delmas et al., 2002) ou la candidose (L. Zarif et al., 2000).

1.6.2.6 Nanoparticules hybrides lipides-polymères

Sur la base d'une combinaison synergique des propriétés, des systèmes hybrides lipides-polymères ont été développés pour surmonter les problèmes des nanoparticules lipidiques (Faustino & Pinheiro, 2020). Chen et al. (2015) ont étudié des micelles mixtes auto-assemblées contenant l'AmB basées sur une combinaison de lécithine avec des polymères amphiphiles commerciaux (Pluronic, Kolliphor, TPGS et DSPE-N-methoxy-PEG2k). Parmi ces systèmes, les micelles d'AmB composées de lécithine et de DSPE-PEG2k (Ampicelles) ont montré les meilleurs résultats dans l'amélioration de la solubilité de l'AmB avec une biodisponibilité parentérale et orale accrue chez le rat par rapport à Fungizone® et une cytotoxicité *in vitro* réduite (Faustino & Pinheiro, 2020).

Serrano et al. (2015) ont encapsulé l'AmB dans des nanoparticules amphiphiles à base de N-palmitoyl-N-méthyl-N,N-diméthyl-N,N,N-triméthyl-6-O-glycol chitosane (GCPQ) (Serrano et al., 2015). Les particules avaient une structure cœur-couronne avec les unités ioniques formant la couronne des particules et les groupes hydrophobes formant le cœur. Ces systèmes ont fourni une biodisponibilité orale de l'AmB de 24,7% chez la souris (Serrano & Lalatsa, 2017). De plus, l'administration orale de l'AmB encapsulée dans des nanoparticules GCPQ a également montré une efficacité élevée sur des modèles murins de la candidose, de l'aspergillose ou de la LV par rapport à l'AmBisome® administrée par voie parentérale (Serrano & Lalatsa, 2017).

1.7 Perspectives actuelles des systèmes d'administration de l'AmB

Parmi les nombreux systèmes d'administration orale développés pour l'AmB, les cochléates, les systèmes à base de lipides (SEDDS) et les nanoparticules polymères sont indiqués comme les formulations les plus efficaces pour délivrer de plus grandes quantités d'AmB vers les tissus cibles chez les rongeurs (Serrano & Lalatsa, 2017). Ces systèmes sont déjà bien avancés dans leur développement et des essais cliniques sont en cours. Ainsi les systèmes AmB-cochléates développés par Matinas Biopharma sont actuellement en phase II (Aigner & Lass-Flörl, 2020). De plus, METAmphizon (AmB encapsulée dans des nanoparticules GCPQ) développé par Nanomerics est en phase I d'essai clinique tout comme le système iCo-Amphotericin B (AmB-SEDDS) développé par iCo Therapeutics Inc (Faustino & Pinheiro, 2020).

1.8 Caractérisation des cochléates (revue)

Les cochléates sont des systèmes prometteurs pour l'administration orale de principes actifs. Leur composition lipidique et leur structure solide déshydratée sont propices à l'obtention d'un système biocompatible et idéal pour améliorer la stabilité de molécules actives face à l'oxydation, les pHs extrêmes ou l'activité enzymatique mais également à l'amélioration de la biodisponibilité orale de certains médicaments. De nombreuses molécules actives ont été encapsulées dans des cochléates, ainsi que de nombreuses méthodes de préparation ont été décrites dans la littérature pour leur obtention. De plus, leur structure particulière rend leur caractérisation délicate. Ainsi, diverses méthodes pour la caractérisation de leur taille, leur charge, leur morphologie et leur structure interne ont été utilisées pour optimiser les formulations. Dans la partie suivante nous présentons un article de revue (à soumettre à International Journal of Pharmaceutics) où nous décrivons les cochléates et plus particulièrement leur composition et leur structure. Une description des propriétés des cochléates, de leurs méthodes de préparation et des techniques disponibles pour leur caractérisation notamment des informations apportées est également détaillée dans l'article de revue.

COCHLEATE DRUG DELIVERY SYSTEMS: AN APPROACH TO THEIR CHARACTERIZATION

Antonio Lipa-Castro, François-Xavier Legrand and Gillian Barratt*

Université Paris-Saclay, CNRS, Institut Galien Paris-Saclay, 92290, Châtenay-Malabry, France.

* Corresponding author

ABSTRACT

Cochleate systems formed from phospholipids have very useful properties as drug delivery systems with sustained release capabilities, which are able to improve bioavailability and efficacy, reduce toxicity and increase the shelf-life of encapsulated molecules. These nanometric or micrometric structures are usually obtained after interaction of negatively charged liposomes with a positively charged bridging agent. Many different methods are now available to prepare cochleates and there are also numerous techniques that can be used to characterize them, some of which can be easily applied while others require more sophisticated equipment or analysis. The present review describes the important features of this drug delivery system; including their structural properties and potential applications, as well as a brief account of methods for their preparation and an extensive description of the techniques used for their characterization. This information could guide formulators in their choice of methods of characterization that would be best suited to their needs in terms of time, precision and technological difficulty.

Keywords: cochleates, phospholipids, drug delivery, SAXS/WAXS, FT-IR, light scattering

1.8.1 Introduction

Oral drug delivery is the most convenient route for drug administration and is preferred because of safety and good patient compliance (Agrawal et al., 2014). However, many useful drugs have poor oral bioavailability due to their very low water solubility or poor permeation through biological membranes. Over the last few years, drug delivery systems have become gaining importance as a means of promoting the modified release of active ingredients (Patra et al., 2018). They are used to improve the therapeutic index and reduce the side effects of drugs, by overcoming problems such as limited solubility, drug aggregation, chemical instability, low bioavailability, poor biodistribution and lack of selectivity. The most commonly described systems include micelles, liposomes, dendrimers, nanocapsules and nanospheres (Li et al., 2019; Sharma et al., 2016). Among these systems, lipid-based delivery systems have been reported to improve oral bioavailability of poorly water-soluble drugs (Kalepu et al., 2013). Due to their biocompatibility and the similarity of the lipid bilayer with the cell membrane, liposomes are the most widely employed systems at present, but they are limited by their poor stability, particularly by the oral route (Pawar et al., 2015). Another type of phospholipid-based structure, known as cochleates, could have some advantages over liposomes for the oral route (Li et al., 2015). Cochleates, which were first described by Papahadjopoulos et al. in 1975, are stable phospholipid-cation precipitates (Zarif et al., 2000), formed of rolled-up negatively charged phospholipid bilayers bridged by multivalent cations (Pawar et al., 2015). Several methods to prepare this type of drug delivery system have been developed (Ramasamy et al., 2009). However, it is necessary to use a number of characterization techniques to determine the optimal composition for the cochleates and the limits to the amount of drug that can be incorporated, as well as to evaluate their stability over time. Therefore, a number of different techniques have been used to characterize cochleate systems. Methods such as dynamic light scattering (DLS), microscopy (Asprea et al., 2019), differential scanning calorimetry (DSC) (Sarig et al., 2011), infrared spectroscopy and X-ray diffraction have been used to study the morphology, size, surface charge and internal structure of the cochleates (Bozó et al., 2017). For a complete characterization of cochleates, and to distinguish them from other phospholipid-based drug delivery systems, it is necessary to combine a number of complementary techniques. In this context, it is important to understand what information can be obtained from each technique. In this review we outline the advantages of cochleates as drug delivery systems, present the different protocols of preparation and describe the different methods available for their characterization in detail.

1.8.2 Cochleates: physicochemical description

Cochleates are stable phospholipid-cation precipitates comprised of a tightly multilayered packed structure formed by a continuous, solid, lipid bilayer sheet rolled up in a spiral, with no internal aqueous space, as shown in Figure 12 (Nagarsekar et al., 2016; Santangelo et al., 2000).

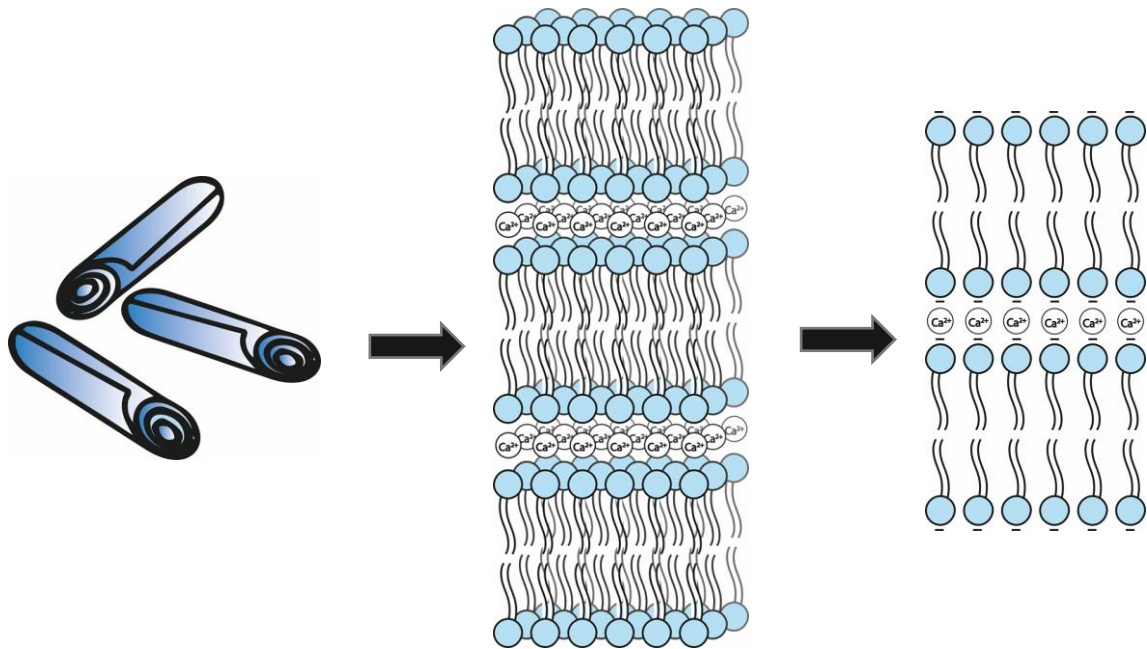


Figure 12. Internal structure of cochleates.

They are formed by the interaction of negatively charged liposomes with divalent cations (Syed et al., 2008) triggering a dehydration and self-assembly process followed by a spontaneous arrangement to form more complex systems with a typical cigar shape. Figure 13 illustrates this mechanism (Nagarsekar et al., 2016).

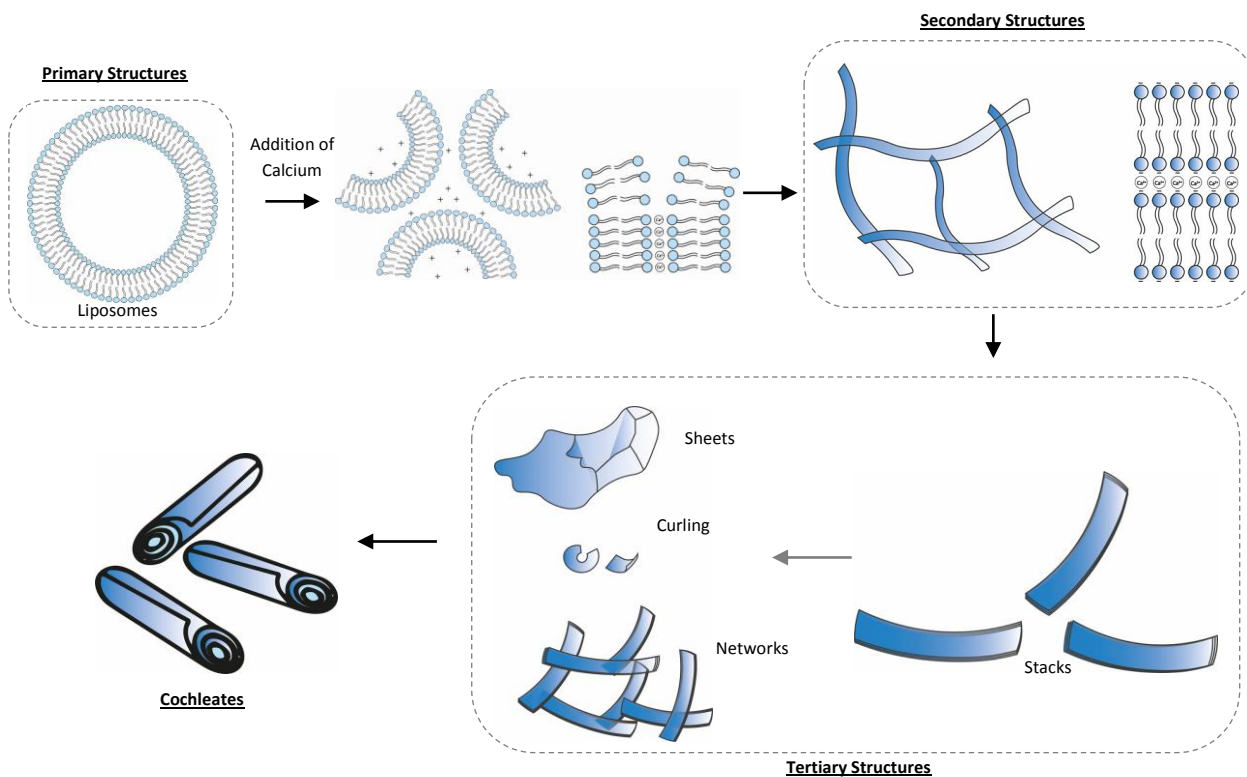


Figure 13. Intermediate structures after the addition of calcium ions that give the cochleates as a final product (adapted from Nagarsekar et al., 2016).

Although cochleates are usually described as cigar-shaped nanostructures, different morphologies have been observed depending on the type of phospholipid and bridging agent used. Hence, when dioleoyl phosphatidylserine (DOPS) was used homogenous cigar-shaped particles were obtained whereas planar and spherical sheets were obtained when palmitoyl-oleoyl phosphatidylserine (POPS) and soy PS were employed respectively (Landge et al., 2013). Furthermore, fibrils and spherical cochleates was observed when bridging agents other than divalent cations were used (Syed et al., 2008). Depending on their physico-chemical properties, drugs can be incorporated either within the phospholipid bilayers or sandwiched between the bilayers (Harkare et al., 2013) (Figure 14). Thus, due to the special internal structure of the cochleates, they can protect the encapsulated material against harsh conditions and thereby provide a unique and efficient way of formulating drug molecules (Bozó et al., 2017).

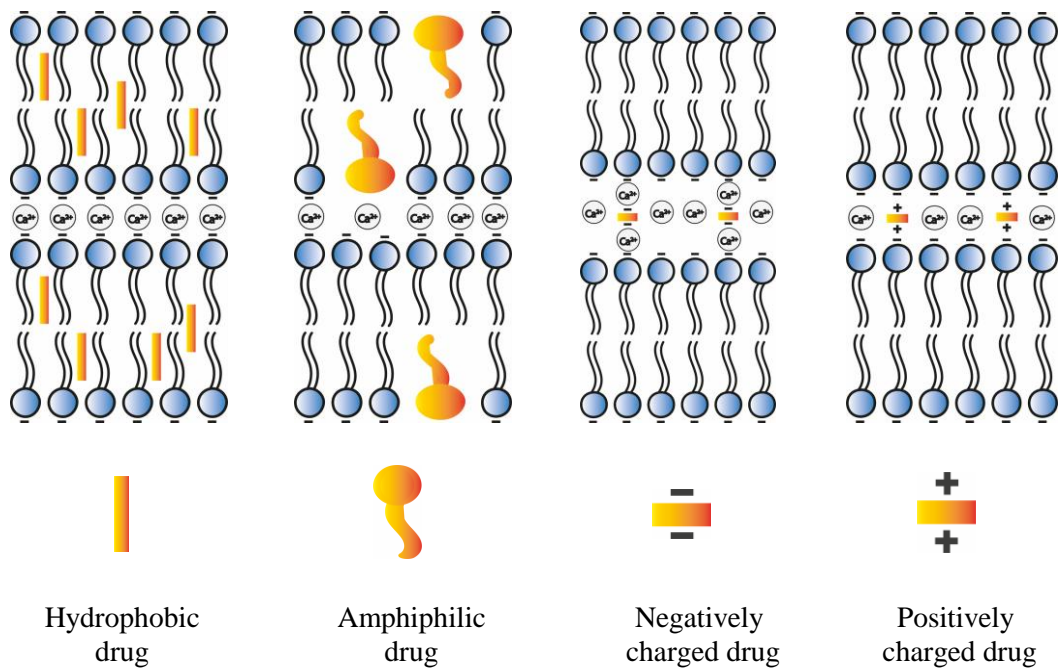


Figure 14. Arrangements of the drugs loaded as cochleates (adapted from Zarif, 2005).

1.8.3 Raw materials

1.8.3.1 Lipids

These are the main ingredients for obtaining the cochleates. The process usually begins with the preparation of negatively charged liposomes, for which the most commonly used phospholipid with a negative charge on the headgroup at physiological pH is phosphatidylserine (PS), and the synthetic dioleoylphosphatidylserine (DOPS) is frequently employed (Bozó et al., 2017; Nagarsekar et al., 2016; Syed et al., 2008). As shown in Figure 4, other negatively charged phospholipids, such as phosphatidic acid (PA), phosphatidyl glycerol (PG) and phosphatidylinositol (PI), have also been shown to form cochleates. In addition, mixtures of negatively phospholipids and other phospholipids (PS/PC where PS > 50%) can also yield cochleates but require a higher concentration of bridging agents (Li et al., 2015). Mixtures containing at least 75% of PS, PI, PA, PG with PC, PE and other less abundant phospholipids have also been used (Sankar & Reddy Y, 2010). It is not necessary to use synthetic phospholipids with defined acyl chains; cochlate structures can also obtained from naturally occurring phospholipids such as soy PS (Mannino et al., 2004) and soy PC (Asprea et al., 2019). This latter result is surprising because PC is zwitterionic with no net charge. However, the liposomes from which the soy PC cochleates were formed had a fairly high negative zeta potential so it is possible that the natural PC used contained other, charged, lipids that could be bridged by the Ca^{2+} ions (Asprea et al., 2019).

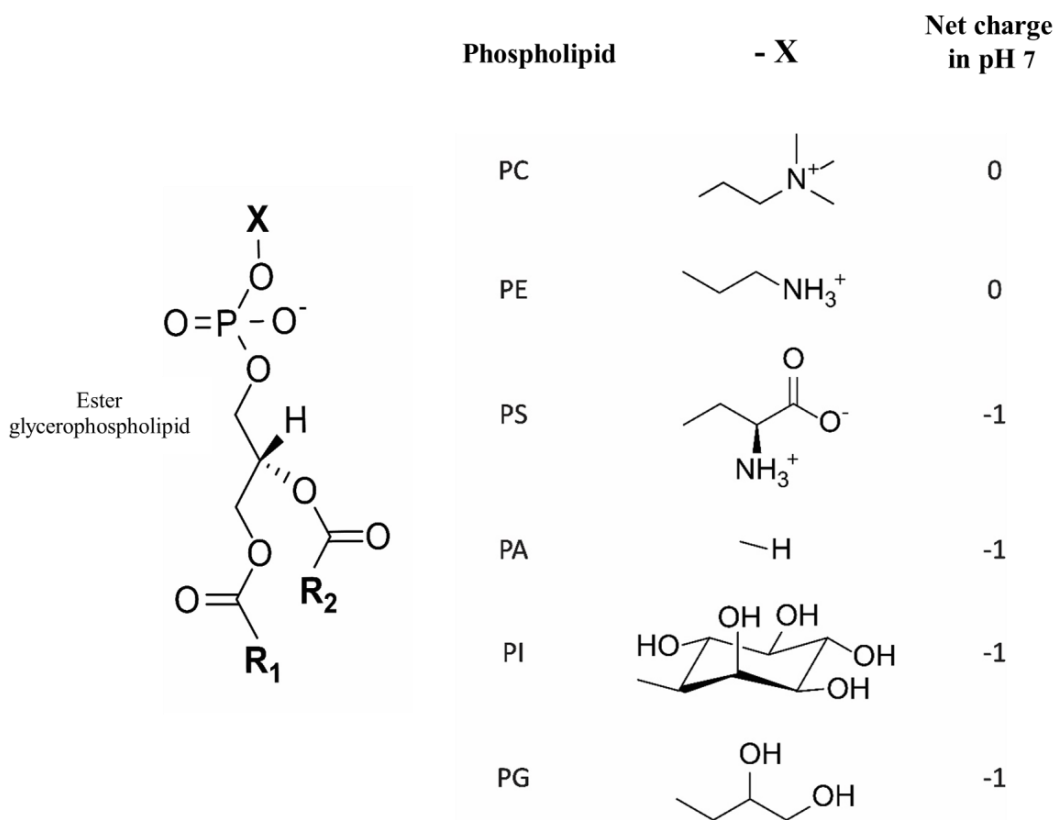


Figure 15. Structure of phospholipids used in obtaining cochleates (adapted from Li et al., 2015).

1.8.3.2 Bridging agent

The divalent cations maintain the rolled sheet structure by electrostatic interaction between their positive charge and that of the negatively charged lipid head groups in the bilayer (Koomer, 2009). Divalent cations such as Ca++, Mg++, Ba++ and Zn++ can all be used, but the calcium ion have been reported to be the most efficient (Landge et al., 2013). Cochleates bridged by calcium have smaller dimensions and a higher degree of dehydration than those formed with magnesium. Furthermore, calcium-based cochleates were found to be more tightly packed, highly ordered and required a much lower concentration of bridging ions (Flach & Mendelsohn, 1993). Some researchers have reported the use of some biologically active molecules, such as tobramycin, polylysine and oligo-acyl-lysyls, as an alternative to metal cations as bridging agents for cochleates, thus combining encapsulation and cochleate stabilisation (Sarig et al., 2011; Syed et al., 2008).

1.8.3.3 Cholesterol

Despite not being essential for obtaining the cochleate structure, several cochleate formulations have included the sterol cholesterol (Asprea et al., 2019; Pham et al., 2013) that can influence its structure, enhancing the dehydration and further immobility of the phospholipids without changing the stoichiometry of the binding agent and the phospholipid by altering the acyl chain packing (Choi et al., 1991).

1.8.3.4 Other components

Aggregation is a commonly described drawback of cochleates (Bozó et al., 2017). It has been shown that aggregation can be inhibited by changing the surface properties of the cochleates and thereby inhibiting cochleate-cochleate interaction. Therefore some aggregation inhibitors, such as casein, methylcellulose or albumin, may be included to maintain the cochleates as individual particles (Mannino et al., 2005).

1.8.3.5 Encapsulated drug

Many reports have described the successful encapsulation of vaccines, antibiotics, antifungals and other drugs in cochleates (Bozó et al., 2017) (Ramasamy et al., 2009), as shown in Table 2. The physicochemical properties of the drug will define its location in the cochleate structure, as shown in Figure 14. Thus hydrophobic, amphiphilic, negatively or positively charged drug can be incorporated and delivered by cochleates (Leila Zarif et al., 2000).

Table 2. Examples of active molecules reported to have been incorporated into cochleates. NSAIDs: non-steroidal anti-inflammatory drugs, CVS: cardiovascular system, CNS: central nervous system, BCS: biopharmaceutical classification system

Drug Name	Activity	BCS Class	Reference
5-Fluorouracil	Anticancer	III	Pawar et al., 2015
Acetaminophen	NSAID	III	Mannino et al., 2014
Acyclovir	Antiviral	III	Pawar et al., 2015
Amiloride	CVS	III	Pawar et al., 2015
Amitriptyline	CNS	I	Pawar et al., 2015
Amoxicillin	Antibiotic	III	Pawar et al., 2015
Amphotericin B	Antifungal	IV	Mannino et al., 2014
Andrographolide	Anti-inflammatory	IV	Asprea et al., 2019
ApoA1	Apolipoprotein	N/A	Ramasamy et al., 2009
Aspirin	NSAID	I	Ramasamy et al., 2009
Atenolol	CVS	III	Pawar et al., 2015
Atropine	Antispasmodic	III	Pawar et al., 2015
Benzodiazepines	CNS	II	Pawar et al., 2015
Bidisomide	CVS	III	Pawar et al., 2015
Bisphosphonates	Antiosteoporosis	III	Pawar et al., 2015
Buspirone	CNS	I	Pawar et al., 2015
Capecitabine	Anticancer	I	Pawar et al., 2015
Captopril	CVS	I	Pawar et al., 2015
Caspofungin	Antifungal	III	Mannino et al., 2014
Cefazolin	Antibiotic	III	Pawar et al., 2015
Celecoxib	NSAID	II	Pawar et al., 2015
Cetirizine	Antihistamine	III	Pawar et al., 2015
Chlorothiazide	Diuretic	IV	Pawar et al., 2015
Chlorpromazine	CNS	II	Pawar et al., 2015
Chlorthalidone	Antihypertensive	IV	Pawar et al., 2015
Cimetidine	Antihistamine	III	Pawar et al., 2015
Ciprofloxacin	Antibiotic	III	Pawar et al., 2015
Cisplatin	Anticancer	II	Pawar et al., 2015
Clofazimine	Antibiotic	II	Ramasamy et al., 2009
Cloxacillin	Antibiotic	III	Pawar et al., 2015
Clozapine	CNS	II	Pawar et al., 2015
Colistin	Antibiotic	IV	Pawar et al., 2015
Cyclosporine A	Immunosuppression	II	Liu et al., 2017
Diclofenac	NSAID	II	Pawar et al., 2015
Dicloxacillin	Antibiotic	III	Pawar et al., 2015
Diltiazem	CVS	I	Pawar et al., 2015
DNA	Gene therapy	N/A	Ramasamy et al., 2009
Docetaxel	Anticancer	IV	Pawar et al., 2015
Doxorubicin	Anticancer	II	Pawar et al., 2015
Encainide	CVS	III	Pawar et al., 2015
Erythromycin	Antibiotic	III	Pawar et al., 2015

Etoposide	Anticancer	IV	Pawar et al., 2015
Factor VIII	Blood clotting	N/A	Miclea et al., 2007
Famotidine	Anti-ulcer	III	Pawar et al., 2015
Fludarabine	Anticancer	II	Pawar et al., 2015
Fluoxetine	CNS	I	Pawar et al., 2015
Furosemide	Diuretic	IV	Pawar et al., 2015
Gemcitabine	Anticancer	III	Pawar et al., 2015
Haloperidol	CNS	II	Pawar et al., 2015
Hydralazine	CVS	III	Pawar et al., 2015
Hydrochlorothiazide	Diuretic	IV	Pawar et al., 2015
Ibuprofen	NSAID	II	Ramasamy et al., 2009
Indomethacin	NSAID	II	Pawar et al., 2015
Irinotecan	Anticancer	II	Pawar et al., 2015
Ketoconazole	Antibiotic	II	Shaikh et al., 2013
Ketorolac	NSAID	I	Pawar et al., 2015
Maprotiline	CNS	III	Pawar et al., 2015
Meloxicam	NSAID	II	Pawar et al., 2015
Mexiletine	CVS	III	Pawar et al., 2015
Naproxen	NSAID	II	Ramasamy et al., 2009
Neomycin	Antibiotic	IV	Pawar et al., 2015
Paclitaxel	Anticancer	IV	Pawar et al., 2015
Phenylbutazone	NSAID	II	Pawar et al., 2015
Piroxicam	NSAID	II	Pawar et al., 2015
Protein antigens	Vaccines	N/A	Ramasamy et al., 2009
Quinidine	CVS	I	Pawar et al., 2015
Rifampicin	Antibiotic	II	Yadav & Chaudhary, 2016
Risperidone	CNS	II	Pawar et al., 2015
Streptomycin	Antibiotic	III	Mannino et al., 2014
Sulindac	NSAID	II	Pawar et al., 2015
Tobramycin	Antibiotic	IV	Mannino et al., 2014
Tolmetin	NSAID	II	Pawar et al., 2015
Topotecan	Anticancer	I	Pawar et al., 2015
Valdecoxib	NSAID	II	Pawar et al., 2015
Vancomycin	Antibiotic	IV	Mannino et al., 2014
Verapamil	CVS	II	Pawar et al., 2015
Vinblastine	Anticancer	II	Pawar et al., 2015
Vincristine	Anticancer	III	Pawar et al., 2015
Vinorelbine	Anticancer	II	Pawar et al., 2015
Zolpidem	CNS	I	Pawar et al., 2015

1.8.4 Advantages of cochleates as a drug delivery system

Although cochleates were first described in 1975, it was not until twenty years later that they began be considered as a vehicle for drug delivery (Gould-Fogerite and Mannino, 1997; Jin et al, 2001). Since they are composed of natural materials, cochleates offer a biocompatible drug delivery system that is well tolerated without producing an immunogenic response (Ramasamy et al., 2009; Zarif, 2002). It has been shown that repeated oral and intra-peritoneal dosing in mice was well tolerated, non-toxic and non-inflammatory (Gibson et al., 2004; Zarif & Mannino, 2002). Their ability to provide controlled release of drugs in vitro (Asprea et al., 2019, Pham et al., 2014) and in vivo (Miclea et al., 2007, Santangelo et al., 2000; L. Zarif et al., 2000) has been demonstrated.

The properties of a drug delivery system do not depend solely on the components (such as the type of lipid) but also the way in which they are organized in the structure. Thus, the dehydrated, tightly packed nature of cochleates creates a stable structure (Landge et al., 2013) that can have advantages for the encapsulation and retention of drugs when compared with liposomes, although the basic phospholipid components of the two systems are very similar. Drugs can be easily inserted into or between the PS bilayers where they are protected against harsh condition such as gastrointestinal media (Pham et al., 2014), and proteolytic enzymes (Koomer, 2009; Rao et al., 2007). Furthermore, the multilamellar structure can provide a slow release profile for the drug (Rao et al., 2007). Finally, due to their dehydrated structure, cochleates are less susceptible to oxidation of both the phospholipids and the encapsulated drug than liposomes and, in contrast to vesicular systems, they retain their structure after freeze-drying without any cryoprotectant being necessary, thus greatly increasing their shelf life (Pham et al., 2014).

In particular, cochleates can improve the oral bioavailability of hydrophilic and hydrophobic drugs (Aigner and Lass-Flörl, 2020; Bhosale et al., 2013; Harkare et al., 2013; Vijeta et al, 2011). As illustrated in Figure 16, the high tension at the bilayer edges of the cochleates when they interact with the membrane of intestinal cells is suggested to be the driving force for fusion with these membranes, thereby enhancing the absorption of the encapsulated drug (Syed et al., 2008). In addition, as particulate material, cochleates may be captured by M cells in Peyer's patches and translocated across the epithelial barrier in this way. Cochleates that reach the circulation intact could be taken up by macrophages and delivered to sites of infection, for example, in the case of amphotericin B-loaded cochleates (Rongen, 2016).

However, within cells, in response to the low calcium levels in the cytoplasm, the cochleate structure could be destabilized and release the loaded drug. Since direct contact between the drug and the intestinal cells is avoided, toxic effects may be avoided.

Despite these advantages, no cochleate-based drug delivery formulation is on the market yet. A phase II trial with amphotericin B-loaded cochleates administered by the oral route was recently conducted with patients suffering from Candida infections, as described by Aigner and Lass-Flörl (2020). No significant toxicity was recorded, but the outcomes were not superior to those obtained with the reference drug, fluconazole. A better knowledge of the mechanisms involved in cochleate interaction with the gastrointestinal tract would help to optimize their use, but research is hampered by the quite complicated methods of preparation and the difficulty in characterizing the systems produced, as well as the cost of the starting material when phospholipids of synthetic origin are used. The information below could contribute to orientating the choice of methods and further developing these interesting drug delivery systems.

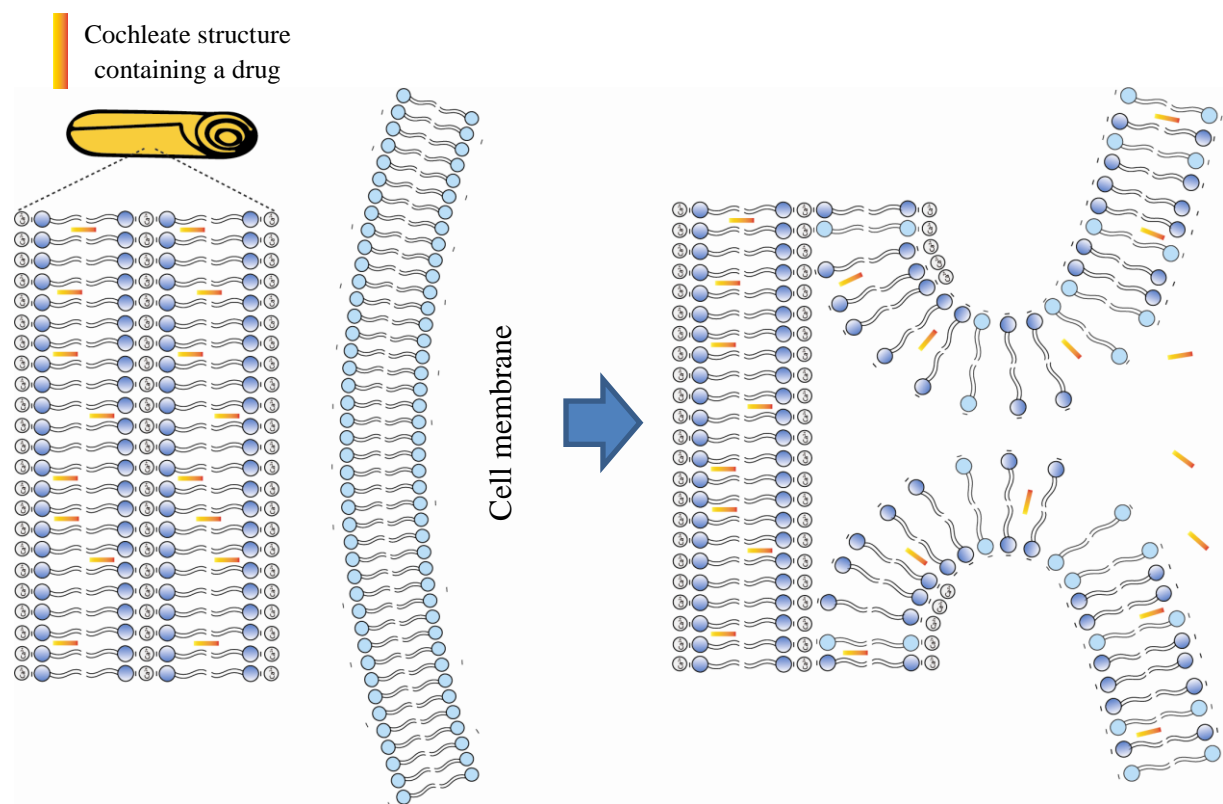


Figure 16. Schematic of the interaction of cochleate particles when the dehydrated bilayers approach a membrane cell resulting in cochleate fusion with cell membrane (reproduced with permission from Lipa-Castro et al. 2021)..

1.8.5 Methods for cochleate preparation

Cochleate preparation is generally based on the interaction of negatively charged liposomes with a positively charged cation, which generates fusion, dehydration and precipitation of larger structures corresponding to cochleates. The methods of preparing cochleates differ in the dispersing medium used and in the way in which the bridging agent is incorporated. Depending on these parameters, cochleates of different sizes can be obtained in the nanometric or micrometric range.

1.8.5.1 Trapping method

This is a simple method that involves the mixing of an aqueous lipid suspension (liposomes, micelles, etc) with a bridging agent. However, it rarely yields a narrow size distribution of the particles (Mannino et al., 2005; Zarif & Mannino, 2002). Modifications to improve the entrapment efficiency based on the use of solvents such as dimethylsulfoxide, ethanol, acetonitrile have been evaluated, allowing a wider range of molecules to be incorporated into the cochleates and also permitting the optimal lipid:molecule ratio to be determined without excessive experimentation (Mannino et al., 2005).

1.8.5.2 Hydrogel Method

This method, the most frequently used, allows small-sized cochleates to be formed from unilamellar liposomes. The liposomes are suspended in an aqueous two-phase medium formed by immiscible polymer solutions. Firstly, liposomes are added to polymer A (dextran, polyethylene glycol, etc.), after which the dispersion is suspended in polymer B (polyvinylpyrrolidone, polyvinylalcohol, Ficoll™, polyvinyl methyl ether, polyethylene glycol, etc.). A two-phase aqueous system is formed, with the liposomes dispersed in small droplets of polymer A. The bridging agent is then added to the system, forming a cochleate precipitate with a particle size of less than one micron. The precipitate must then be washed to remove the polymers (Jin et al., 2001; Zarif et al., 2003).

1.8.5.3 Dialysis method

Two methods employing dialysis have been described. In the first (liposomes before cochleates (LC) method), liposomes are formed by dialyzing the detergent from a solution containing lipid and the material to be encapsulated. These vesicles are then subjected to a second dialysis step in presence of the bridging agent (Gould-Fogerite & Mannino, 1997). In

the second method, called the direct calcium (DC) dialysis method, the mixture of lipid and detergent is directly dialyzed against buffer containing the bridging agent. It has been reported that drug encapsulation is lower than with the LC method (Gould-Fogerite & Mannino, 1997). and unlike the LC method, the DC dialysis method forms large cochleates (Harkare et al., 2013). The detergent used can be ionic such as cholate salts, deoxycholate salts and similar, or nonionic such as Tween, Brig or Triton. The most suitable nonionic detergents are those containing sugar head groups such as the alkyl glucosides, preferably 3-D-octyl glucopyranoside (Gould-Fogerite & Mannino, 1997).

1.8.5.4 Emulsification-lyophilization method

This method involves an emulsification-lyophilisation procedure in which the lipid is dissolved in the oil phase (O), one aqueous phase containing the bridging agent and a cryoprotectant in water (W1) and a buffer as the outer water phase (W2). After preparation of a W1/O/W2 emulsion, a lyophilisation procedure is carried out and nano-sized cochleates are obtained on rehydration of the lyophilized powder (Wang et al., 2014).

1.8.5.5 Microfluidic method

This method avoids elaborate preparation procedures and provides a monodispersed spherical system (3-5 µm in diameter) that retains a typical cochleate structure. The lipid is dissolved in ethanol and the bridging agent is dissolved in aqueous buffer. Mixing of the two phases is controlled by a microfluidic device with herringbone channels and the resulting suspension is collected. The morphology of the cochleates is strongly influenced by the flow rate of mixing and the lipid concentration. Thus, while at lower speeds aggregate structures are formed, at higher speeds spherical and regular particles are obtained. On the other hand, lower lipid concentrations can give extremely uniform structures, as shown in Figure 17. In comparison with conventional techniques, this approach is rapid and easy to handle (Nagarsekar et al., 2017).

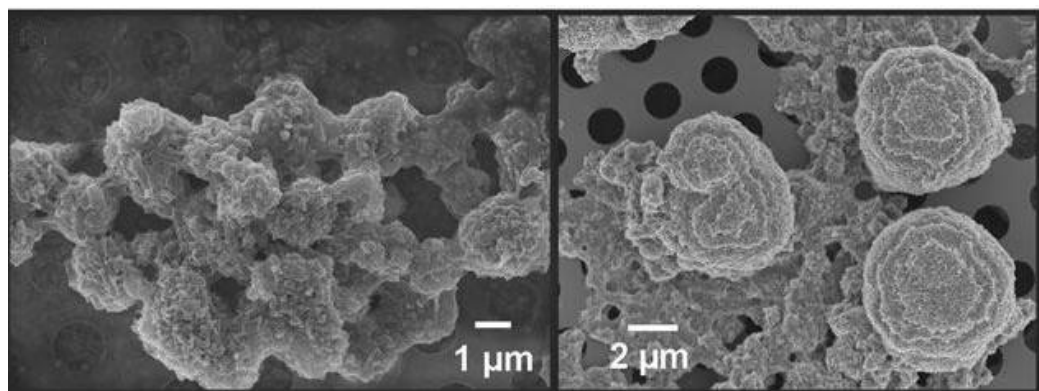


Figure 17. SEM image of optimized DOPS cochleate composites obtained from the NanoAssembler™ microfluidic device (reproduced from Nagarsekar et al., 2017, with permission).

1.8.5.6 Solvent injection method

Unlike the methods mentioned above that use phospholipids as the basis for cochleates, this approach employs cholesterol dispersed in organic solvent injected quickly into a water phase at a controlled temperature between 40°C and 75°C. An aqueous cholesterol microcrystal suspension is obtained. Electron microscopy revealed a hollow, cylindrical, tightly-coiled, multi-bilayer form of cholesterol that resembles classical cochleate cylinders (Harris et al., 2011).

1.8.6 Characterization techniques for cochleates

The formulation of cochleates remains a challenge and a wide range of characterization techniques are necessary to evaluate the objects that are produced and optimize the procedures. Based on their typical morphology, different states of aggregation and their particular internal structure, among other features, cochleates can be characterized by many methods. In the sections below, we review the different methods that can be used to characterize cochleate systems and the information that can be obtained from each of them. Table 3 provides a summary of these remarks.

Table 3. Main experimental techniques used for cochleate characterization

Technique	Main information derived	Commentary	Section
DLS	Size, size distribution, detection of agglomerates	This provides a quick and inexpensive analysis, but the main limitation is that it assumes that the cochleates are spherical in shape.	1.8.6.1.1
Optical microscopy	Size, shape, detection of agglomerates	Low-cost method that provides quick and inexpensive analysis without sample pretreatment; however, it detects only large cochleates	1.8.6.1.2
TEM	Size, shape, detection of agglomerates	Nanometer range can be resolved. However, sample pretreatment and sophisticated equipment are required.	1.8.6.1.2
AFM, SEM, Freeze fracture TEM	Size, shape, rolled structure	Three-dimensional images of cochleates can be resolved at the micrometer range by AFM and at the nanometer range by SEM and Freeze fracture TEM. These methods require sophisticated equipment and experienced operators	1.8.6.1.2
Fluorescence microscopy	Size, shape and interaction with other materials	Cheap analysis but samples must be prepared incorporating a fluorescence substance and is limited for large cochleates	1.8.6.1.2
Turbidimetry	Aggregate state	Fast and cheap analysis monitoring intermediate and final structures.	1.8.6.2.1
Zeta potential	Surface charge Aggregation state	Fast and cheap analysis for stability study and identification of the aggregate state.	1.8.6.2.2
Laurdan fluorescence	Hydration level Aggregation state	Fast and cheap technique useful to evaluate the impact of the inclusion of different drugs. However, incorporation of the fluorescent substance Laurdan is necessary.	1.8.6.2.3
DSC	Aggregate state	Fast analysis that studies phase transition and gives information about drug-lipid interaction but samples are subjected to temperature variations.	1.8.6.2.4
X-ray diffraction	Aggregate state Internal Structure (multilamellar packing)	SAXS and WAXS explore changes in phospholipid bilayers and acyl chain packing respectively. These techniques are also useful to identify intermediate structures accurately and to evaluate the impact of the inclusion of drugs; however sophisticated equipment is necessary.	1.8.6.3.1
FT-IR spectroscopy	Aggregate state Internal Structure	Fast and cheap analysis of the phospholipid headgroups, giving information about dehydration or packing state. Useful to study the impact of drugs in the internal structure.	1.8.6.3.2
NMR	Internal structure	Molecular structure information giving fundamental information about membrane fusion. Main limitation is the sophisticated equipment required.	1.8.6.3.3

1.8.6.1 Morphology, size and polydispersity

Size and shape are two of the most important parameters for colloidal dispersions. Cochleates are described as having a typical cigar shape and are therefore anisotropic, which renders them more difficult to characterize than spherical particles, for example, by light scattering methods where the algorithms assume spherical objects. It is also important to determine their polydispersity and degree of agglomeration that need to be controlled if they are to be used as drug delivery systems.

1.8.6.1.1 Light scattering techniques

Dynamic light scattering (DLS) is a widely employed technique for the measurement of size and polydispersity distribution (Asprea et al., 2019) that is often applied to colloidal suspensions in the nanometric or low micrometric ranges. This technique analyses fluctuations of scattering of laser light to determine the Brownian movement of the particles and hence their average hydrodynamic diameter. A single-frequency laser is directed towards the sample dispersed in liquid in a cuvette. The incident laser light is scattered in all directions and detected at one or more angles over time and the fluctuations in intensity are used to determine the diffusion coefficient and the particle size by the Stokes-Einstein equation (Equation 1). Commercial instruments that are simple to use with a minimum of sample preparation are available. In contrast to microscopic techniques, the results of DLS measure a mean parameter over the whole population rather than individual particles, although the data processing algorithms are able to detect a mixture of two or three distinct populations. A more serious limitation for cochleates is that the algorithms usually assume that the particles are spherical. This can lead to errors in the mean diameter of cigar-shaped particles. Nevertheless, the quick, easy and precise operation of the technique and the sensitivity to large particles (allowing it to detect aggregation) means that it is a useful standard procedure for cochleates (Mourdikoudis et al., 2018), especially when combined with a microscopic technique as described below.

$$D = k_B T / (6 \pi \eta R_H) \quad (\text{Equation 1})$$

D: Translational diffusion coefficient; K_B: Boltzmann constant; T: Temperature; η : Viscosity; R_H: Hydrodynamic radius

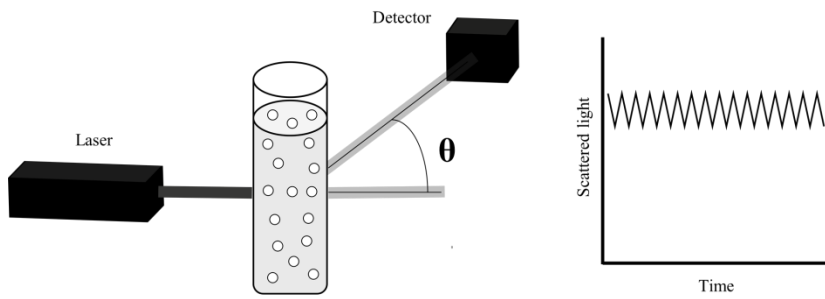


Illustration 1. Basic setup of a DLS measurement system. The sample is contained in a cuvette.

1.8.6.1.2 Microscopic Techniques

Optical microscopy has been used as a straightforward method for characterization of cochleates in several studies (Bozó et al., 2017; Syed et al., 2008; L. Zarif et al., 2000). It is very useful when evaluating cochleates of large size, for observing the cylindrical form of the particles and also for detecting the presence of agglomerations, a very common drawback in the manufacture of cochleates (Figure 18A). However, the resolution of the technique means that cochleates cannot be observed in detail and nano-sized cochleates cannot be resolved at all. Therefore, more advanced microscopic characterization techniques have been brought into play to improve the structural characterization of cochleates and elucidate the mechanisms of their formation. These include atomic force microscopy (Bozó et al., 2017), transmission electron microscopy (Asprea et al., 2019), as illustrated in Figure 18B, scanning electron microscopy and freeze-fracture electron microscopy (Nagarsekar et al., 2016). Amongst these, freeze-fracture electron microscopy is considered to be the most appropriate technique to evaluate the morphology of cochleates because it allows the rolled structure and the closely apposed bilayers to be visualized (Papahadjopoulos-Sternberg, 2012; Zarif, 2005). A disadvantage is that sophisticated equipment and experienced operators are required. These microscopic techniques can also be used to determine the size and polydispersity of cochleates but this requires the observation of a sufficiently large number of particles (Zarif & Mannino, 2002), Nagarsekar et al., 2016). It also has to be remembered that sample preparation may modify the size of the cochleates. Atomic force microscopy, which has a better resolution than optical microscopy, can provide a series of well-resolved snapshots that can be used to calculate the precise aspect ratio (length to diameter ratio) (Gao et al., 2019).

Fluorescence microscopy has also been used to determine the particle size and shape of large cochleates after incorporation of a fluorescent probe into the bilayer. Thus, Miclea et al., included rhodamine-labelled dioleoylphosphatidylethanolamine in cochleates and measured their size on images obtained from fluorescent microscopy (Miclea et al., 2007). The formation of cochleates from proteoliposomes derived from bacteria was revealed by the binding of Texas Red-labelled albumin to their surface (Acevedo et al., 2012). Thus, monitoring by fluorescent microscopy has also been useful in the evaluation of cochleates in the retention of their morphology under external influences such as an ion-complexing substance (EDTA) (Mannino, 2016) and sonication (Acevedo et al., 2012).

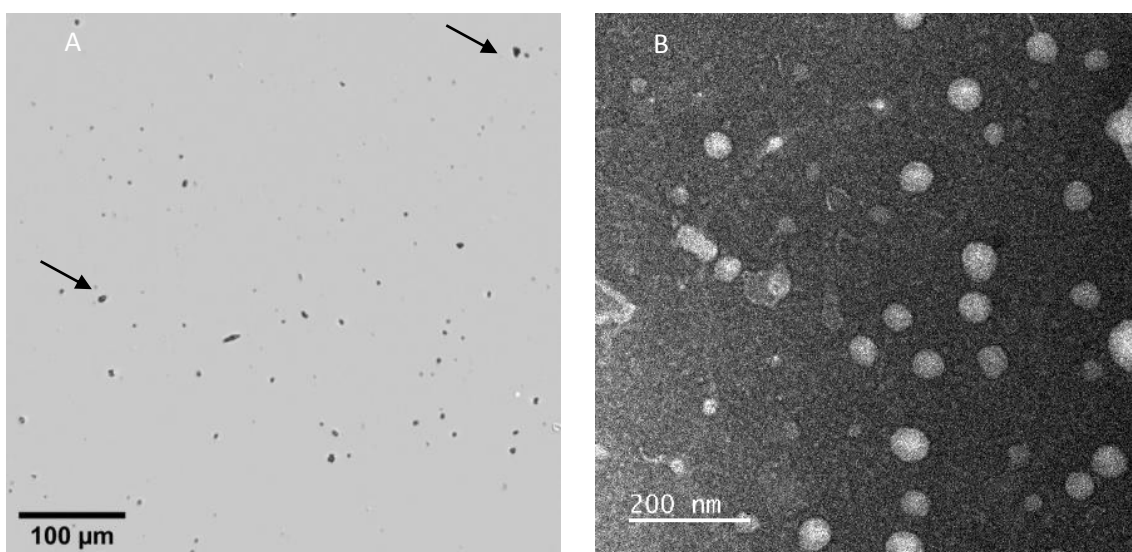


Figure 18. Images of cochleates by optical microscopy (A) and transmission electron microscopy (B). Black arrows indicate larger cochleates not detected by transmission electron microscopy (reproduced with permission from Lipa-Castro et al. 2021).

1.8.6.2 Vesicle fusion and aggregation state

1.8.6.2.1 Turbidity

Turbidity is a form of light scattering. While scattering is usually detected at an angle θ to the incident wave, turbidity it is detected by the reduction in the transmitted light at $\theta=0$. Thus, turbidity can be used to monitor the evolution of particle size or shape through changes in the light scattering properties or the optical density of vesicle suspensions (Beugin et al., 1995; Rachkauskas, 2014; Zerkoune et al., 2016). So, these techniques had been used to follow the fusion of liposomes into cochleates on the addition of divalent cations (Düzgüneş & Ohki, 1977; Portis et al., 1979; Wilschut et al., 1980). This technique, which is easy to perform with an UV spectrophotometer, is able to distinguish the fusion of vesicles and reversible agglomeration (Nir et al., 1983) and so follow the stability of cochleates.

1.8.6.2.2 Zeta potential

Zeta potential, also called electrokinetic potential, is a physical property that is exhibited by any particle in suspension. It can be defined as the electrical potential at the slipping/shear plane of a colloid particle moving under an electric field (Bhattacharjee, 2016). This technique is useful to investigate the stability of cochleates in the environment because variation of zeta potential can indicate whether the physicochemical properties of the cochleates are altered. Thus Asprea et al. (2019) and Pham et al. (2014) used zeta potential measurements to monitor the stability of cochleates over time and after lyophilisation process. In addition, on the principle that the formation of cochleates occurs after the incorporation of a positively charged agent on negatively charged liposomes, zeta potential is very useful as it can distinguish the different states of aggregation that the systems pass through before reaching the final product (cochleates). Typically, the final product will present more positive potential zeta values than the precursor system (Pham et al., 2014).

1.8.6.2.3 Fluorescence Spectroscopy

Fluorescence spectroscopy can be used to probe the state of the lipid membrane and in this way confirm the cochleate structure. In this respect, laurdan (6-dodecanoyl-*N,N*-dimethyl-2-naphthylamine) is often employed because of the sensitivity of its fluorescence properties to the surrounding environment (Parassassi et al., 1991). As shown in Figure 20, due to its localization at the interface between the polar head group and the acyl chains of phospholipids, the emission and excitation spectra of laurdan undergo a red shift, to higher

wavelengths, on the transition of the bilayer from a gel phase to a liquid crystalline phase and, furthermore, the extent of this shift, due to dipolar relaxation, is influenced by the presence of water molecules (Ramani & Balasubramanian, 2003). Thus, monitoring changes in laurdan fluorescence has been proposed as a method to detect the formation of cochleates (Miclea et al., 2007). These authors observed that the fluorescence spectrum of laurdan in liposomes prepared from brain phosphatidylserine showed a maximum of fluorescence emission at around 430 nm, a typical laurdan profile for liposomes in the gel phase. A second peak at 490 nm was also obtained when the temperature was raised. This peak at 490 nm was reduced in intensity when cations were added, and a blue shift was observed for the peak at 430 nm, suggesting dehydration between the bilayers, as would be expected when the cochleate state is obtained (Miclea et al., 2007). Thus this technique has been very useful to evaluate the impact of the inclusion of different drugs such as the blood-clotting protein factor VIII (Miclea et al., 2007) and an anti-microbial peptide (Livne et al., 2010) in the cochleate structure, and also to study different phosphatidylcholine/phosphatidylserine molar ratios and the effect of ionic strength (Ramani & Balasubramanian, 2003).

Another fluorescence-based technique, contents mixing, was used by Wilschut et al. (1980) to study vesicle fusion in the presence of calcium. In this case, two populations of liposomes were prepared, one containing a citrate chelate of terbium and the other dipicolinic acid (DPA). If the vesicles fuse and their contents mix, the resulting terbium/DPA complex is fluorescent. Using this technique, they were able to determine the threshold calcium concentration that would trigger fusion.

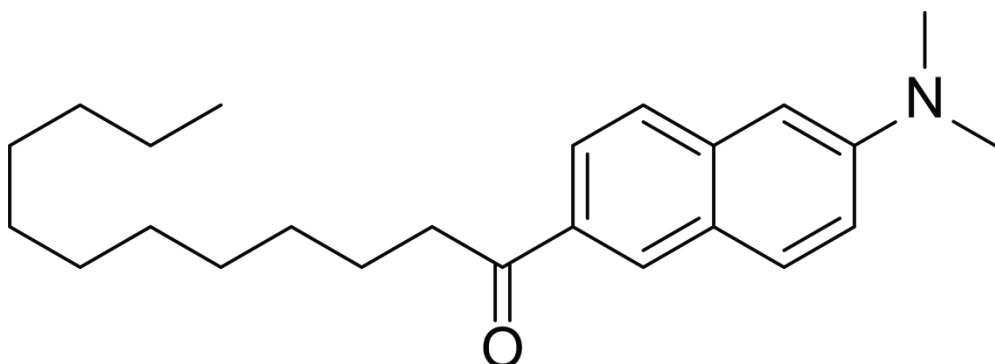


Figure 19. Structural formula of laurdan.

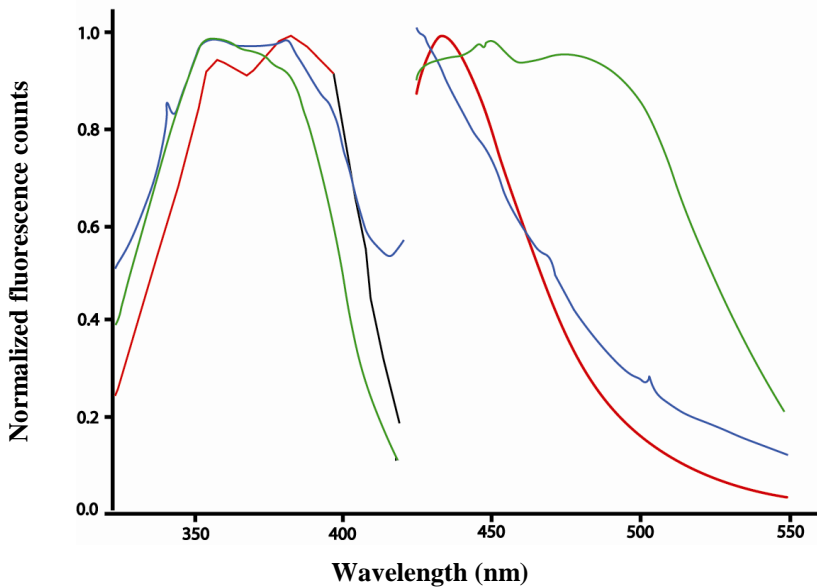


Figure 20. Normalized excitation and emission spectra of laurdan in SUV corresponding to liquid-crystalline phase (green line), cochleate phase (blue line) and gel phase (red line) (adapted with permission from Ramani & Balasubramanian, 2003).

Another fluorescence-based technique, contents mixing, was used by Wilschut et al. (1980) to study vesicle fusion in the presence of calcium. In this case, two populations of liposomes were prepared, one containing a citrate chelate of terbium and the other dipicolinic acid (DPA). If the vesicles fuse and their contents mix, the resulting terbium/DPA complex is fluorescent. Using this technique, they were able to determine the threshold calcium concentration that would trigger fusion.

1.8.6.2.4 Differential scanning calorimetry

Differential scanning calorimetric (DSC) measures heat flow in a sample when it is exposed to a gradual controlled temperature change. This technique is frequently used to characterize phospholipid-based systems because pure phospholipids demonstrate a clear phase transition from a solid to a liquid state of the acyl chains at a specific temperature, known as the transition temperature. Modifications of this temperature and the heat flow during the transition can give information about drug-lipid interaction, the state of the lipid and melting and recrystallization behaviour in the drug delivery system (Chiu & Prenner, 2011).

In this way, the formation of cochleate structures after addition of divalent cations to bovine brain PS vesicles was accompanied by an increase in the transition temperature to an

extremely high value, indicating highly ordered crystalline acyl chains, although this naturally occurring phospholipid contains a mixture of different chains (Portis et al., 1979). Silvius and Gagne (1984) studied the phase transitions of different mixtures of single molecular species of phosphatidylserine and phosphatidylcholine in the presence and absence of calcium and used the results to produce phase diagrams. Although the two phospholipids were miscible in the absence of calcium, when the divalent cation was present, some phase separation was observed, corresponding to cochleate systems containing a high proportion of PS. This allowed them to define the proportions of lipids that could be used to form cochleates. This sort of study was also applied to cochleates constructed using cationic glycopeptides as bridging agents, with or without the antibiotic erythromycin (Sarig et al., 2011). DSC can also be used to probe interactions between the cochleate system and an encapsulated drug. The absence of a melting peak characteristic of the drug when it is contained in cochleates is often observed, demonstrating the interaction of the drug with the phospholipid bilayer (Landge et al., 2013).

1.8.6.3 Internal structure

1.8.6.3.1 X-ray diffraction

X-ray diffraction gives information on a molecular scale about lipid bilayer structure. X-ray scattering/diffraction experiments are usually divided into experiments at small angles (SAXS/D) and at wide angles (WAXS/D). Both techniques are based on the same physical principles because they observe the coherent scattering from a sample as a function of the electron distribution in the sample. The distinction is that SAXS has diffraction 2θ in the range from 0.03° up to roughly 9° , while WAXS has a diffraction 2θ angle range of $9-100^\circ$. Illustration 2 shows the experimental set-up.

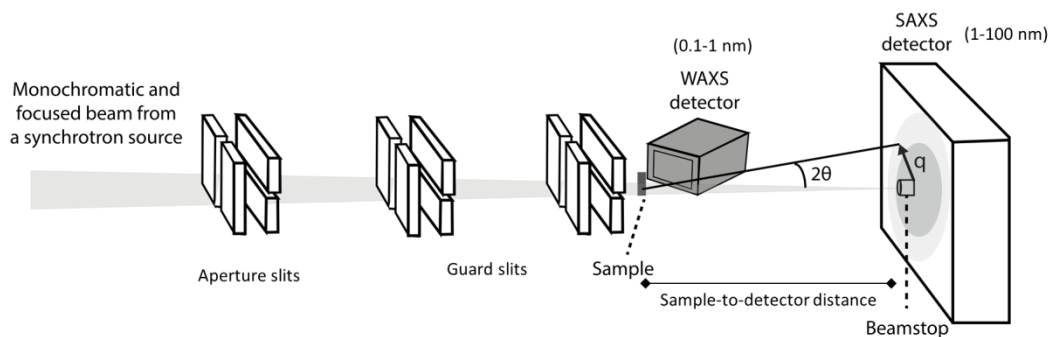


Illustration 2. Schematic diagram of SAXS and WAXS setup measurements

SAXS gives information about structures with dimensions between 10 and 1000 Å (1-100 nm) whereas WAXS normally reports distances in the range of 1-10 Å (< 1 nm) (He, 2018). Bragg's law (Equation 2) is used to relate peaks in the X-ray diffraction pattern to real repeat spacing:

$$n \lambda = 2d \sin \theta \text{ (Equation 2)}$$

where n is an integer corresponding to the order of reflection, λ is the wavelength of the X-ray being used, d is the structural repeat distance (McCarthy & Brooks, 2016).

Therefore, X-ray diffraction is a useful technique for studying the internal structure of cochleates and how this can be affected by encapsulated drug. In particular, it is possible to distinguish between the tightly packed bilayers of cochleates and the more distanced bilayers of multilamellar vesicles (MLV) (Hui et al., 1983). More precisely, SAXS can reveal the changes in correlation and ordering of phospholipid bilayers (Bozó et al., 2017) while WAXS can explore the acyl chain packing (Gao et al., 2019; Hui et al., 1983). The SAXS pattern of cochleates can be measured for scattering vector values comprised between 0.03 and 0.6 Å⁻¹ corresponding to the range of bilayer thickness and periodicity (Bozó et al., 2017) whereas WAXS patterns are measured for scattering vector values greater than 1.0 Å⁻¹ (Gao et al., 2019). SAXS studies of cochleates normally reveal a highly ordered lamellar structure with a Bragg diffraction peak repeat unit spacing of first, second and third order, multiple reflections from which the repeat distance of the cochleate bilayers can be calculated from the different order reflections; in particular the first reflection that shows the highest intensity (Bozó et al., 2017; Nagarsekar et al., 2017).

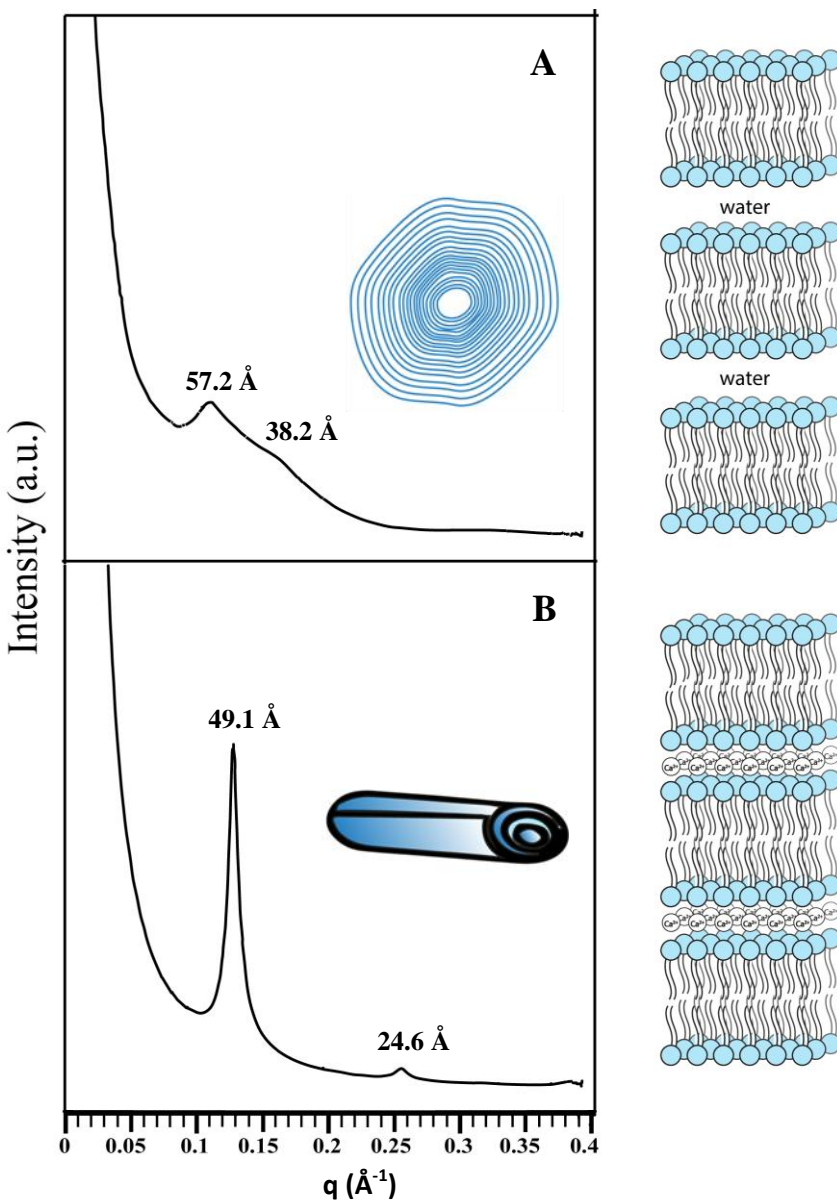


Figure 21. Small-angle X-ray scattering (SAXS) patterns of MLV (A) and cochleates (B) formed from soy phosphatidylserine. (Reproduced with permission from Lipa-Castro et al. 2021).

Thus, in Figure 21, a hydrated system in the absence of divalent cations, which would be expected to form MLVs, shows a very broad signal typical of an entirely uncorrelated multilamellar system. The addition of Ca^{2+} causes a change in the layer organization, showing sharp and equidistant Bragg reflection (Bozó et al., 2017). Hence SAXS can be employed to determine the proportion of negative lipid necessary to obtain the cochleate structure in combination with other components (Hui et al., 1983). Furthermore, X-ray diffraction may be used as an alternative approach for further characterization and to understand the

distinguishing characteristics of the intermediate structures based on the gradual reduction of the repeat distances in the process of transforming multilamellar vesicles to cochleates by addition of a bridging agent (Nagarsekar et al., 2016).

Electron density profiles from SAXS patterns can be obtained after mathematical treatment and give a very precise view of the bilayer arrangement with or without an active molecule (Nagle and Wiener, 1989). In some case, they can provide an idea of the position of the molecule in the bilayer (Chemin et al., 2009). In the case of DOPS cochleates, for example, the addition of 5 mol% of amphotericin B does not induce structural modifications and the electron density difference between amphotericin B and DOPS is too small to induce significant differences between the two electron density profiles (Figure 22, Lipa, Bourgaux, Legrand, Barratt, unpublished results).

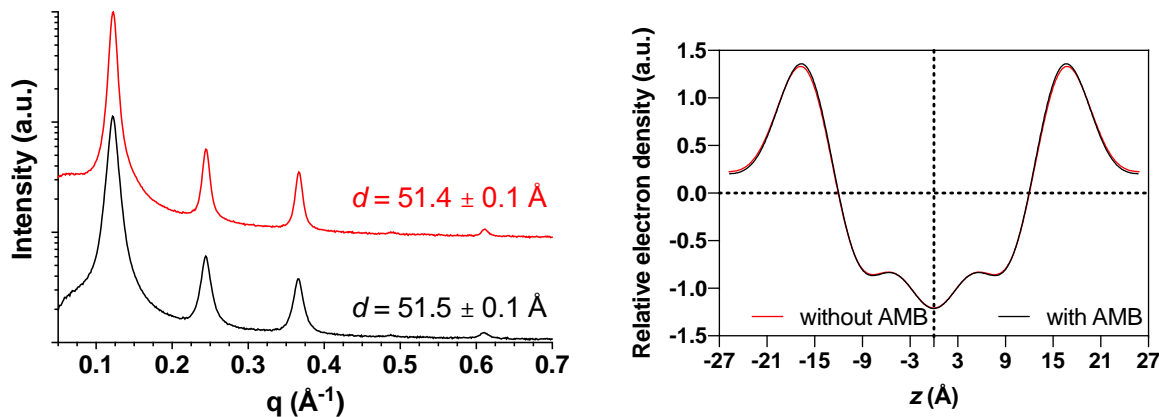


Figure 22. Electron density patterns from cochleates formed from dioleoylphosphatidylserine with and without incorporated amphotericin B. (Lipa, Bourgaux, Legrand, Barratt, unpublished results).

1.8.6.3.2 Fourier transform infrared (FT-IR) spectroscopy

The structural organization of phospholipids can also be probed by FT-IR spectroscopy. This technique can detect ion-induced perturbations at particular phospholipid sites directly without the extensive sample modifications required for other techniques. FT-IR data can also provide useful structural correlations of phase behaviour that has been deduced from experiments (such as DSC) that do not yield direct molecular structure information. In this way it is possible to identify a particular phase of phospholipid organization and to study the interaction of the bridging agent with the phospholipid headgroups (Bozó et al., 2017). In

Figure 23, the complete FT-IR spectra of dimyristoylphosphatidylserine (DMPS) showing the phospholipid molecule and their characteristic vibrational bands in the following regions: The symmetric stretching vibration of the methylene band ($\nu_s\text{CH}_2$) at 2850 to 2855 cm^{-1} , ester carbonyl stretch ($\nu_s\text{C=O}$) at 1685 to 1780 cm^{-1} , NH_3^+ antisymmetric bending ($\nu_{as}\text{NH}_3^+$) at 1620 to 1600 cm^{-1} , carboxylate antisymmetric stretching band ($\nu_{as}\text{COO}^-$) at 1640 to 1620 cm^{-1} and the asymmetric stretching vibration of the phosphate moiety ($\nu_{as}\text{PO}_2^-$) from 1250 to 1220 cm^{-1} (Manrique-Moreno et al., 2016).

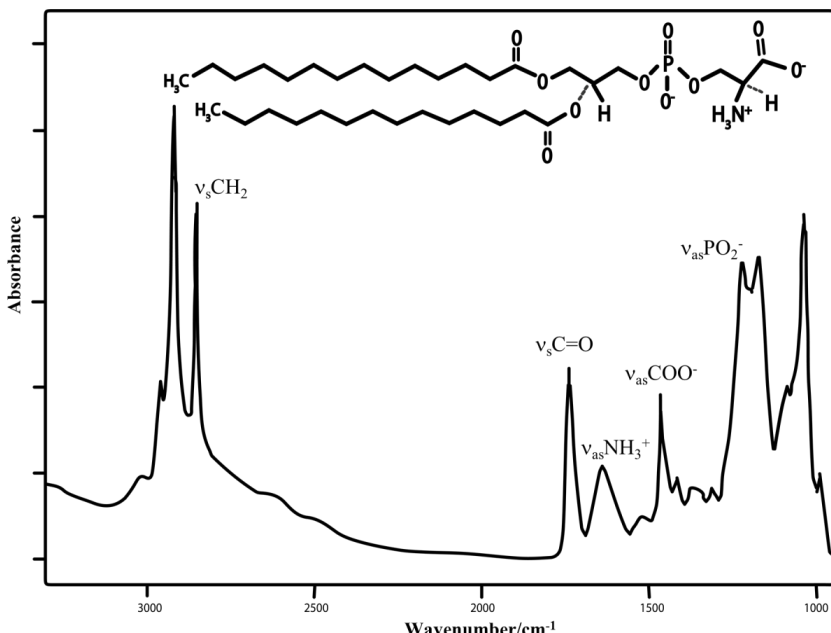


Figure 23. FT-IR attenuated total reflectance spectrum of hydrated film of DMPS (adapted from Manrique-Moreno et al., 2016).

In this respect, PS-ion interactions during cochleate formation have been reported by several groups (Flach & Mendelsohn, 1993). The information obtained from FT-IR studies of cochleate formation focuses on the stretching vibrations of three regions of phospholipid structure.

Acyl Chain Region: Flach and Mendelsohn (1993) observed an increase in frequency of about 8 cm^{-1} in the methyl symmetric bending mode near 1386 cm^{-1} , the so-called “methyl umbrella” when calcium was added to dimyristoylphosphatidylserine bilayer to form cochleates. This modification had not previously been observed in phospholipid phase changes, for example the transition from the gel to the liquid crystal phase, and can therefore be considered as an indication of the formation of tightly packed bilayers in cochleates that modifies the environment of these methyl groups. These changes in the FT-IR correlate with a

reduction in the lamellar repeat distance observed by X-ray diffraction (Flach & Mendelsohn, 1993). Shifts in both the asymmetric and symmetric methylene stretching modes of the acyl chain methylene groups at 2925 and 2854 cm⁻¹ respectively to about 3-4 cm⁻¹ lower when calcium ions were added to dioleoylphosphatidylserine (Choi et al., 1991). This lower frequency indicates an increase in the order of the chains induced by Ca²⁺ binding to the head groups. Interestingly, the addition of cholesterol to the complex causes the bands to be upshifted by 1 cm⁻¹ and the asymmetrical stretching band to become wider, indicating the influence of cholesterol on acyl chain packing. A tighter lipid packing attributed to the strong interaction of Ca²⁺ with lipid head groups was also observed by Bozó et al. (2017). These authors also noted that these changes were reversed when the cochleate structure was destroyed by the addition of EDTA or citrate anions.

Carbonyl interfacial region: The ester carbonyl groups of the phospholipid also show modifications in the FT-IR spectrum when cochleates are formed. The Infrared spectrum of DOPS displays bands corresponding to two asymmetric carbonyl stretching vibrations at 1742 and 1727 cm⁻¹ arising from these groups, as observed by Choi et al. (1991) . In a similar study from another laboratory, bands at 1736 cm⁻¹ and at 1725 cm⁻¹ were reported (Bozó et al., 2017). After addition of Ca²⁺, four bands are generated that can be attributed to carbonyl groups with different degrees of hydration. The band with the lowest wave number at 1704 cm⁻¹ has been assigned to one of the C=O groups forming hydrogen bonds molecules of water (Choi et al., 1991), and the bands are also reduced in width, probably reflecting a large reduction in motional freedom as a result of complexation of the polar headgroups by Ca²⁺ (Bozó et al., 2017). The spectrum is also modified when cholesterol is added to the system, with narrowing of the bands (Bozó et al., 2017). Differences in the spectra recorded at 24°C and 41°C were also observed.

Polar Group Region: The interaction between divalent cations and the phospholipid that leads to cochleate formation occurs at the level of the polar head group. Therefore, the FT-IR spectra in this region are extremely informative. The dehydration or hydration state of the phosphate can be identified through a characteristic increase in the asymmetric PO₂⁻ stretching frequency in the band region from 1221 to 1238 cm⁻¹ (Flach & Mendelsohn, 1993). Infrared spectra of phosphate group vibrations show a band at 1223 cm⁻¹ that can be assigned to an asymmetric PO₂⁻ stretching mode and three peaks at 1090, 1067, and 1043 cm⁻¹ related to the symmetric PO₂⁻ mode in fully hydrated DOPS. Upon Ca²⁺ binding asymmetric PO₂⁻

shows a narrower band at 1238 cm^{-1} indicating that Ca^{2+} binds, dehydrates and immobilizes the phosphate ester group. In addition, the symmetric PO_2^- mode after addition of Ca^{2+} shows four bands at 1111, 1102, 1074, and 1063 cm^{-1} that can be attributed to the torsion angles of the two P-O ester bonds (Choi et al., 1991).

Infrared spectroscopy has also been employed to probe the interactions between active molecules and lipids within the cochleate structure. Thus, Landge et al. (2013) saw changes in the FT-IR spectrum of ketoconazole when it was incorporated into cochleates, and also some changes in the peaks corresponding to DOPS.

1.8.6.3.3 Nuclear magnetic resonance

Nuclear magnetic resonance (NMR) is another technique that is able to provide information about the environment of the molecules within phospholipid assemblies and the changes that can occur when divalent cations are added. ^{31}P in the head group and ^2H (deuterium) in different parts of the molecule are the isotopes that are most often monitored. Thus, Tilcock et al. (1984) used both ^{31}P NMR and deuterium NMR with phospholipids labelled in the acyl chain. They investigated the effect of adding calcium ions to mixed systems of phosphatidylserine with phosphatidylcholine or phosphatidylethanolamine. In some cases, cholesterol was also added. When DOPS was mixed in equimolar proportions to DOPC or DOPE the ^{31}P NMR signal is modified progressively as the proportion of Ca^{2+} is increased, and the signal intensity decreases. This is interpreted as the segregation of DOPS into condensed cochleate cylinders, which was confirmed by freeze-fracture electron microscopy and small-angle X-ray diffraction. A difference was seen between DOPS and DLPS with more unsaturated acyl chains in the former that led to less condensed structures. When cholesterol was added to the DOPS/DOPE system (1:1:1 proportions) there was no phase separation but calcium converted the system to a hexagonal lattice. A DOPS/DOPC bilayer was also studied with and without cholesterol. In this case, no segregation was seen but the signal intensity again decreases with increasing calcium concentration. The results with phosphorous NMR were confirmed using DOPS with deuterium-labelled oleic acid (Tilcock et al., 1984).

Roux and Bloom (1990) studied the binding of different metal cations to bilayers of POPC and POPS in different proportions using deuterium NMR. In this work, the deuterium atoms were on the polar headgroup of the phospholipid. The quadrupolar splitting of both phospholipids was strongly affected by the presence of calcium. The modification in the

NMR spectrum of POPS was correlated with Ca^{2+} binding measured using a radioactive isotope. This binding seemed to occur in two steps. Similar results were obtained with Mg^{2+} , while monovalent cations (Na^+ , K^+) were less deeply inserted into the membrane. In a follow-up paper (Roux and Bloom 1991), pure POPS membranes were also examined. The results give fundamental information about membrane fusion, including cochleate formation.

1.8.7 Interaction with biological systems

Since cochleates have been proposed as drug delivery systems for various types of molecules, it is important to study their interactions with cells. To do this, a fluorescent lipid can be incorporated into the cochleate membrane. Gibson et al. (2004) proposed cochleates as gene delivery vehicles and to investigate their interaction with phagocytic cells (macrophages) the cochleates were prepared with a rhodamine-containing lipid. To follow the cargo within the cochleates, a gene coding for green fluorescent protein was incorporated. Uptake by the 4T1 mouse breast cancer and H36.12 mouse macrophage cell lines and primary cultures of monocyte-derived mouse macrophages was detected by fluorescence microscopy. Similarly, cochleates bridged with drug molecules were labelled with fluorescent phosphatidylserine to study their interaction with bacteria and to compare this with liposomes made from the same materials (Syed et al., 2008). Asprea et al. (2019) encapsulated fluorescein isothiocyanate into cochleates to follow their uptake by the mouse macrophage-like cell line J774a.1 by confocal microscopy. Both cochleates and liposomes were taken up rapidly, with a similar location in the cytoplasm.

1.8.8 Other studies related to cochleates

Since cochleates have been postulated as a drug delivery system for the oral route, it is also necessary to understand their fate in gastrointestinal conditions. Thus, Asprea et al. (2019) tested the stability of a natural product, andrographolide, in cochleates after incubation in synthetic gastric fluid (pH 1.8) and synthetic intestinal fluid (pH 7.0). In this study, in both media the stability of the encapsulated drug (sensitive to the gastrointestinal environment) was evaluated demonstrating that encapsulation in the cochleates significantly improves their stability, as well as showing the stability of the cochleate particles themselves with respect to maintaining their size and shape during the incubation. In addition, a drug release profile shows non-significant liberation serving to demonstrate the retention of the drug in cochleate structure. However, a similar study was performed by Pham et al. (2014) with cochleates

containing two anti-parasitic drugs: amphotericin B and miltefosine. In this proposed formulation, as well as demonstrating some alteration of the size and morphology of the nanoparticle after incubation, drug release was shown to occur preferentially in intestinal medium, driven by presence of bile salts.

1.8.9 Conclusion

Cochleates appear to be a promising drug delivery system that could improve the bioavailability of many drugs and protect them from harsh conditions. Many techniques have been used to characterize these particles and at the same time to optimize the formulation. Among these techniques, electron microscopy and X-ray diffraction are the preferred methods for exact identification and characterization. In addition, complementary studies using simpler methods for an easier or less expensive characterization such as optical microscopy, infrared spectroscopy, laurdan fluorescence, differential calorimetric scanning and others can be used. Future work on the formulation of cochleates will certainly produce alternative manufacturing technology as well as new methods for better characterization and optimization.

Acknowledgements

A. L-C. received a Ph.D. grant from FONDECYT, Peru. We thank Dr. Vincent Faivre (Institut Galien Paris-Saclay) for useful discussions.

This work did not receive any specific grant from funding agencies in the public, commercial or not-for-profit sectors for running costs.

REFERENCES

- Aigner, M., & Lass-Flörl, C. (2020). Encochleated Amphotericin B: is the oral availability of amphotericin B finally reached? *Journal of Fungi*, 6(2), 66. <https://doi.org/10.3390/jof6020066>
- Acevedo, R., Pérez, O., Zayas, C., Pérez, J. L., Callicó, A., Cedré, B., García, L., McKee, D., Mullen, A. B., & Ferro, V. A. (2012). Cochleates derived from *Vibrio cholerae* O1 proteoliposomes: the impact of structure transformation on mucosal immunisation. *PLoS ONE*, 7(10), e46461. <https://doi.org/10.1371/journal.pone.0046461>
- Agrawal, U., Sharma, R., Gupta, M., & Vyas, S. P. (2014). Is nanotechnology a boon for oral drug delivery? *Drug Discovery Today*, 19(10), 1530–1546. <https://doi.org/10.1016/j.drudis.2014.04.011>
- Asprea, M., Tatini, F., Piazzini, V., Rossi, F., Bergonzi, M. C., & Bilia, A. R. (2019). Stable, monodisperse, and highly cell-permeating nanocochleates from natural soy lecithin liposomes. *Pharmaceutics*, 11(1), 34. <https://doi.org/10.3390/pharmaceutics11010034>
- Beugin, S., Grabielle-Madelpont, C., Paternostre, M., Ollivon, M., & Lesieur, S. (1995). Phosphatidylcholine vesicle solubilization by glucosidic non-ionic surfactants: A turbidity and x-ray diffraction study. In J. Appell & G. Porte (Eds.), *Trends in Colloid and Interface Science IX* (Vol. 98, pp. 206–211). Steinkopff. <https://doi.org/10.1007/BFb0115239>
- Bhattacharjee S. (2016) DLS and zeta potential - What they are and what they are not? *Journal of Controlled Release*, 235, 337-351. doi: 10.1016/j.jconrel.2016.06.017.
- Bhosale, R. R., Ghodake, P. P., Nandkumar, A., & Ghadge, A. A. (2013). Nanocochleates: A novel carrier for drug transfer. *Journal of Scientific and Innovative Research*, 2 (5): 964-969. Available online at: www.jsirjournal.com
- Bozó, T., Wacha, A., Mihály, J., Bóta, A., & Kellermayer, M. S. Z. (2017). Dispersion and stabilization of cochleate nanoparticles. *European Journal of Pharmaceutics and Biopharmaceutics*, 117, 270–275. <https://doi.org/10.1016/j.ejpb.2017.04.030>
- Chemin, C., Péan, J.M., Bourgaux, C., Pabst, G., Wüthrich, P., Couvreur, P. & Ollivon, M. (2009). Supramolecular organization of S12363-liposomes prepared with two different remote loading processes. *Biochim Biophys Acta*. 1788(5), 926-935. doi: 10.1016/j.bbamem.2008.11.017.
- Chiu, M. H., & Prenner, E. J. (2011). Differential scanning calorimetry: An invaluable tool for a detailed thermodynamic characterization of macromolecules and their interactions. *Journal of Pharmacy and Bioallied Sciences*, 3(1), 39–59. <https://doi.org/10.4103/0975-7406.76463>
- Choi, S., Ware, W., Lauterbach, S. R., & Phillips, W. M. (1991). Infrared spectroscopic studies on the phosphatidylserine bilayer interacting with calcium ion: effect of cholesterol. *Biochemistry*, 30(35), 8563–8568. <https://doi.org/10.1021/bi00099a011>
- Düzungeş, N., & Ohki, S. (1977). Calcium-induced interaction of phospholipid vesicles and bilayer lipid membranes. *Biochimica et Biophysica Acta (BBA) - Biomembranes*, 467(3), 301–308. [https://doi.org/10.1016/0005-2736\(77\)90307-8](https://doi.org/10.1016/0005-2736(77)90307-8)

Flach, C. R., & Mendelsohn, R. (1993). A new infrared spectroscopic marker for cochleate phases in phosphatidylserine-containing model membranes. *Biophysical Journal*, 64(4), 1113–1121. [https://doi.org/10.1016/S0006-3495\(93\)81477-2](https://doi.org/10.1016/S0006-3495(93)81477-2)

Gao, C., Kewalramani, S., Valencia, D. M., Li, H., McCourt, J. M., Olvera de la Cruz, M., & Bedzyk, M. J. (2019). Electrostatic shape control of a charged molecular membrane from ribbon to scroll. *Proceedings of the National Academy of Sciences of the United States of America*, 116(44), 22030–22036. <https://doi.org/10.1073/pnas.1913632116>

Gibson, B., Duffy, A. M., Foggerite, S. G., Krause-Elsmore, S., Lu, R., Shang, G., Chen, Z.-W., Mannino, R. J., Bouchier-Hayes, D. J., & Harmey, J. H. (2004). A novel gene delivery system for mammalian cells. *Anticancer Research*, 24, 483-488.

Gould-Fogerite, S., & Mannino, R. J. (1997). Protein- or peptide-cochleate vaccines and methods of immunizing using the same. United States Patent No. US5643574A. <https://patents.google.com/patent/US5643574A/en>

Harkare, B., Kulkarni, A., Aloorkar, N., Suryawanshi, J., Wazarkar, A., & Osmani, R. (2013). Nanocochleate: a new cornucopia in oral drug delivery. *International Journal of Innovations in Pharmaceutical Sciences*, 2, 1–9.

Harris, J. R., Lewis, R. J., Baik, C., Pokrajac, L., Billington, S. J., & Palmer, M. (2011). Cholesterol microcrystals and cochleate cylinders: Attachment of pyolysin oligomers and domain 4. *Journal of Structural Biology*, 173(1), 38–45. <https://doi.org/10.1016/j.jsb.2010.07.010>

He, B. B. (2018). Two-dimensional X-ray Diffraction. John Wiley & Sons. doi:10.1002/9781119356080

Hui, S. W., Boni, L. T., Stewart, T. P., & Isac, T. (1983). Identification of phosphatidylserine and phosphatidylcholine in calcium-induced phase separated domains. *Biochemistry*, 22(14), 3511–3516. <https://doi.org/10.1021/bi00283a032>

Jin, T., Mannino, R., & Zarif, L. (2001). Novel hydrogel isolated cochleate formulations, process of preparation and their use for the delivery of biologically relevant molecules. US Patent US6153217A <https://patents.google.com/patent/US6153217A/en>.

Kalepu, S., Manthina, M., & Padavala, V. (2013). Oral lipid-based drug delivery systems – an overview. *Acta Pharmaceutica Sinica B*, 3(6), 361–372. <https://doi.org/10.1016/j.apsb.2013.10.001>

Kay, J. G., & Grinstein, S. (2011). Sensing phosphatidylserine in cellular membranes. *Sensors* (Basel, Switzerland), 11(2), 1744–1755. <https://doi.org/10.3390/s110201744>

Koomer, A. (2009). Formulation of NPDDS for gene delivery. In "Drug Delivery Nanoparticles Formulation and Characterization" (ed. Pathak, Y. & Thassu, D.) CRC Press, pp 51-56.

Landge, A., Pawar, A., Shaikh K. (2013). Investigation of cochleates as carriers for topical drug delivery. *International Journal of Pharmacy and Pharmaceutical Sciences*, 5(2), 314-320.

Li, C., Wang, J., Wang, Y., Gao, H., Wei, G., Huang, Y., Yu, H., Gan, Y., Wang, Y., Mei, L., Chen, H., Hu, H., Zhang, Z., & Jin, Y. (2019). Recent progress in drug delivery. *Acta Pharmaceutica Sinica B*, 9(6), 1145–1162. <https://doi.org/10.1016/j.apsb.2019.08.003>

Li, J., Wang, X., Zhang, T., Wang, C., Huang, Z., Luo, X., & Deng, Y. (2015). A review on phospholipids and their main applications in drug delivery systems. *Asian Journal of Pharmaceutical Sciences*, 10(2), 81–98. <https://doi.org/10.1016/j.japs.2014.09.004>

Lipa-Castro, A., Nicolas, V., Angelova, A., Mekhloufi, G., Prost, B., Chéron, M., Faivre, V., & Barratt, G. (2021). Cochleate formulations of Amphotericin b designed for oral administration using a naturally occurring phospholipid. *International Journal of Pharmaceutics*, 603, 120688. <https://doi.org/10.1016/j.ijpharm.2021.120688>

Liu, M., Zhong, X., & Yang, Z. (2017). Chitosan functionalized nanocoachleates for enhanced oral absorption of cyclosporine A. *Scientific Reports*, 7(1), 1–10. <https://doi.org/10.1038/srep41322>

Livne, L., Epand, R. F., Papahadjopoulos-Sternberg, B., Epand, R. M., & Mor, A. (2010). OAK-based coachleates as a novel approach to overcome multidrug resistance in bacteria. *The FASEB Journal*, 24(12), 5092–5101. <https://doi.org/10.1096/fj.10-167809>

Mannino, R. J. (2016). Lipid-crystal nanoparticles: formulation and delivery of oligonucleotides. https://d1io3yog0oux5.cloudfront.net/_e3f59a1dab64bfddcc4617df443c6e61/matinasbiopharma/db/284/2351/pdf/CHI+Oligonucleotide+Poster+04052016.pdf Accessed 27 May 2021.

Mannino, R. J., Gould-Fogerite, S., Krause-Elsmore, S. L., Delmarre, D., & Lu, R. (2005). Novel encochleation methods, coachleates and methods of use. <https://patents.google.com/patent/WO2004091578A8/en>.

Manrique-Moreno, M., Heinbockel, L., Suwalsky, M., Garidel, P., & Brandenburg, K. (2016). Biophysical study of the non-steroidal anti-inflammatory drugs (NSAID) ibuprofen, naproxen and diclofenac with phosphatidylserine bilayer membranes. *Biochimica et Biophysica Acta (BBA) - Biomembranes*, 1858(9), 2123–2131. <https://doi.org/10.1016/j.bbamem.2016.06.009>

McCarthy, N. L. C., & Brooks, N. J. (2016). Using high pressure to modulate lateral structuring in model lipid membranes. In A. Iglić, C. V. Kulkarni, & M. Rappolt (Eds.), *Advances in Biomembranes and Lipid Self-Assembly* (Vol. 24, pp. 75–89). Academic Press. <https://doi.org/10.1016/bs.abl.2016.04.004>

Miclea, R. D., Varma, P. R., Peng, A., & Balu-Iyer, S. V. (2007). Development and characterization of lipidic coachleate containing recombinant factor VIII. *Biochimica et Biophysica Acta*, 1768(11), 2890–2898. <https://doi.org/10.1016/j.bbamem.2007.08.001>

Mourdikoudis, S., Pallares, R. M., & Thanh, N. T. K. (2018). Characterization techniques for nanoparticles: Comparison and complementarity upon studying nanoparticle properties. *Nanoscale*, 10(27), 12871–12934. <https://doi.org/10.1039/C8NR02278J>

Nagarsekar, K., Ashtikar, M., Steiniger, F., Thamm, J., Schacher, F., & Fahr, A. (2016). Understanding coachleate formation: Insights into structural development. *Soft Matter*, 12(16), 3797–3809. <https://doi.org/10.1039/C5SM01469G>

Nagarsekar, K., Ashtikar, M., Steiniger, F., Thamm, J., Schacher, F. H., & Fahr, A. (2017). Micro-spherical cochleate composites: Method development for monodispersed cochleate system. *Journal of Liposome Research*, 27(1), 32–40. <https://doi.org/10.3109/08982104.2016.1149865>

Nagle, J. F., & Wiener, M. C. (1989). Relations for lipid bilayers. Connection of electron density profiles to other structural quantities. *Biophysical Journal*, 55(2), 309–313. [https://doi.org/10.1016/S0006-3495\(89\)82806-1](https://doi.org/10.1016/S0006-3495(89)82806-1)

Nir, S., Bentz, J., Wilschut, J., & Duzgunes, N. (1983). Aggregation and fusion of phospholipid vesicles. *Progress in Surface Science*, 13(1), 1–124. [https://doi.org/10.1016/0079-6816\(83\)90010-2](https://doi.org/10.1016/0079-6816(83)90010-2)

Papahadjopoulos, D., Vail, W.J., Jacobson, K. & Poste, G. (1975) Cochleate lipid cylinders: formation by fusion of unilamellar lipid vesicles. *Biochim Biophys Acta*. 394(3):483-491. doi: 10.1016/0005-2736(75)90299-0.

Papahadjopoulos-Sternberg, B. (2012). Secondary structure formation by bilayer-active peptides studied by freeze-fracture electron microscopy:from disc micelles to cochleate cylinder. *Biophysical Journal*, 102(3, Supplement 1), 290a. <https://doi.org/10.1016/j.bpj.2011.11.1603>

Parassassi, T., De Stasio, G., Ravagnan, G., Rusch, R. M., & Gratton, E. (1991). Quantitation of lipid phases in phospholipid vesicles by the generalized polarization of Laurdan fluorescence. *Biophysical Journal*, 60(1), 179–189. doi: 10.1016/S0006-3495(91)82041-0

Patra, J. K., Das, G., Fraceto, L. F., Campos, E. V. R., Rodriguez-Torres, M. del P., Acosta-Torres, L. S., Diaz-Torres, L. A., Grillo, R., Swamy, M. K., Sharma, S., Habtemariam, S., & Shin, H.-S. (2018). Nano based drug delivery systems: Recent developments and future prospects. *Journal of Nanobiotechnology*, 16(1), 71. <https://doi.org/10.1186/s12951-018-0392-8>

Pawar, A., Bothiraja, C., Shaikh, K., & Mali, A. (2015). An insight into cochleates, a potential drug delivery system. *RSC Advances*, 5(99), 81188–81202. <https://doi.org/10.1039/C5RA08550K>

Pham, T. T. H., Barratt, G., Michel, J. P., Loiseau, P. M., & Saint-Pierre-Chazalet, M. (2013). Interactions of antileishmanial drugs with monolayers of lipids used in the development of amphotericin B–miltefosine-loaded nanocochelates. *Colloids and Surfaces B: Biointerfaces*, 106, 224–233. <https://doi.org/10.1016/j.colsurfb.2013.01.041>

Pham, T. T. H., Gueutin, C., Cheron, M., Abreu, S., Chaminade, P., Loiseau, P. M., & Barratt, G. (2014). Development of antileishmanial lipid nanocomplexes. *Biochimie*, 107, 143–153. <https://doi.org/10.1016/j.biochi.2014.06.007>

Portis, A., Newton, C., Pangborn, W., & Papahadjopoulos, D. (1979). Studies on the mechanism of membrane fusion: Evidence for an intermembrane calcium(²⁺) ion-phospholipid complex, synergism with magnesium(²⁺) ion, and inhibition by spectrin. *Biochemistry*, 18(5), 780–790. <https://doi.org/10.1021/bi00572a007>

Rachkauskas, R. (2014). Structural and functional effects of non-steroidal anti-inflammatory drugs rofecoxib and valdecoxib on DSPC model membranes. M.Sc. thesis, Middle East Technical University. <https://open.metu.edu.tr/bitstream/handle/11511/23844/index.pdf>

Ramani, K., & Balasubramanian, S. V. (2003). Fluorescence properties of Laurdan in cochleate phases. *Biochimica et Biophysica Acta (BBA) - Biomembranes*, 1618(1), 67–78. <https://doi.org/10.1016/j.bbamem.2003.10.009>

Ramasamy, T., Kandasamy, U., Hinabindhu, R., & Kona, K. (2009). Nanocochleate – a new drug delivery system. *FABAD J. Pharm. Sci.*, 34, 91–101

Rao, R., Squillante, E., & Kim, K. H. (2007). Lipid-based cochleates: A promising formulation platform for oral and parenteral delivery of therapeutic agents. *Critical Reviews in Therapeutic Drug Carrier Systems*, 24(1), 41–61. <https://doi.org/10.1615/critrevtherdrugcarriersyst.v24.i1.20>

Rongen, R. (2016). Delivery platform - encochleated drug formulations: enhancing efficacy, minimizing toxicity. *Drug Development & Delivery*, 16 (6), p8.

Roux, M. & Bloom, M. (1990). Ca^{2+} , Mg^{2+} , Li^+ , Na^+ , and K^+ distributions in the headgroup region of binary membranes of phosphatidylcholine and phosphatidylserine as seen by deuterium NMR. *Biochemistry* 29, 7077-7089. doi: 10.1021/bi00482a019.

Roux, M. & Bloom, M. (1991) Calcium binding by phosphatidylserine headgroups. Deuterium NMR study. *Biophys J.*, 60(1), 38-44. doi: 10.1016/S0006-3495(91)82028-8.

Sankar, R., & Reddy Y, D. (2010). Nanocochleate—A new approach in lipid drug delivery. *International Journal of Pharmacy and Pharmaceutical Sciences*, 2, 220–223.

Santangelo, R., Paderu, P., Delmas, G., Chen, Z.-W., Mannino, R., Zarif, L., & Perlin, D. S. (2000). Efficacy of oral cochleate-amphotericin B in a mouse model of systemic candidiasis. *Antimicrobial Agents and Chemotherapy*, 44(9), 2356–2360. <https://doi.org/10.1128/AAC.44.9.2356-2360>.

Sarig, H., Ohana, D., Epand, R. F., Mor, A., & Epand, R. M. (2011). Functional studies of cochleate assemblies of an oligo-acyl-lysyl with lipid mixtures for combating bacterial multidrug resistance. *The FASEB Journal*, 25(10), 3336–3343. <https://doi.org/10.1096/fj.11-183764>

Sharma, M., Sharma, R., & Jain, D. K. (2016). Nanotechnology based approaches for enhancing oral bioavailability of poorly water soluble antihypertensive drugs. *Scientifica*, 2016, 8525679. <https://doi.org/10.1155/2016/8525679>

Silvius, J. R., & Gagne, J. (1984). Calcium-induced fusion and lateral phase separations in phosphatidylcholine-phosphatidylserine vesicles. Correlation by calorimetric and fusion measurements. *Biochemistry*, 23(14), 3241–3247. <https://doi.org/10.1021/bi00309a019>

Syed, U. M., Woo, A. F., Plakogiannis, F., Jin, T., & Zhu, H. (2008). Cochleates bridged by drug molecules. *International Journal of Pharmaceutics*, 363(1–2), 118–125. <https://doi.org/10.1016/j.ijpharm.2008.06.026>

Tilcock, C.P., Bally, M.B., Farren, S.B., Cullis, P.R. & Gruner, S.M. (1984) Cation-dependent segregation phenomena and phase behavior in model membrane systems containing phosphatidylserine: influence of cholesterol and acyl chain composition. *Biochemistry*, 23(12), 2696-2703. doi: 10.1021/bi00307a025.

Vijeta, P., Vivek, M., Panwar, A.S., Darwhekar, G.N. & Jain, D.K. (2011). Nanocochleate as drug delivery vehicle. *International Journal of Pharmacy and Biological Sciences*, 1(1), 31-38.

Wang, N., Wang, T., Zhang, M., Chen, R., & Deng, Y. (2014). Using procedure of emulsification-lyophilization to form lipid A-incorporating cochleates as an effective oral mucosal vaccine adjuvant-delivery system (VADS). *International Journal of Pharmaceutics*, 468(1), 39–49. <https://doi.org/10.1016/j.ijpharm.2014.04.002>

Wilschut, J., Duzgunes, N., Fraley, R., & Papahadjopoulos, D. (1980). Studies on the mechanism of membrane fusion: Kinetics of calcium ion induced fusion of phosphatidylserine vesicles followed by a new assay for mixing of aqueous vesicle contents. *Biochemistry*, 19(26), 6011–6021. <https://doi.org/10.1021/bi00567a011>

Yadav, A., & Chaudhary, S. (2016). Formulation development and characterization of nanocochleates for the improvement of permeability of drug. *Journal of Advanced Pharmacy Education and Research* 6(3), 14-21. Available on-line at www.japer.in

Zarif, L., Graybill, J. R., Perlin, D., Najvar, L., Bocanegra, R., & Mannino, R. J. (2000). Antifungal activity of amphotericin B cochleates against *Candida albicans* infection in a mouse model. *Antimicrobial Agents and Chemotherapy*, 44(6), 1463–1469. <https://doi.org/10.1128/AAC.44.6.1463-1469.2000>

Zarif, Leila, Graybill, J. R., Perlin, D., & Mannino, R. J. (2000). Cochleates: New Lipid-Based Drug Delivery System. *Journal of Liposome Research*, 10(4), 523–538. <https://doi.org/10.3109/08982100009031116>

Zarif, L. (2002). Elongated supramolecular assemblies in drug delivery. *Journal of Controlled Release*, 81(1–2), 7–23. [https://doi.org/10.1016/s0168-3659\(02\)00010-x](https://doi.org/10.1016/s0168-3659(02)00010-x)

Zarif, L. (2005). Drug delivery by lipid cochleates. In *Methods in Enzymology* (Vol. 391, pp. 314–329). Academic Press. [https://doi.org/10.1016/S0076-6879\(05\)91018-5](https://doi.org/10.1016/S0076-6879(05)91018-5)

Zarif, L., Jin, T., Segarra, I., & Mannino, R. J. (2003). Hydrogel-isolated cochleate formulations, process of preparation and their use for the delivery of biologically relevant molecules (United States Patent No. US6592894B1). <https://patents.google.com/patent/US6592894B1/en>

Zarif, L. & Mannino, R. J. (2002). Cochleates. In N. A. Habib (Ed.), *Cancer Gene Therapy: Past Achievements and Future Challenges* (pp. 83–93). Springer US. <https://doi.org/10.1007/0-306-46817-49>.

Zerkoune, L., Lesieur, S., Putaux, J.-L., Choisnard, L., Gèze, A., Wouessidjewe, D., Angelov, B., Vebert-Nardin, C., Doutch, J., & Angelova, A. (2016). Mesoporous self-assembled nanoparticles of biotransesterified cyclodextrins and nonlamellar lipids as carriers of water-insoluble substances. *Soft Matter*, 12(36), 7539–7550. <https://doi.org/10.1039/C6SM00661B>

2. TRAVAUX EXPERIMENTAUX

Objectif du travail

L'administration orale de l'AmB pour le traitement de la leishmaniose est attractive pour plusieurs raisons : le ciblage de la molécule vers les organes d'intérêt, surtout vers le foie par la veine porte, augmentant l'efficacité, l'utilisation de concentrations moins importantes en AmB notamment au niveau des organes sensibles conduisant à une réduction de la toxicité et la facilité de l'administration orale par rapport à l'administration parentérale conventionnelle, surtout dans des pays en voie de développement.

Dans ce travail, nous étudions les systèmes à base de cochléates pour l'administration orale de l'AmB pour le traitement de la leishmaniose. Aussi, dans le but de proposer un système efficace, faisable et accessible pour les pays en voie de développement, des particules composées de phospholipides d'origine naturelle ont été développées. Les études expérimentales seront décrites en trois chapitres.

- I. Préparation et étude de l'efficacité des cochléates contenant l'AmB à base de phospholipides synthétiques
- II. Etude de formulation et de caractérisation des cochléates contenant l'AmB à base de phospholipides d'origine naturelle (article en révision pour International Journal of Pharmaceutics)
- III. Etude de la pharmacocinétique, de la biodistribution et de l'efficacité *in vivo* contre la leishmaniose des cochléates contenant l'AmB à base de phospholipides d'origine naturelle

2.1 Chapitre 1 : AmB-cochléates à base de lipides d'origine synthétique

Antonio LIPA CASTRO¹; Sébastien POMEL²; Philippe LOISEAU²; Gillian BARRATT¹

¹ Institut Galien Paris-Saclay, UMR CNRS 8612, Faculty of Pharmacy,

Univ. Paris-Saclay, 92296 Chatenay-Malabry Cedex, France

² BioCIS, UMR CNRS 8076, Faculty of Pharmacy,

Univ. Paris-Saclay, 92296 Chatenay-Malabry Cedex, France

Dans les travaux antérieurs, nous avons décrit les cochléates en termes de leur structure, leur composition et leurs avantages en tant que système de délivrance des principes actifs et nous avons résumé les différentes méthodes de préparation et de caractérisation. Dans ce chapitre nous décrivons la préparation des cochléates à base d'un phospholipide d'origine synthétique (DOPS) contenant l'AmB (AmB-cochléate) et leur évaluation *in vivo* dans un modèle de leishmaniose viscérale chez la souris.

La formulation d'AmB-cochléates a été préparée selon une formulation préalablement optimisée dans notre laboratoire dont la composition est la suivante : DOPS/Cholestérol/AmB/Vitamine E (9:1:0,5:0,06 en proportions molaires) (Pham et al., 2013). Nous avons conservé la même méthode de préparation : la méthode hydrogel. Les cochléates ont été caractérisés en termes de taille, de morphologie et de rendement d'encapsulation de l'AmB par diffusion dynamique de la lumière (DLS), par microscopies électronique et optique et par HPLC respectivement. En plus l'interaction avec les cellules intestinales a été réalisée dans le modèle cellulaire Caco-2.

2.1.1 Matériaux

La DOPS a été fourni gracieusement par Lipoid (Germany). L'AmB et le taurocholate de sodium ont été obtenus chez Alfa Aesar. Le cholestérol, la vitamine E, le dextran (500 000 Da), le polyéthylène glycol (PEG 8000), l'acide éthylènediaminetraacétique (EDTA), le chlorure de calcium, le glucose, le chlorure de sodium, le chlorure de potassium, le sulfate de magnésium, le trisaminométhane-base, l'hydroxyde de sodium, le phosphate dibasique de sodium, le bicarbonate de sodium, le phosphate monobasique de potassium et le phosphate monobasique de sodium ont été achetés chez Sigma-Aldrich. Le méthanol, le chloroforme, l'acétonitrile, le tétrahydrofurane et les autres solvants ont été achetés chez Merck. L'eau utilisée a été purifiée par osmose inverse (Milli-Q Millipore). Le milieu Eagle modifié de Dulbecco, la solution saline de phosphate (PBS), le sérum de veau fœtal (FBS), la solution d'acides aminés non essentiels (NEAA 10 mM, 100x), la solution de pénicilline-streptomycine (10000 unités/mL de pénicilline et 10 mg/mL de streptomycine), la solution de trypsine-EDTA (0,05% de trypsine, 0,53 mM d'EDTA), le méthylthiazoltétrazolium (MTT) et le diméthylsulfoxyde ont été achetés chez Sigma-Aldrich. Les membranes de polyester Corning Transwell® de 12 mm, avec une porosité de 0,4 µm ont été obtenues chez Costar Corning Corporation (NY).

2.1.2 Méthodologie

2.1.2.1 Préparation d'AmB-cochlées

Les cochlées contenant l'AmB ont été préparés par la méthode d'hydrogel (Leila Zarif et al., 2000). Tout d'abord, des liposomes unilamellaires ont été préparés.

2.1.2.2 Préparations d'AmB-liposomes unilamellaires

Les liposomes ont été formés par la technique d'hydratation du film lipidique, (Figure 24). Un mélange de lipides, préalablement optimisé dans notre laboratoire, constitué de DOPS, de cholestérol, d'AmB et de vitamine E dans des proportions molaires 9:1:0.5:0.06 a été utilisé pour leur préparation (Pham et al., 2013).

Des volumes appropriés de solutions contenant 39 µmoles de DOPS, 4,3 µmoles de cholestérol et 0,26 µmoles de vitamine E dissous dans un mélange chloroforme/méthanol (60/40) et un volume contenant 2,16 µmoles d'AmB dissous dans le méthanol alcalin (2,5 mMol NaOH) ont été mélangés et évaporés sous vide à l'aide d'un rotavapeur (Buchi R-210 Rotavapor) à 54°C afin de permettre le dépôt des différents constituants sous forme d'un film

mince sur la paroi du ballon. Ensuite le film est hydraté avec 35 mL de Tris 0,01M à pH 7,4 et est maintenu pendant 1 heure sous agitation. Après évaporation sous vide à 54 °C afin de réduire le volume à 7 mL de tampon, une suspension de liposomes multilamellaires (MLV) dont la concentration lipidique est de 5,6 mM est obtenue.

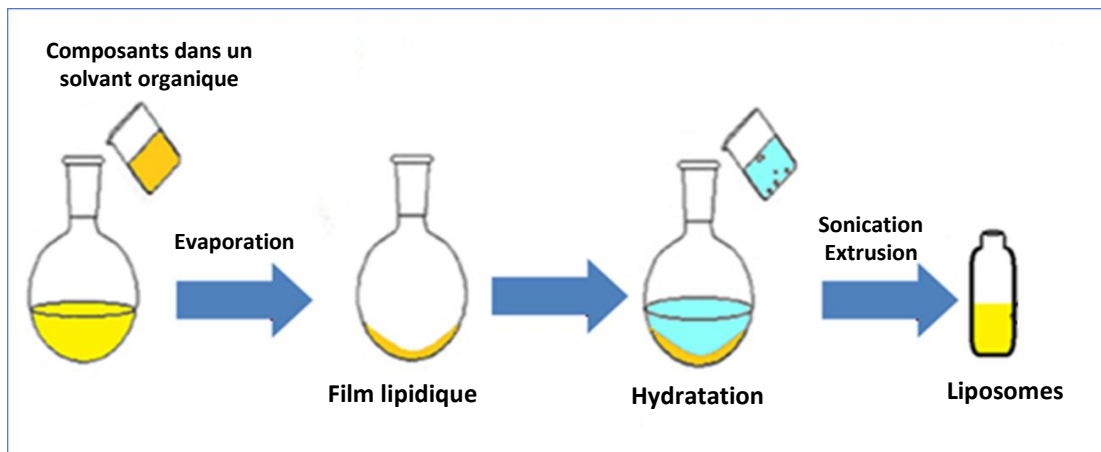


Figure 24. Technique de film lipidique

La taille des liposomes a été réduite à l'aide d'une sonde à ultrasons (Bioblock Scientific vibracell 72441 ultrasons). La suspension de MLV a été soumise à 7 cycles d'une minute d'ultrasons séparés par des intervalles d'une minute de pause. Afin d'éviter la dégradation des lipides par réchauffement, la procédure a été réalisé dans la glace. Ensuite une centrifugation a été réalisée pendant 30 min avec une centrifugeuse Awel MF 20-R (3000g) pour éliminer toute trace de titane. Enfin, une procédure d'extrusion successive sur des membranes de polycarbonate avec des pores de 200 nm (1 passage) et de 100 nm (3 passages) (Whatman® Nuclepore) a été réalisée pour obtenir une suspension de liposomes unilamellaires d'un diamètre autour de 100 nm.

2.1.2.3 Conversion des liposomes en AmB-cochleates

Cette procédure est illustrée dans la Figure 25. 5 mL de la suspension de liposomes ont été mélangés avec 10 mL d'une solution de dextran 40% (m/m). Ensuite le mélange a été ajouté dans 20 mL d'une solution de polyéthylène glycol 15% (m/v) sous agitation magnétique à 1 000 tour/min jusqu'à homogénéisation de la suspension. Ensuite 35 mL d'une solution de 0,1M CaCl₂ ont été ajoutés lentement et le tout est laissé sous agitation pendant 15 minutes. Finalement, une solution de 1 mM CaCl₂/150 mM NaCl (solution de stockage) a été ajoutée pour compléter le volume à 200 mL puis la suspension est laissée sous agitation pendant 10

minutes. Le précipité de cochléates a été récupéré par centrifugation et filtration. Pour cela, la suspension a été répartie entre 4 tubes de centrifugation et est centrifugée pendant 30 minutes à 22°C à l'aide d'une centrifugeuse Awel MF 20-R (3000g). Le précipité a été rincé 3 fois avec 10 mL de la solution de stockage et est centrifugé à nouveau. En parallèle tous les surnageants ont été filtrés et rincés avec 10 mL de la solution de stockage pour récupérer les cochléates non précipités par la centrifugation. Les cochléates récupérés lors de la centrifugation et de la filtration ont été réunis puis dispersés dans 5 mL de la solution de stockage. Enfin la suspension a été lyophilisée pendant 24 heures (Freeze dryer CRYOTEC Cosmo 20K-80) pour obtenir des cochléates sous forme de poudre qui sont conservés à -25°C dans un récipient teinté. Les cochléates sans AmB ont été préparés de la même façon.

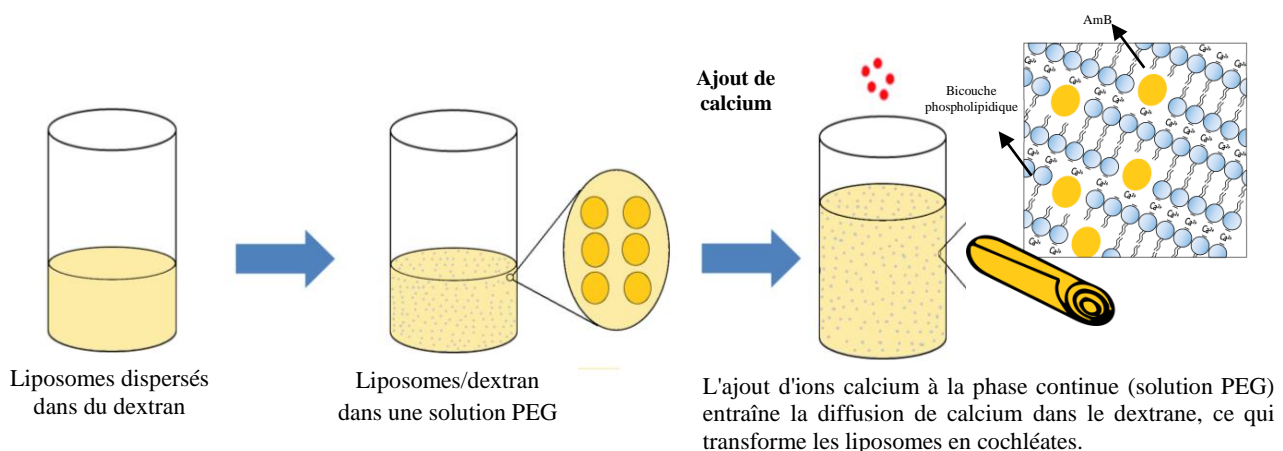


Figure 25. Schéma de la méthode hydrogel

2.1.2.4 Caractérisation d'AmB-cochléates

Les cochléates ont été caractérisés en termes de leur morphologie, leur taille et de leur rendement d'encapsulation en AmB par microscopie, DLS et HPLC respectivement.

2.1.2.4.1 Microscopie électronique

La microscopie électronique en transmission (JEOL JEM-1400 opérant à 120 kV) a été réalisée sur les nanoparticules sur la plateforme de l'I2BC (Gif-sur-Yvette, France). Des suspensions de cochléates ont été préparées en les dispersant dans la solution de stockage à une concentration de 0,1g cochléates/mL. Les suspensions ont été déposées sur des grilles de cuivre. L'excès de liquide a été enlevé avec du papier filtre. Ensuite une coloration négative avec une solution à 1% de phosphotungstate de sodium a été réalisée pendant 1 min, l'excès de solution a été enlevé avec du papier filtre. Les grilles ont été séchées à l'air avant

l'observation par TEM. Les images ont été acquises à l'aide d'une caméra haute résolution (Orius SC1000).

2.1.2.4.2 Granulomorphométrie

Une analyse par microscopie optique a été réalisée afin d'identifier d'éventuelles agglomérations ou particules au-dessus de l'échelle nanométrique. Un flux de cochléates, préalablement mis en suspension à 0,8 mg/mL dans une solution à 2 mM de CaCl₂, a été observé à travers d'une cellule optique de 50 µm d'épaisseur dans un granulomorphomètre Flow-Cell 200 S-M (Occhio, Belgique) et des images numériques ont été enregistrées par une caméra haute résolution avec une résolution spatiale de 0,185 µm (facteur de zoom 9). Les images ont été analysées avec le logiciel Callisto (Occhio, Belgique).

2.1.2.4.3 Analyse de Taille

L'analyse de taille a été réalisée par diffusion dynamique de la lumière (DLS) à l'aide d'un Zetasizer Nano ZS90 instrument (Malvern, France). Avant l'analyse, les échantillons de cochléates ont été suspendus à 0,1 mg/mL dans la solution de stockage. Les mesures ont été effectuées en triplicat à 25 °C avec un angle de détection de 90°.

2.1.2.4.4 Evaluation du rendement d'encapsulation de l'AmB

L'AmB, qui n'était pas incluse dans les cochléates, se retrouve déposée sur les membranes d'extrusion, la molécule étant très peu soluble dans les milieux aqueux. Ainsi, un dosage de la molécule dans les cochléates finaux permet d'évaluer l'efficacité d'encapsulation. La quantification de l'AmB contenue dans les cochléates a été effectuée avec la technique de chromatographie en phase liquide de haute performance (HPLC). L'analyse a été réalisée sur un système HPLC équipé d'une pompe quaternaire 600, un détecteur à barrette de diodes (2996 Photodiode Array Detector, Waters) et un injecteur automatique (717 Autosampler, Waters). La colonne utilisée est une colonne une Symmetry® C₁₈ de 150mm x 4,6 cm en dimensions avec une taille de particules de 5 µm (Waters). La phase mobile était un mélange d'une solution de 0,5% de triéthylamine (ajustée à pH 5,2 avec de l'acide formique), d'acetonitrile et du tétrahydrofurane (1000/385/154 v/v). Le débit était de 1 mL/min et le volume d'injection de 100 µL. L'AmB a été quantifiée par son absorbance à une longueur d'onde de 408 nm. Une courbe d'étalonnage a été préparée à partir d'une série de dilutions d'un étalon de référence AmB dans MeOH / H₂O (1/1) dans une gamme entre 0,1 et 5 µg/mL. Le coefficient de corrélation (R^2) était de 0,9992 et la limite de quantification était de 0,1 µg/mL. Les lyophilisats de cochléates ont été préalablement traités avec de l'EDTA à 0,05 M

et ensuite dissous avec 3 volumes de MeOH pour extraire l'AmB puis dilués avec un mélange MeOH/H₂O (1/1). Enfin, les échantillons ont été centrifugés avec une mini-centrifugeuse VWR Galaxy C1413 8 (2000 g) pour éliminer les éventuelles traces de précipités. L'efficacité d'encapsulation (EE%) pour chaque préparation a été calculée à l'aide de l'équation suivante :

$$EE\% = (W_t/W_i) \times 100\%$$

où W_t est la quantité totale d'AmB mesurée dans les cochléates lyophilisés et W_i est la quantité totale d'AmB ajoutée au début de la préparation.

2.1.2.5 Culture cellulaire

Les cellules Caco2 (passages 3-20) ont été cultivées dans du DMEM supplémenté avec 20% de FBS, 1% d'acides aminés non essentiels, 1% de L-glutamine, 1% de mélange pénicilline-streptomycine et maintenues à 37°C dans 5% de CO₂ et 95% d'humidité. Les cellules ont été lavées avec du PBS et décollées à l'aide de trypsine-EDTA. Les cellules ont été ensemencées à une densité de 15x10³ cellules/puits dans des plaques à 96 puits pour les études de cytotoxicité et à une densité de 50x10³ cellules/puits lors des études à l'aide d'insert Corning Transwell® (12 mm, 0,4 µm), puis maintenues à 37°C dans 5% de CO₂ et 95% d'humidité afin de permettre le développement en monocouche et, dans le cas des études de transport, permettre une différenciation qui nécessite une période d'au moins 21 jours.

2.1.2.5.1 Études de viabilité : test MTT

La viabilité cellulaire a été étudiée avec la méthode colorimétrique MTT (Menez et al., 2006). Les cellules Caco2 cultivées dans une plaque de culture à 96 puits ont été exposées apicalement à des concentrations croissantes d'AmB-cochleate (0,1 µg/mL, 1 µg/mL, 10 µg/mL et 100 µg/mL d'AmB) et incubées pendant 24 heures. Des cochléates placebo (sans AmB) ont été évalués à des concentrations lipidiques équivalentes. Après 24 heures d'exposition, 20 µl de solution de MTT (5 mg/mL dans du PBS) ont été ajoutés à chaque puits et les plaques ont été incubées à 37°C pendant 2 h. Le milieu a été éliminé et ensuite 200 µL de DMSO ont été ajoutés. La plaque a été agitée jusqu'à dissolution des cristaux bleu foncé puis la densité optique des échantillons a été mesurée à 570 nm en utilisant un spectrophotomètre à balayage multipuits (LT-5000 MS, Labtech). Cinq puits ont été mesurés pour chaque concentration et les expériences ont été réalisées en triplicat. Les résultats sont exprimés en pourcentages de la densité optique moyenne du contrôle. Les groupes de

traitement ont été comparés à l'aide du test t bilatéral de Student, un p inférieur à 5% étant considéré comme significatif.

2.1.2.5.2 Étude d'interaction d'AmB-cochléates sur monocouches cellulaires Caco2 (test de perméabilité)

Ces expériences ont été réalisées sur des monocouches de cellules Caco2 cultivées pendant au moins 21 jours (Hubatsch et al., 2007). Deux conditions d'incubation ont été réalisées. Dans le premier, les monocouches cellulaires ont été incubées pendant 3 heures avec la formulation d'AmB-cochléate à une concentration fixe d'AmB de 50 µg/mL (milieu HBSS à pH 6,5) dans le compartiment supérieur. Pour la deuxième condition, l'incubation a été similaire mais le milieu du compartiment supérieur était du milieu intestinal FASSIF (tableau 4). Dans les deux cas, le milieu du compartiment inférieur était du HBSS à pH 7,4 contenant 4% (m/v) d'albumine. La résistance transépiteliale (TEER) a été mesurée avant et après incubation pour s'assurer de l'intégrité de la monocouche (valeurs supérieures à 200 Ω.cm²) (Hubatsch et al., 2007).

À la fin de la période d'incubation, la quantité d'AmB transportée à travers la monocouche Caco2 a été déterminée en récupérant la solution du compartiment inférieur qui a été traité avec 2 volumes d'acétonitrile puis centrifugée (2000g, 10 min) pour éliminer l'albumine précipitée. L'excès de solvant a été évaporé sous un courant d'azote suivi d'une lyophilisation pendant 24 heures. Enfin, un mélange eau / méthanol (1/3) a été ajouté pour dissoudre le résidu qui a été analysé par HPLC comme décrit ci-dessus. L'accumulation d'AmB dans la monocouche cellulaire a également été mesurée. Pour cela, la monocouche a été rincée cinq fois avec du PBS à 4°C puis solubilisée avec du Triton X-100 à 1% dans l'eau. 3 volumes de méthanol ont été ajoutés puis une centrifugation (2000g, 10 min) est réalisée. Enfin, le surnageant a été récupéré pour mesurer la concentration en AmB par HPLC.

Tableau 4. Composition de milieu intestinal FASSIF (Pham et al., 2014)

Composant	FASSIF
Taurocholate de sodium	3 mM
Lécithine	0,8 mM
Phosphate monobasique de sodium (anhydre)	28,7 mM
Hydroxyde de sodium	8,7 mM
Chlorure de sodium	105,9 mM
pH	6,5

2.1.2.6 Évaluation de l'activité des AmB-cochléates contre la leishmaniose viscérale par voie orale

L'activité *in vivo* des cochléates a été évaluée à l'aide d'un modèle de leishmaniose viscérale chez la souris (Campos Vieira et al., 2011). Les procédures expérimentales ont été autorisées par le Comité d'éthique d'expérimentation animale N° 26, en accord avec la réglementation de l'Union Européenne. Des souris BALB/c femelles de 18-20 g (âgées 7 à 8 semaines) fournies par JANVIER LABS ont été infectées par voie intraveineuse avec 10^7 amastigotes de *L. donovani* puis ensuite reparties au hasard en groupes de 7 à 9. L'évaluation a été réalisée sur 4 groupes : le premier groupe (groupe contrôle) n'a reçu aucun traitement ; le second groupe (groupe placebo) a reçu des traitements avec cochléates sans AmB par voie orale à une dose équivalente au groupe 3 ; le troisième groupe a reçu le traitement de cochléates contenant l'AmB par voie orale à une dose de 1 mg AmB/kg et le quatrième groupe a reçu un traitement d'AmBisome par voie intrapéritonéale à une dose de 1 mg AmB/kg. Une semaine après infection, trois doses ont été administrées au premier, troisième et cinquième jour. Au jour 14 post-infection, toutes les souris ont été euthanasiées par dislocation cervicale et le foie et la rate ont été prélevés et pesés. Le nombre de parasites a été déterminé par comptage du nombre d'amastigotes par 500 hépatocytes sur des frottis d'empreinte préparés à partir du foie coloré au Giemsa et en multipliant cette valeur par la masse du foie en milligrammes. Les différences statistiques entre les groupes de traitement ont été déterminées par le test non-paramétrique de Kruskal Wallis suivi d'un Dunn's test non corrigé. La significativité a été établie pour une valeur $p < 0,05$ par rapport au contrôle.

2.1.3 Résultat et discussion

2.1.3.1 Morphologie, taille, indice de polydispersité et rendement d'encapsulation

Les cochléates sont définis comme une structure en forme de cigare et, selon la méthodologie utilisée leurs dimensions peuvent être micrométrique ou nanométrique (Shuddhodana et al., 2016). La Figure 26A (flèches noires) montre la forme typique de cigare correspondant aux cochléates dont la taille est de l'ordre du nanomètre, démontrant l'efficacité de la méthodologie hydrogel pour obtenir des cochléates de petite taille (Jin et al., 2001; Leila Zarif et al., 2003). Dans la Figure 26B, la microscopie optique révèle la présence de particules micrométriques (flèches blanches), indiquant une distribution de taille hétérogène qui est un problème fréquent lors de la fabrication des cochléates (Bozó et al., 2017).

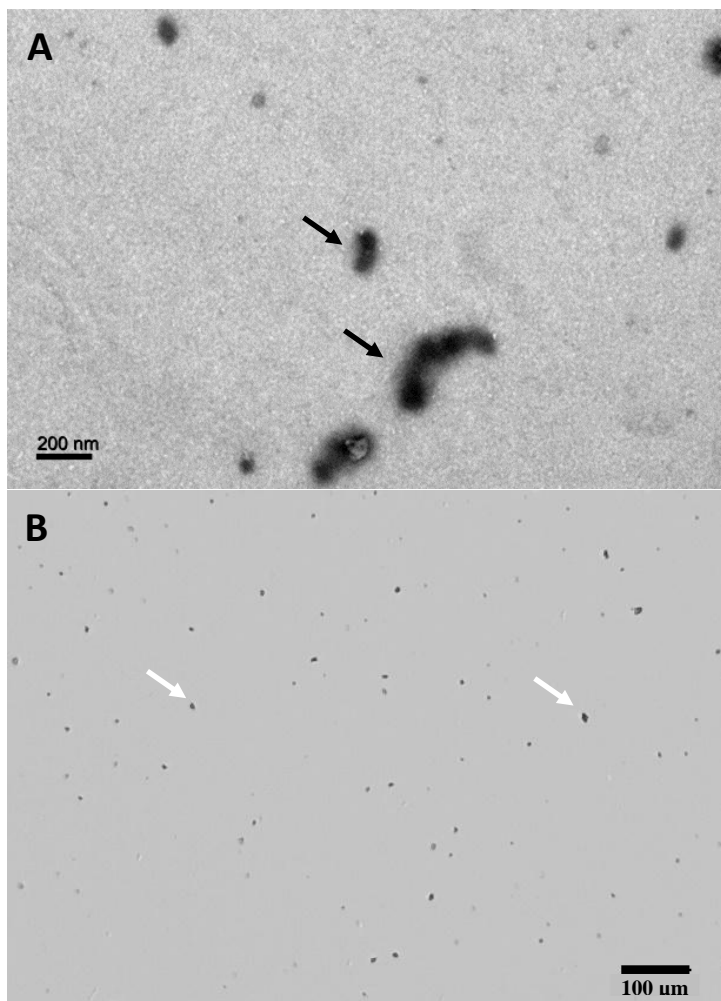


Figure 26. Images de microscopie électronique (A) et optique (B) des AmB-cochléates obtenus à partir du phospholipide synthétique DOPS

Ces résultats sont cohérents avec ceux obtenus par diffusion dynamique de la lumière, où nous obtenons une taille moyenne de 465 nm associée à un indice de polydispersité de 1,00 (dispersion très hétérogène). Il faut prendre en compte que les algorithmes utilisés pour la DLS assument des particules sphériques et isotropes. Or, les cochléates sont anisotropes, ainsi la technique n'est pas complètement adaptée, et il faut toujours une technique complémentaire telle que la microscopie. D'autre part, le rendement d'encapsulation de l'AmB a été de 70%, démontrant la capacité des cochléates à base de DOPS, d'encapsuler l'AmB dans leur structure.

2.1.3.2 Etudes de viabilité

Figure 27, les résultats sur la viabilité cellulaire après 24H d'incubation montrent l'innocuité de la formulation dans l'intervalle de concentration de 0,1 à 100 µg AmB/mL contenu dans les cochléates. Sur la base de ces résultats, la concentration de travail choisie pour les tests de perméabilité a été de 50 µg AmB/mL.

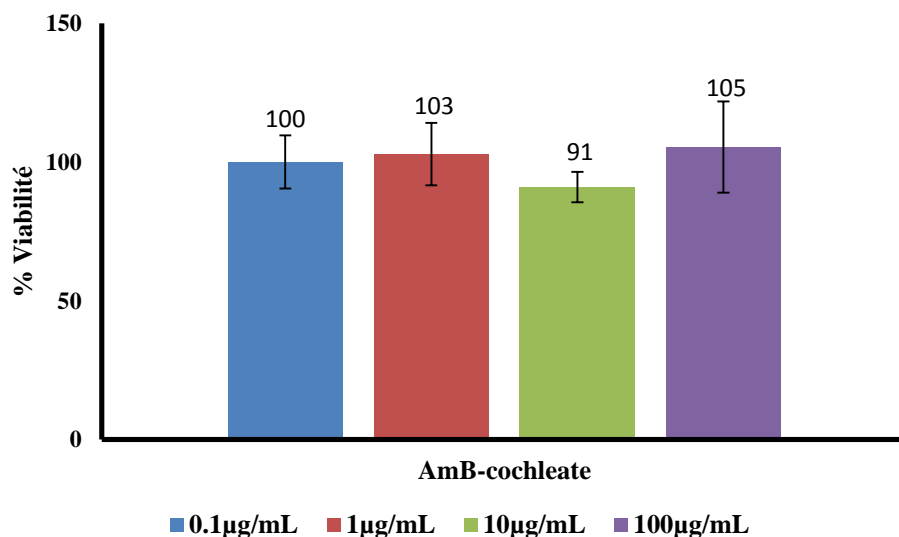


Figure 27. Résultats de viabilité des formulations d'AmB-cochléates à base de DOPS

2.1.3.3 Étude de l'interaction d'AmB-cochléates avec des monocouches cellulaires Caco2

Après 3 heures d'incubation des AmB-cochléates, un pourcentage d'environ 22% d'AmB a été retrouvé dans les cellules en utilisant du HBSS (conditions salines sans sel biliaire) (voir tableau 5). Les mécanismes d'action des cochléates pour améliorer la biodisponibilité orale des molécules actives ne sont pas clairs mais plusieurs auteurs mentionnent l'interaction de la structure cochléaire avec la membrane, suivie de la fusion des phospholipides et d'une libération postérieure du principe actif contenu dans les cochléates à l'intérieur des cellules (L. Zarif et al., 2000). Sur la base de ce mécanisme, la formulation AmB-cochélées à base de DOPS montre un résultat prometteur pour libérer l'AmB par voie orale. Cependant, la présence des sels biliaires contenus dans le milieu FASSIF diminue fortement les propriétés d'adhésion et de fusion de la formulation, phénomène qui a été mis en évidence par la récupération d'environ 0,82% d'AmB dans la monocouche cellulaire. Pourtant, certains auteurs ont montré que l'interaction et la dissolution des nanoparticules par les sels biliaires pourrait favoriser l'absorption des médicaments (Mikov et al., 2006). Par ailleurs, malgré les avantages du modèle cellulaire Caco2, ces modèles ne simulent pas totalement les conditions intestinales. De plus, ces systèmes n'ont pas les caractéristiques morphologiques et physiologiques de l'intestin, principalement la perméabilité impliquant un processus médié par les transporteurs. Des modèles *ex vivo* comme la chambre de Using pourrait mimer différentes régions du tractus gastro-intestinal en utilisant des tissus intégraux de rats (Mendes et al., 2018). Ainsi cela pourrait constituer des expériences complémentaires à réaliser par la suite pour élucider le mécanisme d'action des cochléates et en même temps obtenir un profil d'absorption plus véritable. Nous pouvons toutefois affirmer que les cochléates présentent un mécanisme de fusion en l'absence de sel biliaire et un mécanisme de dissolution avec libération de la substance active en présence de sels biliaires, ce mécanisme ayant déjà été observé par Pham et al. (2014).

Table 5. Pourcentage de récupération d'AmB après 3H d'incubation sur Caco2

Valeurs exprimées en moyenne \pm SD (n=3)

Niveau	Condition	%AmB récupéré
Couche Cellulaire	HBSS	22.1 \pm 4
	FASSIF	0.82 \pm 0.3
Compartiment Basolatéral	HBSS	ND (<0.1%)
	FASSIF	ND (<0.1%)

2.1.3.4 Activité *in vivo*

Comme le montre la Figure 28, après le traitement avec trois doses de formulations étudiées, une réduction de 26,5% de la charge parasitaire dans le foie a été observée suite à l'administration orale de la formulation cochléate placebo. Toutefois, cette réduction n'est pas significative. En revanche, l'administration orale d'AmB-cochleates a provoqué une réduction significative de 32,9% de la charge parasitaire et l'AmBisome®, administré par voie intrapéritonéale, a provoqué une réduction de 77,3% de la charge parasitaire, comme ce qui pouvait être attendu pour la formulation de référence.

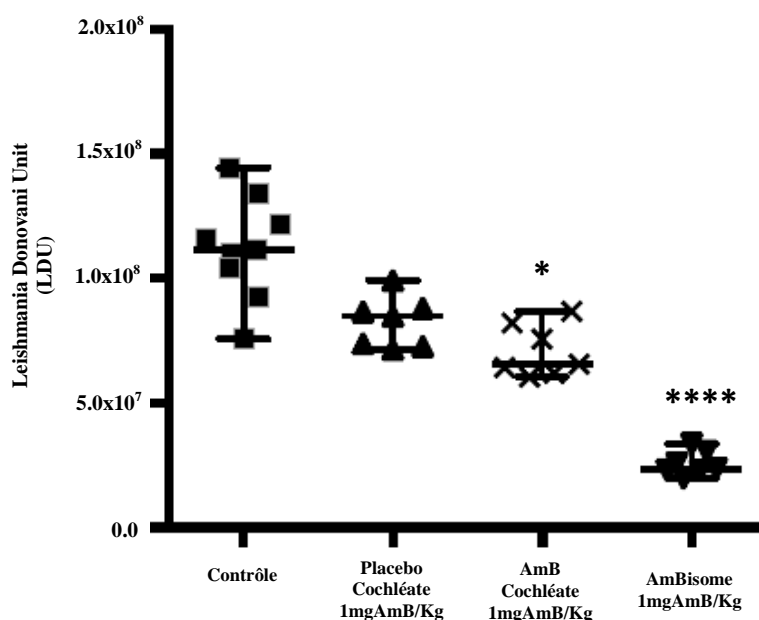


Figure 28. Activité antileishmanienne *in vivo* d'AmB-cochleates. Test non paramétrique de Kruskal Wallis suivi d'un Dunn's test non corrigé. La significativité a été établie pour une valeur * $p < 0.05$ et *** $p < 0.0001$ par rapport au contrôle.

Ces résultats démontrent une possibilité du traitement de la leishmaniose en administrant l'AmB par voie orale quand elle est associée aux cochléates.

2.1.4 Conclusion

Les cochléates, élaborés à partir d'un phospholipide synthétique comme la DOPS, s'avèrent être un système prometteur pour délivrer l'AmB par voie orale mais également prometteur comme traitement accessible pour la leishmaniose par voie orale par rapport à l'administration parentérale exigée par les formes commerciales d'AmB. Cependant, malgré le bon profil de taille (nanométrique), le taux d'encapsulation (70%) et l'interaction avec les cellules intestinales, leur préparation à base de phospholipide synthétique comme la DOPS conduit à une formulation onéreuse, inaccessible pour les pays en voie de développement. Par conséquent, d'autres sources de lipides capables de former des cochléates doivent être étudiées pour encapsuler l'AmB et ainsi permettre de proposer un traitement beaucoup plus accessible. Enfin, l'élucidation du mécanisme d'action des cochléates reste nécessaire pour comprendre la libération afin d'améliorer à terme la biodisponibilité des médicaments mais aussi l'optimisation de la présence ou l'absence de sels biliaires est indispensable dans l'objectif mieux comprendre les interactions sous-jacentes.

2.2 Chapitre 2 : AmB-Cochléates d'origine naturelle (article)

Dans ce chapitre nous étudions l'incorporation de l'AmB dans des formulations de cochléates préparés à partir d'un lipide naturel (Lipoid PS P 70). Pour cela, quatre formulations contenant l'AmB ont été préparées :

LipoidPSP70/Cho/AmB/VitE (9:2:0,5:0,06)

LipoidPSP70/Cho/AmB/VitE (9:2:1:0,06)

LipoidPSP70/Cho/AmB/VitE (9:2:2:0,06)

LipoidPSP70/Cho/AmB/VitE (9:2:0,1:0,06)

La méthode de préparation de cochléates a été la même que pour les préparations précédentes (méthode de l'hydrogel). Ensuite des caractérisations comme la morphologie, la taille, le rendement d'encapsulation, l'état d'agrégation d'AmB et la structure interne ont été obtenues par microscopie, DLS, HPLC, dichroïsme circulaire et SAXS respectivement.

De plus, des études de stabilité des formulations dans un milieu gastrique simulé et de libération *in vitro* dans des milieux gastro-intestinaux modèles ont été réalisées en dosant l'AmB par HPLC. Enfin, des études d'interaction avec un modèle cellulaire de Caco2 ont été réalisées afin de connaître le mécanisme d'internalisation des cochléates et aussi évaluer la capacité de chaque formulation à interagir avec la membrane intestinale.

COCHLEATE FORMULATIONS OF AMPHOTERICIN B DESIGNED FOR ORAL ADMINISTRATION USING A NATURALLY OCCURRING PHOSPHOLIPID

Antonio Lipa-Castro,^a Valérie Nicolas,^b Angelina Angelova,^a Ghozlene Mekhloufi,^a Bastien Prost,^c Monique Chéron^d, Vincent Faivre,^a and Gillian Barratt^{a,*}

^aUniversité Paris-Saclay, CNRS, Institut Galien Paris-Saclay, 92290, Châtenay-Malabry, France.

^bUniversité Paris-Saclay, Inserm, IPSIT, Plateforme MIPSIT, 92290, Châtenay-Malabry, France

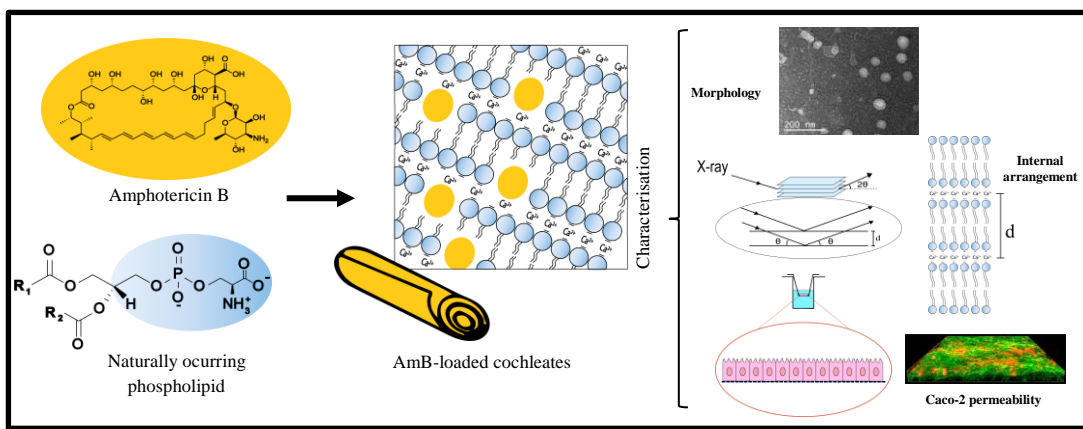
^cUniversité Paris-Saclay, Inserm, IPSIT, Plateforme SAMM, 92290, Châtenay-Malabry, France

^dFaculté de Pharmacie, Université Paris-Saclay, 92290, Châtenay-Malabry, France

* Corresponding author

Abstract

The purpose of this work is to formulate the poor soluble antifungal and antiparasitic agent Amphotericin B (AmB) in cost-effective lipid-based formulations suitable for oral use in developing countries, overcoming the limitations of poor water solubility, nephrotoxicity and low oral bioavailability. The antifungal agent was formulated, at different molar proportions, in cochleate nanocarriers prepared using an accessible naturally occurring phospholipid rich in phosphatidylserine (Lipoid PSP70). These nanoassemblies were prepared by condensation of negatively charged phospholipid membrane vesicles with divalent cations (Ca^{2+}). Small-angle X-ray scattering studies revealed the Ca^{2+} -triggered condensation of loosely packed multilamellar vesicles into tightly packed bilayers of strongly dehydrated multilamellar organization characterized by narrow Bragg peaks. Transmission electron microscopy and quasi-elastic light scattering studies demonstrated the formation of nanosized particles. AmB drug loading was above 55% in all formulations. Circular dichroism demonstrated the prevalence of monomeric and complexed forms of AmB over toxic aggregates. The stability of AmB in gastric medium was improved by loading in cochleates and its release in gastrointestinal media was retarded. Confocal microscopy studies revealed the *in-vitro* interactions of Lipoid PSP70-based cochleates with Caco2 intestinal cell monolayers. The results suggest that the low-cost AmB-loaded cochleates may increase the therapeutic range of this drug.



Keywords: phosphatidylserine, cochleates, Amphotericin B, oral bioavailability, Caco2 cells, synchrotron SAXS, circular dichroism

2.2.1 Introduction

Amphotericin B is a polyene antibiotic belonging to the macrolide family that is used to treat serious, life-threatening fungal infections as well as infections caused by the protozoan parasite *Leishmania* (Berman, 2005; Chattopadhyay & Jafurulla, 2011; No, 2016). AmB is poorly soluble in both water (10^{-7} M) and many organic solvents. It has a molecular mass of 924 g/mol and an estimated octanol/water partition coefficient of -2.80. In its pharmaceutical form sodium deoxycholate is used to solubilize the antibiotic in the form of mixed micelles (Fungizone®). However, instability of this form in the plasma gives rise to dose-limiting toxicity (notably nephrotoxicity and infusion-related reactions) (Espada et al., 2008; Huang et al., 2002). Lipid-based formulations, and in particular a liposomal speciality (AmBisome®; LAmB), can reduce toxicity but are expensive (Hamill, 2013). Furthermore, none of the commercial formulations provide significant bioavailability of AmB when administered by the oral route, due to the high molecular weight and poor water solubility of the drug. However, an orally active formulation would be advantageous, particularly for the treatment of leishmaniasis in developing countries where this disease is endemic and presents a major public health problem (Torres-Guerrero et al., 2017).

Several experimental formulations have been reported to improve the bioavailability of AmB by the oral route (Faustino and Pinheiro, 2020). These have been based on mixed micelles (Chen et al., 2015), emulsions or self-emulsifying systems (Ibrahim et al., 2013; Khan et al., 2019), cubosomes (Jain et al., 2018; Yang et al., 2014), solid-lipid nanoparticles (Chaudhari et al., 2016) and chitosan-covered nanoparticles (Serrano et al., 2015). These formulations can prolong the residence time of the drug in the intestine and allow its release in the molecular form. Recently, a prodrug of AmB covalently linked to oleic acid was shown to increase the bioavailability of the drug by a factor of almost 5 after oral administration to rats (Thanki et al., 2019). This type of prodrug is designed to use physiological routes of lipid absorption.

One of the forms that has been most frequently exploited for the oral administration of AmB is cochleates (Lu et al., 2019; Santangelo et al., 2000; Zarif et al., 2000). These are stable phospholipid-cation precipitates that consist of cigar-like spiral rolls formed of negatively charged phospholipid bilayers with divalent metal counter ions as bridging agents between the bilayers. Due to the tightly rolled structure, they possess little or no aqueous phase, in contrast to liposomes. This dehydrated internal structure renders them an ideal vehicle for delivering

lipid-soluble drugs, proteins or nucleic acids into biological systems because they protect the encapsulated material against enzymatic or chemical degradation (Pawar et al., 2015). As a highly hydrophobic molecule, AmB would be localized in the lipid bilayers of the tightly rolled cochleates and in this way would be protected from degradation when exposed to harsh environmental conditions and enzymes. Furthermore, it could be released in a form with a higher possibility of passing the intestinal barrier. Initial biodistribution studies of AmB encapsulated in cochleates administered orally in a mouse model showed that the cochleates could deliver therapeutic levels of AmB to target organs. Cures were observed after oral administration of AmB-loaded cochleates to mice infected with *Candida albicans* (Santangelo et al., 2000) or *Cryptococcus neoformans* (Lu et al., 2019). A phase II clinical trial was recently undertaken in patients with mucocutaneous candidiasis (Aigner and Lass-Flörl, 2020). Low toxicity was observed, but the improvement in symptoms was not better than that observed with fluconazole.

Despite the encouraging results with AmB-loaded cochleates that have been obtained over the last decades, their use for the treatment of leishmaniasis has not been developed. The negatively charged phospholipid most commonly employed for the formation of cochleates is phosphatidylserine (PS). Often, the synthetic 18-carbon monounsaturated 1,2-dioleoyl-sn-glycero-3-phospho-L-serine (DOPS) is chosen. However, this synthetic lipid is expensive, limiting the use of such formulations in the developing countries where leishmaniasis is prevalent. The objective of this study was to develop cochlate formulations using a naturally occurring phosphatidylserine from soy (Lipoid PSP70) able to encapsulate AmB and to evaluate their suitability for oral administration. Different molar proportions of AmB within the cochleates were evaluated for its influence on the shape, size and internal structure of the cochleates. The aggregation state of the AmB, its stability in the gastric environment, its *in vitro* release and its toxicity to intestinal cells were also investigated.. Lastly, studies of interactions with Caco2 cells were carried out by confocal microscopy.

2.2.2 Material

DOPS, Lipoid PSP70 and lecithin were gifts from Lipoid (Grasse, France). AmB and sodium taurocholate were purchased from Alfa Aesar™. Cholesterol, vitamin E, dextran (500,000 Da), poly (ethylene glycol) (PEG 8000), ethylenediaminetetraacetic (EDTA), calcium

chloride, glucose, sodium chloride, potassium chloride, magnesium sulphate, Tris base, pepsin, Tween 80, sodium hydroxide, sodium chloride, sodium dibasic phosphate, sodium bicarbonate, potassium monobasic phosphate and sodium monobasic phosphate were purchased from Sigma-Aldrich. AMBERLITE™ 200CNa resin was a gift from Dow Water & Process. Methanol, chloroform, isopropanol, heptane, acetic acid, hydrochloric acid and other solvents were purchased from Merck. Water was purified by reverse osmosis (Milli-Q Millipore). Fungizone® was purchased from Bristol-Myers Squibb. Dulbecco's modified Eagle's medium (DMEM), phosphate buffered saline (PBS), foetal bovine serum (FBS), non-essential amino acids solution (10 mM, 100x), penicillin-streptomycin solution (10,000 units/mL penicillin and 10 mg/mL of streptomycin), trypsin-EDTA solution (0.05% trypsin, 0.53 mM EDTA), methylthiazoltetrazolium (MTT), FITC-dextran 4.4 kDa, FITC-labelled phalloidin and dimethyl sulfoxide were obtained from Sigma-Aldrich. The fluorescent phospholipid 1,2-dioleoyl-sn-glycero-3-phosphoethanolamine-N- (lissamine rhodamine B sulfonyl) (ammonium salt) was obtained from Avanti Polar Lipids (Alabaster, Alabama, USA). Corning Transwell® inserts of 12 mm diameter, with 0.4 µm pore-size polyester membranes, and 24 mm diameter, with 0.4 µm pore-size polycarbonate membranes, were purchased from the Costar Corning Corporation (New York, USA).

2.2.3 Method

2.2.3.1 Ion exchange treatment of the Lipoid PSP70

Lipoid PSP70 was obtained as a calcium salt that was insoluble in organic solvent. Therefore, an ion exchange treatment was necessary to convert it to the sodium salt. 1g of Lipoid PSP70 was dissolved in chloroform/methanol/water (20/10/2) at a concentration of 5 mg/mL, after which 75g of resin (previously dried over 24 hours at 50°C due to its high water content) was added and stirred for 12 hours. The suspension was filtered (PTFE 0.2 µm) and the solvent was removed by vacuum evaporation (Buchi R-210 Rotavapor System). The lipid film was recovered in chloroform/methanol/water (20/10/2) solvent to obtain a concentration of 5 mg/mL of lipid. A second exchange treatment was performed with 10 g of resin stirred for 2 hours. The suspension was filtered and the solvent removed by vacuum evaporation. Finally, the lipid film was recovered in chloroform/methanol (60/40) at 5 mg/mL total lipid concentration.

Identification and quantification of phosphatidylserine were carried out by normal phase high-performance liquid chromatography coupled to electrospray mass spectrometry (HPLC-MS). The analysis was done by coupling a quaternary RSLC Dionex-U3000 liquid chromatography (Thermo Scientific) with a Corona-CAD Ultra aerosol charge detector (Thermo Scientific) and a hybrid mass spectrometer equipped with ion trap and an orbital trap LTQ- Orbitrap Velos Pro (Thermo Scientific) for PS species identification. The separation was performed on an YMC PVA-Sil column (150 mm × 2.1 mm I.D., 5 µm particles, pore size 120Å). The column was operated under gradient conditions with mobile phase A: heptane/ Isopropanol 98/2, mobile phase B: chloroform/ Isopropanol 65/35, mobile phase C: methanol/water 95/5 and mobile phase D: Isopropanol where A, B and C contained 1% acetic acid and 0.08% triethylamine. The quaternary gradient program used is shown in Table S1. The flow rate was 400 µL/min and the injection volume was 5 µL. Absolute ethanol was added with a second mixing tee, with a flow rate of 200 µL/min to increase the flow entering the Corona CAD and thereby maintain aerosol stability. All data corresponding to mass spectrometry were collected in negative ionization mode. Fullscan high resolution MS (HRMS) was performed in the orbitrap with a scan range of m/z 300–1800 and a resolution of 100000 and data-dependent MS² and MS³ with collision-induced dissociation in the CID (Collision Induced Dissociation) fragmentation. Acyl chain (AC) composition of the different PS species was performed in negative ESI data-dependent mode in the LTQ ion trap (low resolution) (Moulin et al., 2015).

2.2.3.2 Preparation of AmB-loaded cochleates

The molar proportions of Lipoid PSP70 and cholesterol of 9/2 were established based on the impact on the internal structure of cochleates determined by SAXS and on the stability of AmB in gastric medium (Supplementary Figure S1 and Table S2 respectively). Thereafter, cochleates were prepared by the hydrogel isolation method (Zarif et al., 2000) using Lipoid PSP70, cholesterol and vitamin E (as antioxidant) in molar proportions of 9/2/0.01 with AmB at four different molar ratios: 0.5, 1, 2 and 3. The molecular weight of Lipoid PSP70, containing a mixture of acyl chains, was considered to be the same as that of the sodium salt of dioleoylphosphatidylserine: 810 g/mol. The formulations will be designated as follows in the text and illustrations below:

- F0.5: 9 Lipoid PSP70 / 2 cholesterol / 0.06 vitamin E / 0.5 AmB
F1: 9 Lipoid PSP70 / 2 cholesterol / 0.06 vitamin E / 1 AmB
F2: 9 Lipoid PSP70 / 2 cholesterol / 0.06 vitamin E / 2 AmB
F3: 9 Lipoid PSP70 / 2 cholesterol / 0.06 vitamin E / 3 AmB

Since AmB is photosensitive, all procedures were carried out in a way that protected it from light as much as possible. Amber glassware was used when possible and when not it was covered with aluminium foil. All equipment used was shielded from light. Firstly, small unilamellar liposomes were formed by film hydration. Lipoid PSP70, cholesterol, vitamin E dissolved in chloroform/methanol (60/40) and AmB dissolved in alkaline methanol (containing sodium hydroxide solution at 1mM) were mixed in the desired proportions, dried by rotary evaporation and hydrated with 0.05M Tris buffer pH 7.4 to a lipid concentration of 5.6 mM. The size was reduced and homogenized by probe sonication (Bioblock Scientific vibracell 72441 ultrasons) with a sonic power of 2 for 7 cycles of 1 min at 1-min intervals over ice followed by sequential extrusion on calibrated membranes (Whatman® Nuclepore) to form liposomes with a mean diameter of about 100 nm. Non-encapsulated AmB was retained on the membranes at this stage.

To form cochleates, the liposomes were mixed with 40% (w/w) dextran in a suspension of 2/1 (v/v) dextran/liposome and injected into 15% (w/w) polyethylene glycol 8000 with stirring. CaCl₂ solution was added at a final concentration of 50 mM, and stirring was continued for 15 minutes to form cochleates. The cochleates were recovered by filtration followed by washing with 1mM CaCl₂/150 mM NaCl and freeze-drying for 24 h in the dark to avoid photodegradation (Freeze dryer CRYOTEC Cosmo 20K-80). Unloaded cochleates (designated F0) were prepared in the same way without addition of AmB. Rhodamine-labeled unloaded cochleates were prepared by including 1,2-dioleoyl-sn-glycero-3-phosphoethanolamine-N- (lissamine rhodamine B sulfonyl) ammonium salt (Rho-PE)) at 0.2% molar ratio with Lipoid PSP70, thereby obtaining cochleates with the composition 9 Lipoid PSP70 /2 cholesterol /0.018 Rho-PE/ 0.06 vitamin E.

2.2.3.3 Electronic microscopy

A transmission electron microscope operating at 120KV (JEOL JEM-1400) at the I2BC (Gif-sur-Yvette, France) was used to examine the aggregation state and morphology of the nanoparticles obtained with Lipoid PSP70. The cochleates were suspended in 2mM CaCl₂

solution at 0.4 mg/mL, after which 5 µL of the solution was deposited on a copper grid covered with a formvar film (400 mesh) for 1 hour until air-dried followed by negative staining treatment with 1% sodium phosphotungstate. Excess solution was removed with filter paper from the back of the grids before observation. Images were acquired using a high-resolution camera (Orius SC1000).

2.2.3.4 Morphogranulometry

The aggregation state and morphology of the cochleates obtained from Lipoid PSP70 were also analyzed by flow imaging microscope, using a Flow-Cell 200 S-M instrument (Occhio, Belgium) morphogranulometer. The cochlate suspension was pumped through a 50-µm-wide flow cell and digital images were obtained with a high-resolution camera with a 0.185-µm spatial resolution ($9 \times$ zoom factor). Cochlate samples were suspended in 2mM CaCl₂ solution at 0.8 mg/mL. Images were acquired when the flow was completely stopped to ensure good resolution. The morphogranulometer was equipped with image analysis software Callisto (Occhio, Belgium) designed for particle detection using the grey level difference between the particle and background.

2.2.3.5 Size, polydispersity index and zeta potential analysis

The hydrodynamic diameters (D_h), polydispersity indexes (PDI) and zeta potential of the formulations obtained from Lipoid PSP70 as liposomes and cochleates were studied by dynamic light scattering (DLS) measurements using a Zetasizer Nano ZS90 instrument (Malvern, France). The liposomes were diluted in Tris 0.05M pH 7.4 and cochleates were dispersed in NaCl/CaCl₂ 150 mM/ 1mM solution. Zeta potential measurements were carried out after dilution of the liposomes in Tris (0.0125 M pH 7.4) and cochleates in CaCl₂ solution (2 mM). All measurements were performed in triplicate at 25°C at a detection angle of 90° for size measurements.

2.2.3.6 Determination of AmB content by HPLC and encapsulation efficiency

The AmB content of the formulations was measured by reversed phase HPLC, using the method reported by Ménez et al., (2006a). This was performed with a HPLC system equipped with a quaternary 600 Controller pump, UV-Visible spectrophotometric detector (2996 Photodiode Array Detector, Waters) and an automatic injector (717 Autosampler, Waters). The column was a Symmetry® C₁₈ column 150 mm x 4.6 cm, 5 µm particle size and 100 Å

pore size (Waters). The mobile phase was 0.5% aqueous solution of triethylamine (adjusted to pH 5.2 with formic acid), acetonitrile and tetrahydrofuran (1000/385/154 v/v). The flow rate was 1 mL/min and the injection volume was 100 µL. The column temperature was 30°C and the injection system was at room temperature. AmB was quantified using the peak areas acquired at 408 nm, with a retention time of about 9 minutes. A calibration curve was prepared from a series of dilutions of an AmB reference standard in MeOH/H₂O (1/1) in the range between 0.1 and 5 µg/mL. The correlation coefficient (R^2) was 0.9995, the limit of detection was 40 ng/mL and the limit of quantification was 100 ng/mL. Cochleate samples were treated with EDTA 0.05M and MeOH to extract the AmB then diluted in MeOH/H₂O (1/1). Finally, samples were centrifuged with a VWR Galaxy Mini Centrifuge C1413 8 (2000 x g, 10 min) to remove the impurities. This treatment was sufficient to destroy the cochleate structure and ensure that AmB was present in its molecular form.

Since AmB is very poorly soluble in water, any non-encapsulated drug precipitated when the multilamellar liposomes were formed. These precipitates were retained on the extrusion membranes when the liposome size was reduced. Thus, the AmB recovered in the final cochleates could be considered as encapsulated. The encapsulation efficiency (EE %) for each preparation was calculated using the following equation:

$$EE\% = (W_t/W_i) \times 100\%$$

where W_t is the total amount of the AmB measured in the freeze-dried cochleates and W_i is the total quantity of AmB initially added to the preparation. The AmB content was also expressed with respect to the total weight of freeze-dried cochleates that were recovered.

To confirm that the final cochleate preparation did not contain free AmB, an extraction procedure using 0.2% Tween 80 in 50 mM CaCl₂ solution was performed on formulations diluted to 2µg/ml AmB content. This revealed that 5, 8, 11, and 12% of associated AmB could be extracted from F0.5, F1, F2 and F3 respectively. Thus, we can conclude that the majority of the AmB in the final cochleates was tightly associated with the lipid bilayers.

2.2.3.7 Small- and wide-angle X-ray scattering

For synchrotron SAXS measurements, liquid crystalline vesicular membranes and cochleate samples were introduced into X-ray capillaries with a diameter 1.5 mm and were sealed with paraffin wax. The experiments were performed at the SWING beamline of synchrotron SOLEIL (Saint Aubin, France) with a set-up previously described (David and Pérez, 2009). The samples were oriented in front of the X-ray beam ($25 \times 375 \mu\text{m}^2$) using a designed holder for multiple capillaries positioning (X, Y, Z). The sample-to-detector distance was 3 m. The employed exposure time of 500 ms did not cause radiation damage. The q -vector was defined as $q = (4\pi / \lambda) \sin \theta$, where 2θ is the scattering angle. The synchrotron radiation wavelength was $\lambda = 1.033 \text{ \AA}$. The SAXS patterns were recorded with a two-dimensional Eiger X 4M detector (Dectris) at 12 keV. The q -range calibration was done using a standard sample of silver behenate ($d = 58.38 \text{ \AA}$). Temperature was 22 °C. Data processing of recorded 2D images was performed by the FOXROT software (David and Pérez, 2009). The interlamellar repeat distances, d , of the observed multilamellar structures were calculated from the positions of the Bragg peaks resolved in the SAXS patterns using the relationship $d = 2\pi / q$.

Additional SAXS patterns and some preliminary WAXS patterns were acquired using a microfocus X-ray tube (I μ S, Incoatec), selecting the Cu K α radiation. It was used with an intensity of 1000 μA and a voltage of 50 kV. The incident beam was focused at the detector with multilayer Montel optics and 2D Kratky block collimator. Small-angle (SAXS) and wide-angle (WAXS) X-ray scattering analyses were performed simultaneously using two position-sensitive linear detectors (Vantec-1, Bruker) set perpendicular to the incident beam direction, up to 7° (2θ) and at 19° to 28° (2θ) from it, respectively. The direct beam was stopped with a W-filter. The scattered intensity was reported as a function of the scattering vector $q=4\pi \sin \theta/\lambda$ where θ is half the scattering angle and λ is the wavelength of the radiation. The repeat distances were calculated as above. Silver behenate and tristearin (β form) were used as standards to calibrate SAXS and WAXS detectors, respectively.

In order to prevent sedimentation, all the samples were suspended in 4% (w/w) dextran. Cochleates prepared from Lipoid PSP70 or DOPS, cholesterol and AmB in different ratios were compared. Multilamellar vesicles (MLV) from Lipoid PSP70 were also studied. All samples were introduced into thin-walled glass capillaries (GLAS, Müller, Berlin, Germany) of 1.5 mm external diameter which were then placed in a specially designed temperature-

controlled sample holder (Microcalix, Setaram) maintained at 20°C during the measurements. Acquisition time was 3600 seconds. Igor 6.03 was used for data processing.

2.2.3.8 Circular dichroism and UV-visible spectroscopy

The toxicity of AmB is related to the aggregation state of the molecules, which can be monitored by its absorbance spectrum in the UV/Vis range of 300-450 nm (Rochelle do Vale Morais et al., 2018). Therefore, the formulations were evaluated by UV-visible spectroscopy and circular dichroism. A JASCO J-810 CD Spectropolarimeter (Tokyo, JAPAN and Jasco Spectra Manager v2 software were used for the record these parameters. Cochleates obtained from Lipoid PSP70 containing 3×10^{-5} M AmB (previously treated with 0.05M EDTA) were put in 1-cm path length quartz cuvettes (Pham et al., 2014). Suspensions of cochleates without AmB at the same lipid composition and concentration were used as blanks. Furthermore, concentrated AmB in DMSO was diluted to 3×10^{-5} M in water as a control for the aggregated state of AmB and in methanol to obtain the monomeric state and examined under the same conditions. Measurements were conducted in triplicate at room temperature and the results for CD spectra are expressed as $\Delta\epsilon$ ($M^{-1} \cdot cm^{-1}$) (differential molar absorption dichroic coefficient) and the UV/Vis spectra are presented as molar extinction coefficient (ϵ , $M^{-1} \cdot cm^{-1}$).

2.2.3.9 Stability of AmB in cochleates in gastric medium

It is known that AmB is unstable in the presence of gastric medium (Thanki et al., 2019). Therefore, its stability in the different formulations was studied using simulated gastric fluid (SGF). Samples of AmB-loaded cochleate formulations and a control of AmB dissolved in DMSO were suspended in SGF (0.32% w/v pepsin and pH adjusted to 1.2) (Pham et al., 2014) at an AmB concentration of 10 µg/mL and incubated at 37°C under shaking at a speed of 75 rpm for 2 h. The suspension was immediately neutralised with the same volume of buffer (0.11M NaOH, 0.03M NaH₂PO₄ and 0.05M EDTA) to pH 7, then 1 volume of MeOH was added followed by centrifugation in a VWR Galaxy Mini Centrifuge C1413 8 (2000 × g, 10 min). Finally, the supernatant was recovered to measure the AmB concentration by HPLC as described above. The amount of intact AmB recovered is expressed as a percentage of the original amount.

2.2.3.10 In-vitro release study

The *in-vitro* release of AmB-loaded cochleates was investigated under simulated gastro-intestinal conditions. The media were prepared as described by Pham et al (2014) with some modifications (Table S3). To ensure the solubility of released AmB in sink conditions, the initial concentration was low - 10 µg/mL, and Tween 80 was added to the gastro-intestinal media at 0.1%. Furthermore, an excess of CaCl₂ was added to obtain a concentration of 50 mM under SGF and FaSSIF conditions and 750 mM under FeSSIF conditions to mimic intestinal calcium concentrations and maintain cochleate structure. The cochleate suspensions, at an AmB concentration of 10 µg/mL, were first placed in SGF at 37°C under shaking at a speed of 75 rpm for 1 h, after which an equivalent volume of either FaSSIF or FeSSIF medium at twice the desired final concentration was added.

The temperature and the stirring speed were maintained at 37°C and 75 rpm respectively for 2h. SGF aliquots of 0.3 mL were withdrawn at intervals and immediately neutralised with the same volume of buffer (0.11M NaOH, 0.03M NaH₂PO₄, 0.1% Tween 80) followed by centrifugation with an VWR Galaxy Mini Centrifuge C1413 8 (2000 × g, 10 min). After recovering the supernatant, 1 volume of MeOH was added followed by another centrifugation. FaSSIF and FeSSIF aliquots were filtered (0.2 µm PDVF syringe filter) and treated with 1 volume of MeOH followed by centrifugation. Supernatant from SGF, FaSSIF and FeSSIF samples were analysed for their AmB content by HPLC as described above.

2.2.3.11 Cell culture

Caco2 cells (passages 3-20 after thawing of cryo-preserved cells) were grown in DMEM supplemented with 20% FBS, 1% non-essential amino acids, 1% L-glutamine and 1% penicillin-streptomycin mixture and kept at 37°C in 5% CO₂ and 95% humidity. Cells were washed with PBS and harvested with Trypsin-EDTA. Cells were cultured at a density of 15×10^3 cells/well onto 96-well cluster trays and allowed to grow for 24 hours before cytotoxicity studies. For fluorescence confocal microscopy studies, 5×10^4 cells were added to each Corning Transwell® insert (12 mm diameter, 0.4 µm pore size polyester membrane) and allowed to grow into monolayers for at least 21 days. For transport studies, 1.20×10^5 cells were added to each Corning Transwell® insert (24 mm diameter, 0.4 µm pore size polycarbonate membrane) for AmB permeability study and again grown for at least of 21 days. To verify the integrity of the monolayer the transepithelial electrical resistance (TEER)

was measured using an EVOM2™ Epithelial Voltohmmeter with a STX2 electrode (Sarasota, USA) before and after each experiment. Furthermore, a marker of paracellular passage (FITC-dextran, 4.4 kDa) was also used periodically to check that tight junctions were maintained.

2.2.3.11.1 Cytotoxicity studies: MTT assay

Cell viability in the presence of cochleate formulations was studied using the MTT colorimetric method (Ménez et al., 2006b). Caco2 cells cultured in 96-well culture plate were exposed apically to increasing concentrations of AmB in the form of cochleates (0.1 µg/mL, 1 µg/mL, 10 µg/mL and 100 µg/mL of AmB) and incubated for 24 hours. Unloaded cochleates, F0, were added at lipid concentrations equivalent to F0.5, the formulation with the lowest proportion of AmB and therefore the highest proportion of lipid. After 24h of exposure, 20 µL of MTT solution (5 mg/mL in PBS) were added to each well and the plates were incubated at 37°C for 2 h. The medium was removed and then 200 µL of DMSO was added to each well, and the plate was agitated until dissolution of the dark blue crystals. The optical density of the samples was measured at 570 nm using a multiwell-scanning spectrophotometer (LT-5000 MS, Labtech). The cytotoxicity of a control formulation without AmB was also evaluated, as was a suspension of AmB as the pharmaceutical formulation Fungizone®. Five replicate wells were used in each of triplicate experiments. The results are expressed as percentages of normalized mean control optical density. Treatment groups were compared using Student's two-tailed t test, with a P of less than 5% being considered as significant.

2.2.3.11.2 Interaction of cochleates with Caco2 cells by confocal fluorescence microscopy

Cochleates labeled with 1,2-dioleoyl-sn-glycero-3-phosphoethanolamine-N-(lissamine rhodamine B sulfonyl) (ammonium salt) were used for the purpose of studying the interaction and internalization of cochleates by Caco2 cells that had been cultured for at least 21 days. Before the experiment, the confluence and the integrity of the monolayer was verified by measurement of TEER (values greater than 200 Ω.cm²) (Hubatsch et al., 2007) and cumulative transport values of FITC-Dextran 4.4 kDa after 4 h of incubation (~0.64 µg/mL) (Kowapradit et al., 2010). The Caco2 cells were incubated for 2 hours with the Rhodamine-labeled cochleates (3 mg cochleates/ml equal to 40 µg/mL AmB) added to the upper compartment in HBSS pH 6.5. The medium in the lower compartment was HBSS at pH 7.4

supplemented with albumin at 4% (w/v). After incubation, the medium was removed and washed 3 times with PBS (Hubatsch et al., 2007). Cells were fixed with paraformaldehyde 4% for 15 minutes, washed three times with PBS and treated with 0.1% Triton X-100 for 10 minutes for permeabilization. Three washes of PBS were carried out followed by incubation with 50mMol NH₄Cl for 10 minutes. The inserts were then washed with PBS and treated with 1% BSA for 1h. After removing the medium, the inserts were incubated with FITC-phalloidin (1/1000 in PBS 1% BSA) to label the cytoskeleton. After three washes with PBS, the filters bearing the cell monolayers were cut out of the supports and mounted on coverslips for examination by confocal microscopy with an inverted confocal laser scanning microscope TCS SP8 – gated STED Leica (Leica, Germany) equipped with a WLL Laser (495 nm excitation wavelength for FITC-phalloidin and 552 nm for rhodamine-nanoparticles). Green fluorescence emission was collected with a 505-550 nm wide emission slits and a 565-700 nm wide emission slits for the red signal under a sequential mode. Images were done with the Leica Application Suite X software (Version 3.5.5; Leica, Germany).

2.2.3.11.3 Uptake and transport of AmB by Caco2 cell monolayers

These experiments were performed on Caco2 cell monolayers that had been cultured for at least 21 days. The TEER was measured both before and after the experiment to ensure the integrity and the confluence of the monolayer in the presence of AmB-loaded cochleates. The cell monolayers were incubated for 6 hours with the different cochleate formulations at a fixed AmB concentration of 100 µg/mL added to the upper compartment in HBSS pH 6.5. The medium in the lower compartment was HBSS at pH 7.4 containing 4% (w/v) albumin. At the end of the incubation period, the amount of AmB transported across the Caco2 monolayer was determined by recovering the solution from the lower compartment that was added to 2 volumes of acetonitrile and centrifuged (2000 × g, 10 min) to eliminate precipitated albumin. The excess solvent was evaporated under a nitrogen stream followed by freeze-drying for 24 hours. Finally, a mixture of water/methanol (1/3) was added to dissolve the residue, obtaining a concentrated sample for analysis by HPLC as described above. In this case the limit of detection was 10 ng/mL and the limit of quantification was 25 ng/mL. The accumulation of AmB within the cell monolayers was also measured. The monolayers were rinsed five times with ice-cold PBS and solubilized with 1% Triton X-100 in water before adding to 3 volumes of methanol followed by centrifugation (2000 × g, 10 min). Finally, the supernatant was recovered to measure the AmB concentration by HPLC.

2.2.4 Result and Discussion

2.2.4.1 Identification of phosphatidylserine species in Lipoid PSP70

After ion exchange, HPLC-MS of the Lipoid PSP70 revealed a large majority of phosphatidylserine. Phosphatidylcholine were also identified with a maximum content of 6% with respect to the total amount of phospholipids detected (see Supplementary Information, Figure S2). Further analysis revealed 11 different species of phosphatidylserine with different acyl chain lengths and degrees of unsaturation, as would be expected from a naturally occurring soy phospholipid (Table 6 and Figure S3). The acyl chains contained 16 or 18 carbon atoms, and were either saturated or with 1, 2 or 3 unsaturated bonds, with phosphatidylserine (18:2/18:2) being the most abundant, according to the peak heights. This means that the natural lipid is quite similar to DOPS (18:1/18:1) in terms of chain length and average level of unsaturation but is less homogenous. A $56 \pm 7\%$ recovery of phosphatidylserine was obtained after ion exchange. Therefore, as a negatively charged lipid with a high phosphatidylserine content, Lipoid PSP70 would be suitable for forming cochleates (Nagarsekar et al., 2017).

Table 6. Phosphatidylserine species composition of Lipoid PSP70 identified by MS² mass spectrometry. Where PS (AC1 / AC2) denotes that AC1 is on one of the sn-1 carbon and AC2 is on the sn-2 carbon while PS (AC1-AC2) denotes that the position of the two acyl chains is unknown.

Observed ions [M-H] ⁻	PS Associated
756.4810	PS (16:0 – 18:3)
	PS (16:1 – 18:2)
758.4962	PS (16:0 – 18:2)
760.5083	PS (16:0 – 18:1)
780.4799	PS (18:3 – 18:2)
782.4950	PS (18:2 / 18:2) Majority
	PS (18:3 – 18:1)
784.5082	PS (18:2 – 18:1)
	PS (18:3 – 18:0)
786.5239	PS (18:0 – 18:2)
	PS (18:1 – 18:1)

2.2.4.2 Morphology, size, polydispersity index and encapsulation efficiency

Cochleate structures are described as large, continuous lipid bilayer sheets rolled up into a rigid spiral, with no internal aqueous space (Zarif et al., 2000). To examine the structure of the formulations we studied them by TEM and morphogranulometry using an optical microscope. Figure 29 corresponding to AmB-loaded cochleates obtained from Lipoïd PSP70. Fig. A(1) shows precipitates mainly as cigar-shapes (black arrows) while B(1), C(1) and D(1) show objects with ovoid (white arrows) to spherical shapes (dotted white arrows), indicating an influence of the AmB content on the aggregation of liposomes and their subsequent precipitation as cochleates. Furthermore, the observed particles are in the nanometer range, in agreement with what would be expected by the hydrogel isolation method to obtain nanococheates (Jin et al., 2000). Images A(2), B(2), C(2) and D(2) obtained by optical microscopy shows some larger cochleates, (black arrows), maybe due to the presence of other lipid species in the naturally occurring phospholipid or to the variability of the acyl chains of the phosphatidylserine; leading to less ordered structure, but which could also be caused by calcium ion excess, a serious drawback reported in the fabrication of cochleates where excess calcium can provoke fusion between cochleates (Bozó et al., 2017).

Table 7. Physical and chemical characterization of AmB-loaded liposomes and cochleates. Values expressed as mean \pm SD (n=3). Formulation compositions are defined in Material and Methods. D_h: Equivalent hydrodynamic diameter; PdI: Polydispersity index.

Parameter Formulation	Size (liposomes)		Size (cochleates)		Zeta Potential (mV)		AmB (μ g/mg cochleate)	Encapsulation Efficiency (%)
	D _h (nm)	Pdl	D _h (nm)	Pdl	as liposomes	as cochleates		
F0	90	0.160	221	1.000	-47.8	-13.5	-----	-----
F0.5	71	0.220	469	1.000	-48.6	-12.2	57 \pm 3	64 \pm 4%
F1	78	0.280	470	1.000	-59.2	-10.1	107 \pm 5	62 \pm 3%
F2	83	0.240	626	0.668	-48.9	-9.15	193 \pm 4	56 \pm 1%
F3	71	0.190	752	0.634	-43.8	-15.9	264 \pm 5	65 \pm 1%

The values obtained for zeta potential (Table 7) also indirectly confirm the bridging of the phosphatidylserine bilayers by calcium. While the zeta potential of the liposomes was highly negative (-43 mV or more), the values recorded under the same conditions for the resulting cochleates were between -9 and -16 mV, showing the neutralization of the charge on the phosphatidylserine headgroup by calcium ions.

Unloaded and AmB-loaded cochleates from Lipoid PSP70 were characterized in terms of size and homogeneity by dynamic light scattering. In Table 7 the cochlate dimensions were 221, 469, 470, 626, 752 nm, confirming the nanometric scale found by electronic microscopy. The cochlate dimensions appeared to increase with the proportion of AmB, although the size of the liposomes used to prepare them was always calibrated on 100 nm pore size membranes and was between 71 and 90 nm. However, dynamic light scattering is not the ideal method for determining the average size of anisotropic particles such as cochleates because the algorithms used to deduce size from diffusion constants assume that the particles are spherical. The high PDI that were obtained are partly a reflection of this limitation but are also in agreement with the observations from microscopic techniques. Heterogeneous dispersions are frequently observed for nanocochnleates (Nagarsekar et al., 2017). Since the present formulation is intended for oral use, small and monodisperse particles are not as high a requirement as they would be for parenteral administration. However, smaller particles are desirable to allow better drug release and it is necessary that the fabrication process be reproducible; thus, the procedure needs to be further improved before *in-vivo* use. On the other hand, increasing values of the zeta potential observed in all formulations after the addition of calcium ions shows the complexation of the negative charge on the phospholipid that triggers cochlate formation. Finally, the AmB entrapment efficiency of more than 55% demonstrates the efficiency of the cochleates from Lipoid PSP70 to encapsulate AmB within the lamellar phase. Furthermore, increasing the proportion of AmB in the formulation from 0.5 to 3 moles did not reduce significantly the encapsulation efficiency (~ 64, 62, 56 and 65%). Therefore, the results show that it is possible to increase the proportion of AmB stably encapsulated in the cochleates above that described in the literature (Pham et al., 2013, Zarif et al., 2000).

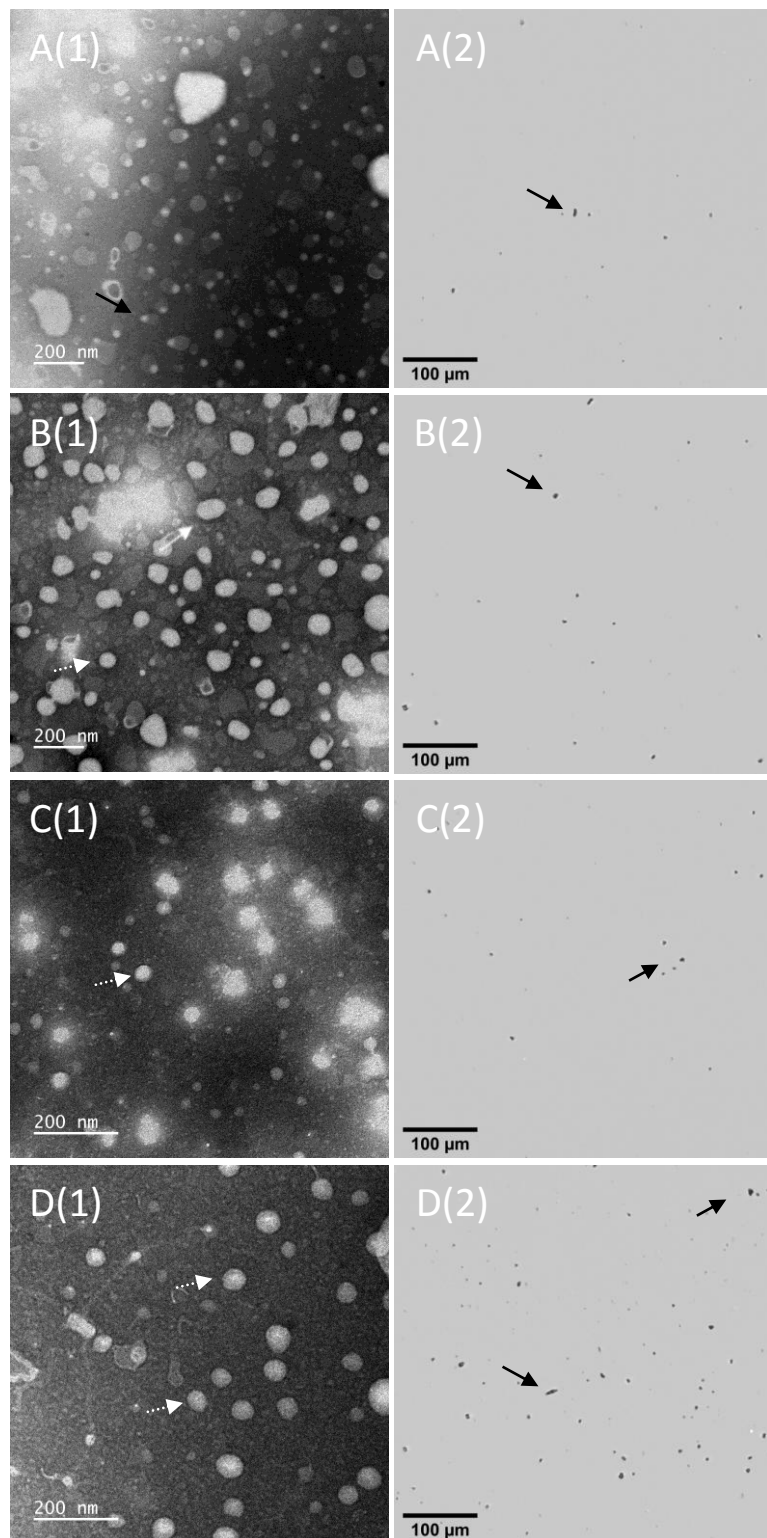


Figure 29. AmB-Lipoid PSP70 cochleates observed by transmission electron (1) and optical microscopy (2). Formulation compositions are given in Materials and Methods. A: F0.5; B: F1; C: F2; D: F3.

2.2.4.3 Small-angle X-ray scattering

The SAXS patterns obtained (Figure 30 and Table S4) clearly show the transformation of the negatively charged fluid-phase Lipoid PSP70 liquid crystalline vesicular membranes into densely packed multilamellar structures (Lipoid PSP70/Ca²⁺ or Lipoid PSP70/cholesterol/Ca²⁺) stabilized by electrostatic interactions with the divalent cations. The formation of salt bridges between the lamellae led to dehydration of the multilamellar phospholipid organization, which was associated with the emergence of well-defined Bragg peaks in the SAXS patterns. The possibility of identifying the formation of cochleate structures by SAXS has been examined for other lipid compositions in the literature (Nagarsekar *et al.*, 2016; Hui *et al.*, 1983). Depending on the ratio between the components in the self-assembled systems, the decrease of the repeated distances (d) of the multilamellar lipid vesicles (MLV) upon the addition of a bridging agent may correspond to either pure cochleate system or to a coexistence of cochleates and the multilamellar vesicles that existed before addition of the bridging agent.

Figure 30 and Table S4 show the SAXS results obtained as a function of the lipid compositions Lipoid PSP70 with and without calcium and Lipoid PSP70/cholesterol with different proportions of AmB in the presence of calcium. Additional results are presented in the Supporting Information for varying contents of cholesterol in the mixtures with a constant proportion of AmB (Figure S1). The structural transition between the different aggregation states of the lipid bilayers in the Lipoid PSP70-based formulations is remarkable. Figure 30A presents the SAXS pattern of a hydrated lamellar structure (Lipoid PSP70 MLV) with a repeat distance of $d=57.2\text{ \AA}$. The observed peak intensity and full width at half maximum (FWHM) indicate the formation of onion-like multilamellar membranes with no dense packing between the lamellae. In contrast, the appearance of narrow Bragg peaks upon the addition of calcium cations to the Lipoid PSP70 MLV demonstrates the condensation of the lamellae into a layered structure with increased packing order. As can be observed in Figure 30B (Lipoid PSP70 cochleates), the SAXS plot shows an intense first-order peak corresponding to a repeat interlamellar distance of 49.1 \AA as well as second and third order reflections characterizing the multilamellar organization.

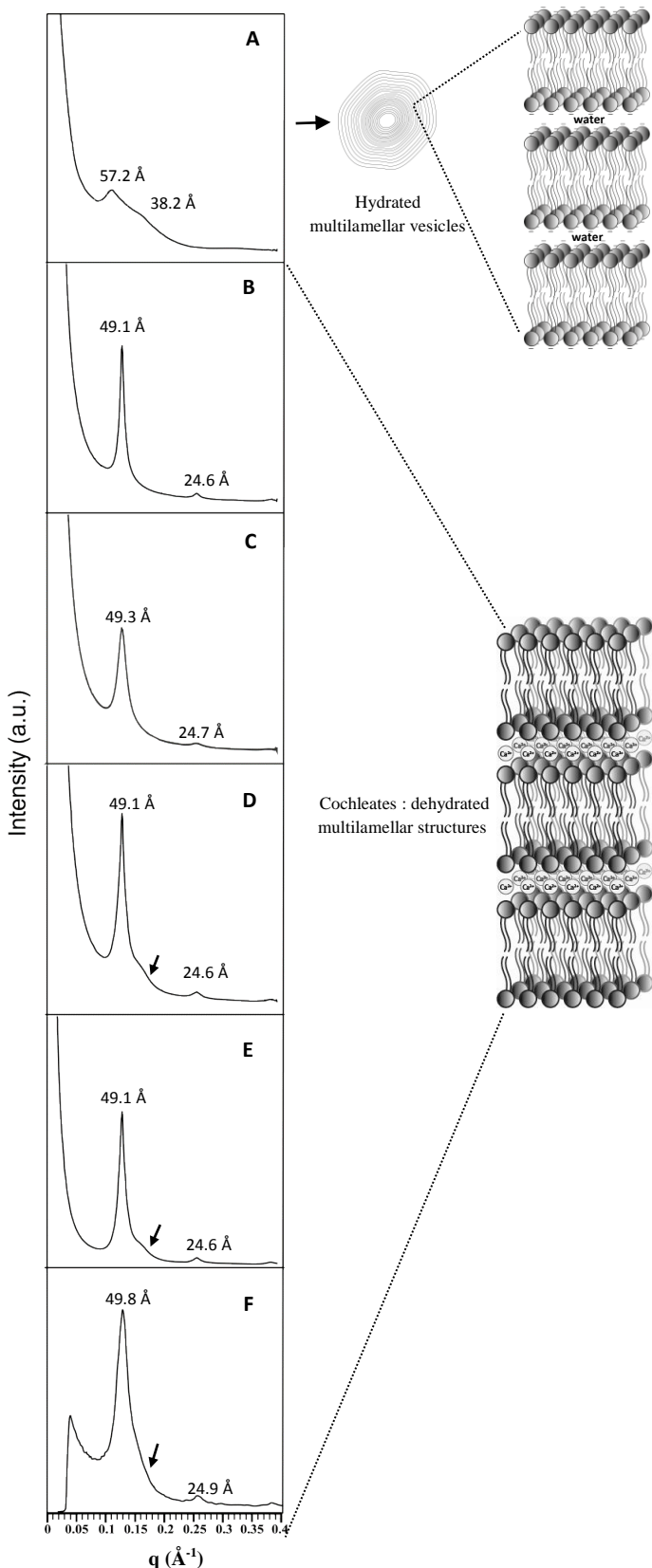


Figure 30. SAXS spectra of Lipoid PSP70 in various formulations (molar proportions).
 A: Lipoid PSP70 as multilamellar vesicles; B: Lipoid PSP70 as cochleates; C: 9 Lipoid PSP70 /2 Cholesterol/ 0.5 AmB as cochleates (F0.5); D: 9 Lipoid PSP70 /2 Cholesterol /1 AmB as cochleates (F1); E: 9 Lipoid PSP70 /2 Cholesterol /2 AmB as cochleates (F2); F: 9 Lipoid PSP70 /2 Cholesterol /3 AmB as cochleates (F3).

These repeat spacings indicate that the cochleates are comprised of dehydrated multilamellar phase assemblies. In this arrangement, the lipid molecules form a well-packed bilayer structure with a multibilayer periodicity, in which the phospholipid head groups are suggested to be oriented parallel to the bilayer plane and the acyl chains are organized in a more confined space (Garidel et al., 2001). The intermembrane space is reduced owing to the attractive interactions between the phosphoserine headgroups and the Ca^{2+} ions that cause considerable changes of the water layer thickness (*i.e.* dehydration). Within the induced topology of this kind of lipid aggregates, Ca^{2+} ions gradually replace water of hydration from the phosphate group forming a tight, anhydrous Ca-lipid chelate. It has been suggested that decreasing in the thickness of the water layer is due to the formation of bridges between the two bilayers (Hauser et al., 1977).

Figure 30C to F demonstrates the formation of cochleates with increasing proportions of the incorporated drug AmB (F0.5, F1, F2 and F3). The cochleates formulated at a constant molar fraction of cholesterol in the bilayers were characterized with a similar interlamellar distance as that for Lipoid PSP70 alone (Fig. 30B). In Figure 30C, the SAXS pattern obtained at a 9/2/0.5 ratio of phospholipid, cholesterol and AmB, the profile was similar to Figure 2B, indicating that the dehydrated lamellar phase was able to accommodate AmB.

As a comparison, formulations made with the synthetic phosphatidylserine DOPS were also examined. Supplementary Figure S4A shows cochleates made from DOPS and cholesterol in 9/1 molar proportions that demonstrate a sharp first-order Bragg peak at 51.7 Å, while a formulation containing DOPS, cholesterol and AmB in 9/1/0.5 molar proportions displayed a peak at 51.2 Å (Supplementary Figure S4B). Therefore, the structures formed by Lipoid PSP70 are similar to those formed by the synthetic phospholipid that has most often been used to form cochleates.

The SAXS patterns shown in Supplementary Figure S1 show that the position of the first-order Bragg peak was not affected by the proportion of cholesterol, at a constant AmB proportion. However, with very high cholesterol content, a small addition peak appeared (indicated by the black arrow in Figure S1E). Therefore, cholesterol contents up to a 9/4 molar ratio with phospholipid does not hamper cochleate formation. However, when the proportion of AmB in Lipoid PSP70 cochleates is increased, a small additional peak can be

seen (indicated by arrows in Figures 30D, E and F), probably due to the formation of a second phase.

Preliminary studies with wide-angle X-ray diffraction (WAXS) did not show any well-defined peaks and could not be interpreted. This was due to the heterogenous nature of the phospholipid as well as the presence of cholesterol, so that no ordered structure could be seen in the plane of the bilayer.

In conclusion, the SAXS results have confirmed the ability of Lipoid PSP70 to form dehydrated multilayer assemblies on interaction with calcium ions in the same way as the synthetic DOPS. They have also defined the limits for the inclusion of cholesterol and AmB in the structures. Complementary studies of stability in the gastric environment and the state of aggregation of AmB will help to clarify whether the appearance of a new phase in the presence of higher proportions of AmB can alter the ability of the cochleates to deliver AmB effectively and to reduce its toxicity.

2.2.4.4 Circular dichroism and UV-visible spectroscopy

The AmB molecule has a particular cyclic structure with seven conjugated double bonds which give rise to intense absorption peaks between 250 and 450 nm. Its spectral properties depend on whether the molecule is in monomeric form, aggregated or complexed with other molecules. In consequence, electronic absorption and CD spectroscopy are useful tools for studying the organization of AmB within formulations (Barwicz et al., 1993; Gaboriau et al., 1997). This is important because the pharmacological activity and the toxic side effects of AmB are strongly dependent on its molecular organization (Barwicz et al., 1992). Therefore, the aggregation state of AmB within the Lipoid PSP70 formulations was investigated. However, samples for UV and CD spectroscopy must be homogeneous and free from highly light-scattering particles to prevent interference (Kelly and Price, 2000). Since the final cochleates do not fulfil these criteria, the measurements were carried out on the cochleates treated with 0.05 M EDTA to reconvert them into liposomes (Pham et al., 2014). Unloaded cochleates treated in the same way were used as blanks.

In Figure 31A, the UV-visible spectrum corresponding to AmB in methanol, shows a small band at 344 nm and pronounced bands at 365, 385 and 406 nm that correspond to the profile of AmB in the monomeric state. On the other hand, for the AmB diluted in water from a high

concentration in DMSO there is a broad intense band around 342 nm, in addition to other bands of low intensity around 368, 387 and 420 nm. All these bands are characteristic of the aggregated state of AmB (Pham et al., 2014). Figure 31A also shows the UV-visible spectrum of AmB-loaded cochleates in which four bands appear at 327 nm, 367 nm, 389 nm, and 415 nm for the F0.5 and F1 formulations and 325 nm, 367 nm, 389 nm, and 415 nm for the F2 and F3 formulations. These spectra differ from that of AmB in the aggregated state, suggesting that a part of the AmB in these formulations is maintained in its monomeric form. The band at 415 nm indicates a complexed form of AmB.

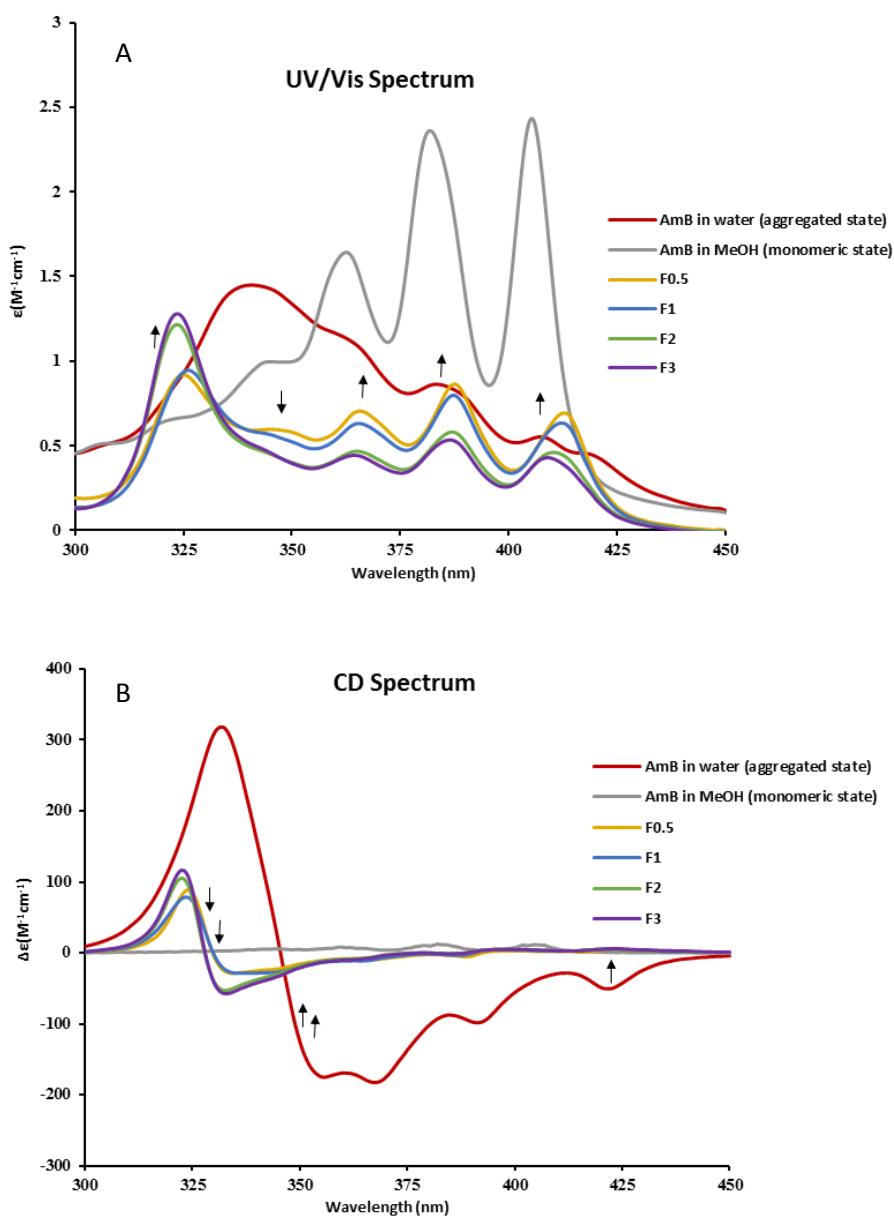


Figure 31. UV spectra ($\epsilon M^{-1} \text{cm}^{-1}$) (A) and CD spectra ($\Delta\epsilon M^{-1} \text{cm}^{-1}$) (B) of AmB-loaded cochleates treated with 0.05M EDTA

The CD spectrum of the aggregated form of AmB is known to display a very intense dichroic doublet with both positive and negative bands (Pham et al., 2014, Shervani et al., 1996, Barwicz et al., 2002). In Figure 31B, the CD spectrum showing AmB diluted in water, the doublet was centered at 334 nm and the negative bands were detected at 370 nm, 394 nm and 424 nm. On the other hand, the monomeric form of AmB in methanol yields a CD spectrum with three weak positive bands at 360 nm, 382 nm, 405 nm, as observed by Pham et al. (2014). The CD spectra of all AmB-loaded cochleate formulations show a much lower intensity of both the positive band and the negative bands compared with AmB in water. Taken together, these findings indicate that some AmB in the formulations is present in the monomeric form. However, the appearance of a strong positive band at 327 nm in the UV-visible spectrum (for F0.5 and F1) or at 325 nm (for F2 and F3) leads to a change in the intense dichroic doublet from 345 nm to 329 nm (or 327 nm), a decrease in intensity of the negative bands and the appearance of a positive band at 425 nm in the CD spectrum. Thus, the molecular state is related to the proportion of AmB in the preparation. These results are characteristic of the interaction of AmB with other components such as cholesterol and/or phospholipid present in the formulation (complexed AmB) (Pham et al., 2014). This suggests that AmB-cochleate formulations contain AmB in both its monomeric and complexed forms and that the complexed form becomes more prevalent as the proportion of AmB increases. These results led us to expect the cochleate formulation to be less toxic than the pharmaceutical form (Fungizone[®]) by avoiding or reducing the self-associated form (aggregated state) (Barwicz et al, 1992).

2.2.4.5 Stability study of AmB-cochleates in SGF medium

Table 8 clearly shows that free AmB, added as a concentrated solution in DMSO, was unstable when exposed to SGF medium, since only about 17% was recovered after 2 h of exposure. In contrast, all formulations of AmB as cochleates show a significant improvement with approximately 81, 73 and 77% recovery for the formulations F0.5, F1 and F2 respectively, while lower protection was observed for the cochleate formulation F3 with the highest proportion of AmB, where the recovery was 64%. Most of the degradation was observed during the first hour, while only a small additional loss during the second hour. Part of the degradation observed during the first hour could be due to the small percentage of AmB that was not tightly associated with the cochleates (see Section 2.2.3.6) and there is probably also some AmB release from the outer layer of the cochleate structure. The higher

susceptibility of the AmB in the formulation containing the highest molar proportion (F3) may be due to the presence of a small amount of a different structure, as indicated by the shoulder in the SAXS pattern in Figure 2F, that does not afford as much protection as the cochleate phase.

Table 8. AmB stability in SGF medium. Formulation compositions are defined in Material and Methods. Values are the percentage of intact AmB recovered, mean \pm SD for 3 determinations.

Formulation	AmB (%) after 1h	AmB (%) after 2h
AmB in DMSO	37 \pm 1	17 \pm 1
F0.5	85 \pm 2	81 \pm 1
F1	81 \pm 1	73 \pm 2
F2	88 \pm 1	77 \pm 2
F3	72 \pm 2	64 \pm 4

2.2.4.6 In-vitro release study

The profiles in Figure 32 show a release of approximately 10%, 6%, 10%, 5% of the encapsulated AmB after incubation for 1h under gastric conditions and 3%, 4%, 5% and 2% after a further 2h of incubation in FaSSIF conditions for formulations F0.5, F1, F2 and F3 respectively; however significant amounts of release of 70%, 56%, 49% and 75% were observed when the second incubation was in FeSSIF intestinal conditions. These values indicate the ability of the cochleates to retain AmB under SGF and fasting conditions (FaSSIF) but to release it in presence of a high concentration of bile salts (FeSSIF). It is known that bile salts form mixed micelles with lipids and disrupt lipid-based drug delivery systems (Andrieux et al. 2009) and similar behavior was observed by Pham et al. (2014) for DOPS-based cochleates. The degree of release in FeSSIF differed between the formulations; the highest release being obtained for the formulation with the lowest molar proportion of AmB (F0.5) and for that with the highest (F3). This could be explained by two phenomena acting at the same time. One is the strength of the association of AmB with the lipids in cochleates which would be lowest with the highest proportion of AmB to lipid, as already shown by the reduced protection of AmB in formulation F3 (Table 8). The other might be the

total surface area developed by the formulation. Since the experiments were carried out at a fixed concentration of AmB, for F0.5 a large number of particles were present, giving a higher surface area to interact with bile salts. Whatever the release from individual formulations, it is clear from the results that AmB release is greatly increased in “fed” conditions. It is interesting to note that mixed lipid-bile salt micelles have been shown to promote the intestinal absorption of AmB (Dangi et al., 1998).

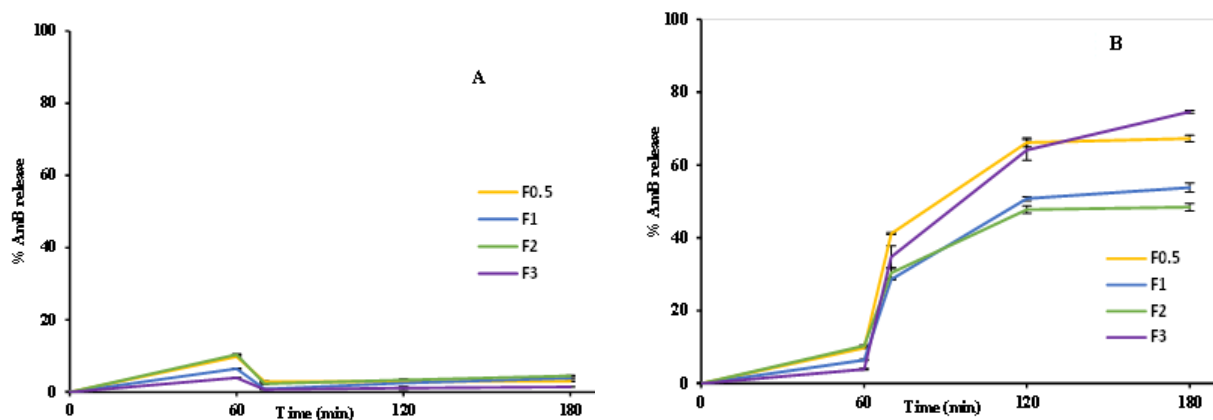


Figure 32. Release profiles of AmB from different formulations in FASSIF and FeSSIF media. The initial AmB concentration was 10 µg/mL. Values are expressed as mean ± SD (n=3).

2.2.4.7 Effects of AmB-loaded cochleates on Caco2 cell viability

As shown in Figure 33, none of the formulations tested reduced Caco2 viability, as determined by MTT reduction, by more than 30% during 24h of exposure. A slight increase in Caco2 cell viability was observed with the F0 and F0.5 formulations at 100 µg/mL after 24 h of exposure, probably due to the higher lipid load that favors cell growth (Hossain et al., 2006). There were no significant differences between F0.5, the formulation with the lowest proportion of AmB and F0 at the same lipid concentrations without AmB. However, for the formulations with higher AmB proportions, F1, F2 and F3, some significant reductions of viability were observed after exposure to at 100 µg/mL of AmB when compared to untreated controls were observed, especially at the highest AmB concentration (P<0.05, as indicated on Figure 5). However, the viability was never lower than 80% with the cochleate formulations, whatever the concentration tested. The pharmaceutical formulation, Fungizone® also reduced

viability compared to untreated controls at concentration of 1 $\mu\text{g}/\text{mL}$ and higher and was slightly more toxic than the cochleate formulations.

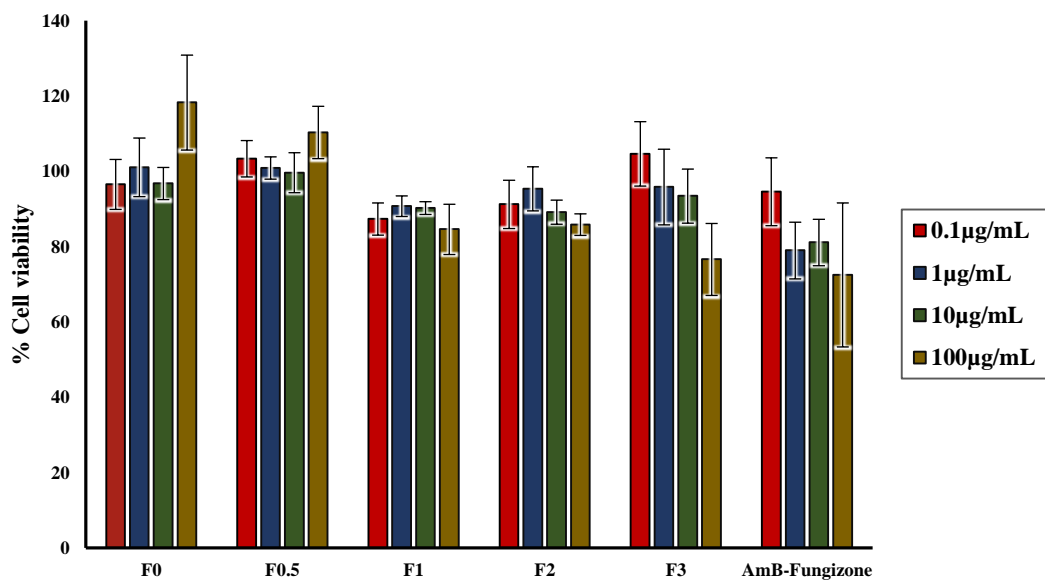


Figure 33. Cytotoxic effects of AmB-loaded cochleates on Caco-2 cell monolayers after 24h as a function of concentration, determined by MTT reduction. Values are expressed as percentages of untreated controls, mean \pm SD of three experiments. * P < 0.05 for comparison with untreated control, # P < 0.05 for comparison with Fungizone at the same concentration, Student's unpaired two-tailed t test.

These results were confirmed by measurements of transepithelial electrical resistance, as shown in Table 9. Caco2 cell monolayers after at least 21 days of culture were incubated for 4h with AmB at 100 $\mu\text{g}/\text{mL}$ as different formulations. The pharmaceutical formulation Fungizone[®] reduced the TEER to 7% of its original value over this period. The cochleate formulations also reduced the TEER, to between 57 and 72% of the starting value, but the resistance remained higher than 200 $\Omega \cdot \text{cm}^2$ that is considered to indicate intact monolayers (Hubatsch et al., 2007).

These observations are consistent with those obtained from circular dichroism that the association with lipids in the cochleates can reduce the proportion of toxic forms of AmB. They are also in agreement with many other studies that demonstrate reduced toxicity of lipid-based formulations of AmB compared with Fungizone[®] in many different cells types; for example in alveolar epithelial cells (Menotti et al., 2017).

Table 9. Transepithelial electrical resistance (TEER) of Caco2 monolayers cultivated on inserts for at least 21 days after 4h of incubation with 100 µg/mL Amphotericine B in different formulations. Values are expressed as mean ± SD of measurements from 3 inserts.

Formulation	TEER (Ω.cm ²)	
	Before incubation	After incubation
AmB-Fungizone®	486 ± 8	34 ± 3
F0.5	435 ± 5	249 ± 8
F1	440 ± 10	317 ± 10
F2	454 ± 7	310 ± 30
F3	452 ± 10	322 ± 20

2.2.4.8 Interactions of Rhodamine-labeled cochleates with Caco2 cells

The interaction of the cochleates with the intestinal cells was followed by labeling unloaded cochleates with Rho-PE while the cytoskeleton of the cells was labeled with FITC-phalloidin. In Figure 34 A1 and B1, the image in the fluorescein channel shows the typical Caco2 cell surface. The rhodamine channel in Figure A2, after exposure of the cells to Rho-PE as micelles in DMSO, shows few fluorescent objects while in Figure B2 after exposure to Rho-PE as cochleates, there is a considerable fluorescence signal, indicating accumulation of the Lipoid PSP70 cochleates on the cell surface. When images were recorded at the level of the cell interior (Figure 34 C and D), the fluorescein channel again showed the confluent Caco2 cells (Figure 34 C1 and D1), while the rhodamine channel showed very low fluorescence in the case of Rho-PE-DMSO micelles (Figure 34 C2) whereas the fluorescence signal from Rho-PE-cochleates Figure 34 (D2) was slightly higher.

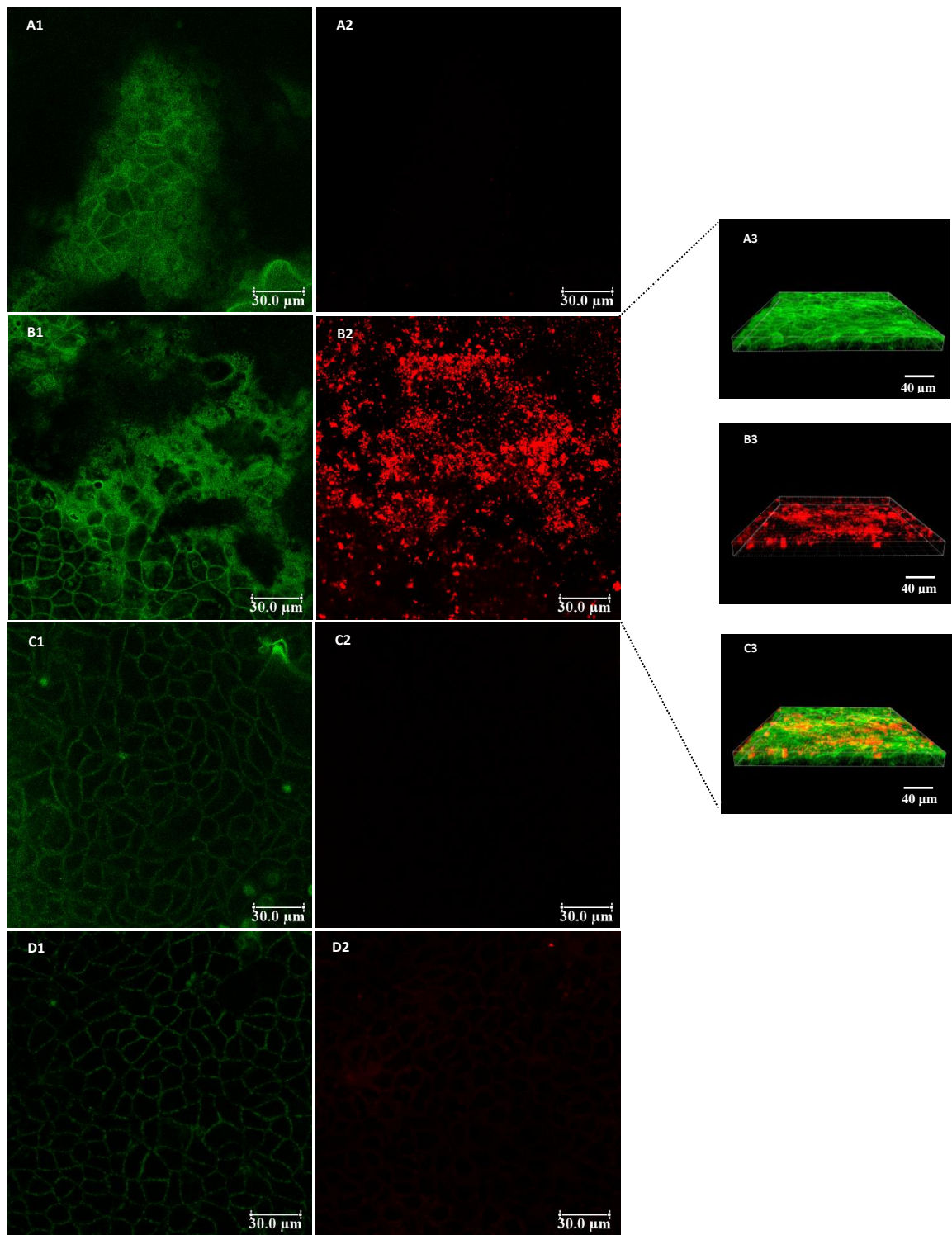


Figure 34. Confocal microscopy images of Caco2 cells taken at the cell surface (A and B) and in the cell interior (C and D). Fluorescein emission (1) and Rhodamine emission (2) after exposure for 2h to Rhodamine-PE micelles (A and C) and Rhodamine-PE cocheates (B and D). On the left, 3D images showing the possible absorption and fusion of the cocheates on the cell membrane: Fluorescein emission (A3), Rhodamine emission (B3) and overlay (C3).

2.2.4.9 Uptake and transport of AmB by Caco2 cell monolayers

The TEER values were unchanged after 6 hours of incubation contact with AmB-loaded cochleates, confirming the MTT results showing that the drug in cochleate form was not highly toxic to Caco2 cells. Table 10 shows that the accumulation of AmB within the cells depended on the proportion of AmB in the cochleates, although the same amount of AmB was added in each case. For the formulations F0.5, F1 and F2, the percentage of added AmB recovered from the cells increased with the proportion of AmB, reaching almost 50% with the cochleates composed of Lipoid PSP70, cholesterol and AmB in 9/2/2 molar proportions. However, the percentage captured decreased when the proportions were 9/2/3 (F3). The amount of AmB measured within the cell monolayer was between 34 and 71 µg.

A similar relationship with AmB proportion in the cochleates was seen when the amount that had been transported across the monolayer was considered. However, the percentage of added AmB that reached the baso-lateral compartment was very low, with a maximum of 0.07% with the formulation F2, corresponding to a concentration of 103 ng/mL, but remained above the limit of quantification of the HPLC method of 25 ng/mL. Taken with the results from confocal microscopy, this suggests that the cochleates can be adsorbed onto the cell surface, followed by fusion and AmB transfer into the cell membranes, to be released later. An increase in the proportion of AmB could favor transfer, but at the highest proportion of AmB (F3) the lower proportion of phosphatidylserine may decrease the ability of the cochleates to fuse with cell membranes. However, it should be taken into account that Caco2 cells do not produce mucus and this could influence cochleate adherence *in vivo*. On one hand, the mucus could contribute to trapping cochleates on the surface of the epithelium; on the other hand, the large size of the cochleates could hamper their diffusion through the mucus later to the cell surface.

These results are consistent with the hypothesis of Zarif et al. (2000) that cochleate structures could improve the bioavailability of drugs by means of adhesion of the particles to the intestinal epithelium followed by fusion and incorporation of phosphatidylserine into the cell membrane to later release the encapsulated drug. Figure 35 shows a schematic representation of this hypothesis.

After absorption through the intestinal epithelium AmB would be expected to bind to plasma lipoproteins (Wasan et al., 1998) and be carried to the liver via the hepatic portal vein. This

“first-pass effect” is often a disadvantage for orally administered drugs but in the case of leishmaniasis treatment it is an advantage because the liver is the main organ harboring the parasites. As pointed out in a review by Serrano and Lalatsar (2017), plasma concentrations after oral administration of AmB formulations are not necessarily the best indication of efficacy; organ concentrations are also important. Thus, although the cochleate formulations that have been tested *in vivo* so far do not lead to high plasma concentrations, they can produce high concentrations in the liver, spleen and lungs. Interestingly, organ concentrations were found to be higher in mice infected with *Candida albicans* than in healthy animals (Mannino and Perlin, 2015).

The administration of cochleates containing AmB in models of fungal infection in mice also showed lower toxicity than Fungizone® (reviewed by Aigner and Lass-Flörl, 2020). Furthermore, in clinical trials, AmB-loaded cochleates were well tolerated in healthy volunteers and no serious side effects were observed in patients with fungal infections in phase II trials (Aigner and Lass-Flörl, 2020). We could therefore expect that our system, with similar physicochemical properties, would display similar *in-vivo* efficacy and tolerability in the case of leishmaniasis. This will be the subject of future investigation.

Table 10. Uptake of AmB into Caco-2 cell monolayers grown on inserts and passage to the lower compartment. Inserts were incubated for 6h with 100 µg/mL AmB in various cochleate formulations added to the upper compartment. Results are expressed as the percentage of added AmB found into cell monolayer and in the lower compartment as the mean ± SD of 3 inserts.

Formulation	AmB in the cell monolayer (%)	AmB in the lower compartment (%)
F0.5	23 ± 3	Non-detectable
F1	31 ± 2	0.019 ± 0.003
F2	47 ± 2	0.069 ± 0.008
F3	43 ± 3	0.035 ± 0.011

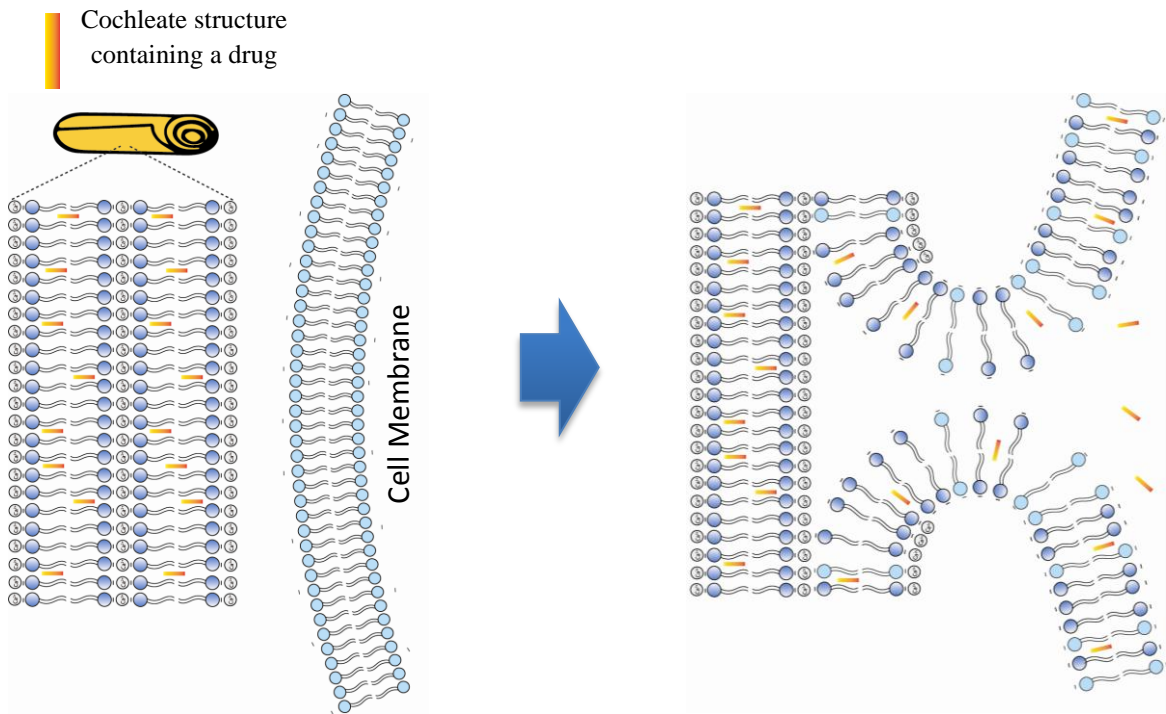


Figure 35. Schematic representation of the interaction of cochleate particles with the cell membrane.

2.2.5 Conclusion

The study shows that it is possible to prepare cochleates containing AmB from an inexpensive and biocompatible naturally occurring phospholipid, Lipoid PSP70, while retaining the morphology, internal structure described for cochleates prepared from more costly synthetic phospholipids such as DOPS. Synchrotron SAXS experiments gave direct evidence the supramolecular organization of the multicomponent cochleate assemblies loaded with AmB. Furthermore, the entrapment efficiency, low toxicity, improved gastric stability and delayed *in-vitro* release of AmB from loaded cochleates were also promising for the oral administration. The formulation F2 (9 Lipoid PSP70 / 2 cholesterol / 0.06 vitamin E / 2 AmB) contains a high proportion of AmB compared with cochleate formulations previously described in the literature. Studies on Caco2 cell monolayers have thrown light on the possible mechanism of action of these drug delivery systems: incorporation of phosphatidylserine into the cell membrane and the subsequent release of the drug into the cell. The use of a naturally occurring phosphatidylserine from soy that is considerably less

expensive than the synthetic phospholipid DOPS means that further experiments can be carried out at reduced cost. These should allow better understanding of cochleates, such as their uptake mechanism and to investigate the improved bioavailability of AmB and activity *in-vivo* after oral administration. The lower raw material cost also allows these systems to be considered for use in developing countries. In this respect, another important point is the ability of cochleates to undergo freeze-drying and reconstitution without any cryoprotector being necessary. All these factors suggest that AmB-loaded cochleates would be a promising tool for oral therapy of leishmaniasis in the regions where it is endemic.

Acknowledgements

A. L-C. received a Ph.D. grant from FONDECYT, Peru. A.A. acknowledges the allocation of beam time at Synchrotron SOLEIL (Saint Aubin, France) through the project 20191836 and the scientific and technical support of Dr. T. Bizien at the SWING beamline. The authors would like to thank Audrey Solgadi (Université Paris-Saclay, Inserm, CNRS, Ingénierie et Plateformes au Service de l’Innovation Thérapeutique) for help with the analysis of phospholipids in Lipoid PSP70; Claire Boulogne and Cynthia Gillet (Imagerie-Gif) for help with electron microscopy; Claire Gueutin (Institut Galien Paris-Saclay) for help with the analysis of AmB. Nicolas Huang and Baptiste Robin (Institut Galien Paris-Saclay) for help with morphogranulometry. We thank Jean-Jacques Vachon (Institut Galien Paris-Saclay) for help with X-ray diffraction experiments and also Claudie Bourgaux (Institut Galien Paris-Saclay) for performing additional SAXS experiments. We are grateful to Christina Sizun (Université Paris-Saclay, CNRS, Institut de Chimie des Substances Naturelles, UPR 2301) for preliminary studies with circular dichroism and François-Xavier Legrand for useful discussions. We thank Joelle Salameh (Mécanismes cellulaires et moléculaires d’adaptation au stress et cancérogénèse, Faculté de Pharmacie, Université Paris-Saclay) for the gift of FITC-phalloidin.

This work did not receive any specific grant from funding agencies in the public, commercial or not-for-profit sectors for running costs

References

- Aigner, M., & Lass-Flörl, C. (2020). Encocleated Amphotericin B: is the oral availability of amphotericin B finally reached? *Journal of Fungi*, 6(2), 66. <https://doi.org/10.3390/jof6020066>
- Andrieux, K., Forte, L., Lesieur, S., Paternostre, M., Ollivon, M. & Grabielle-Madelpont C. (2009). Solubilisation of dipalmitoylphosphatidylcholine bilayers by sodium taurocholate: A model to study the stability of liposomes in the gastrointestinal tract and their mechanism of interaction with a model bile salt, *European Journal of Pharmaceutics and Biopharmaceutics*, 71 346-355. <https://doi.org/10.1016/j.ejpb.2008.09.004>
- Barwicz, J, Christian, S., & Gruda, I. (1992). Effects of the aggregation state of amphotericin B on its toxicity to mice. *Antimicrobial Agents and Chemotherapy*, 36(10), 2310–2315. <https://doi.org/10.1128/AAC.36.10.2310>
- Barwicz, Joanna, Beauregard, M., & Tancrède, P. (2002). Circular dichroism study of interactions of Fungizone or AmBisome forms of amphotericin B with human low density lipoproteins. *Biopolymers*, 67(1), 49–55. <https://doi.org/10.1002/bip.10042>
- Barwicz, Joanna, Gruszecki, W. I., & Gruda, I. (1993). Spontaneous organization of amphotericin B in aqueous medium. *Journal of Colloid and Interface Science*, 158(1), 71–76. <https://doi.org/10.1006/jcis.1993.1230>
- Berman, J. (2005). Recent developments in leishmaniasis: epidemiology, diagnosis, and treatment. *Current Infectious Disease Reports*, 7(1), 33–38. <https://doi.org/10.1007/s11908-005-0021-1>
- Bozó, T., Wacha, A., Mihály, J., Bóta, A., & Kellermayer, M. S. Z. (2017). Dispersion and stabilization of cochleate nanoparticles. *European Journal of Pharmaceutics and Biopharmaceutics*, 117, 270–275. <https://doi.org/10.1016/j.ejpb.2017.04.030>
- Chattopadhyay, A., & Jafurulla, Md. (2011). A novel mechanism for an old drug: Amphotericin B in the treatment of visceral leishmaniasis. *Biochemical and Biophysical Research Communications*, 416(1–2), 7–12. <https://doi.org/10.1016/j.bbrc.2011.11.023>
- Chaudhari, M. B., Desai, P. P., Patel, P. A., & Patravale, V. B. (2016). Solid lipid nanoparticles of amphotericin B (AmbiOnp): In vitro and in vivo assessment towards safe and effective oral treatment module. *Drug Delivery and Translational Research*, 6(4), 354–364. <https://doi.org/10.1007/s13346-015-0267-6>
- Chen, Y.-C., Su, C.-Y., Jhan, H.-J., Ho, H.-O., & Sheu, M.-T. (2015). Physical characterization and in vivo pharmacokinetic study of self-assembling amphotericin B-loaded lecithin-based mixed polymeric micelles. *International Journal of Nanomedicine*, 10, 7265–7274. <https://doi.org/10.2147/IJN.S95194>
- Dangi, J.S., Vyas, S.P. & Dixit, V.K. (1998) Effect of various lipid-bile salt mixed micelles on the intestinal absorption of Amphotericin B in rat, Drug Develop. Ind. Pharm., 24 631-635. <https://doi.org/10.3109/03639049809082364>

David, G. and Pérez, J. (2009) Combined sampler robot and high-performance liquid chromatography: a fully automated system for biological small-angle X-ray scattering experiments at the synchrotron SOLEIL SWING beamline. *J. Applied Crystallography*, 42, 892–900. <https://doi:10.1107/S0021889809029288>.

Espada, R., Valdespina, S., Alfonso, C., Rivas, G., Ballesteros, M. P., & Torrado, J. J. (2008). Effect of aggregation state on the toxicity of different amphotericin B preparations. *International Journal of Pharmaceutics*, 361(1), 64–69. <https://doi.org/10.1016/j.ijpharm.2008.05.013>

Faustino, & Pinheiro. (2020). Lipid systems for the delivery of Amphotericin B in antifungal therapy. *Pharmaceutics*, 12(1), 29. <https://doi.org/10.3390/pharmaceutics12010029>

Gaboriau, F., Chéron, M., Petit, C., & Bolard, J. (1997). Heat-induced superaggregation of amphotericin B reduces its in vitro toxicity: A new way to improve its therapeutic index. *Antimicrobial Agents and Chemotherapy*, 41(11), 2345–2351. <https://doi.org/10.1128/AAC.41.11.2345>

Garidel, P., Richter, W., Rapp, G., & Blume, A. (2001). Structural and morphological investigations of the formation of quasi-crystalline phases of 1,2-dimyristoyl-sn-glycero-3-phosphoglycerol (DMPG). *Physical Chemistry Chemical Physics*, 3(8), 1504–1513. <https://doi.org/10.1039/b009881g>

Hamill, R. J. (2013). Amphotericin B formulations: A comparative review of efficacy and toxicity. *Drugs*, 73(9), 919–934. <https://doi.org/10.1007/s40265-013-0069-4>

Hauser, H., Finer, E. G., & Darke, A. (1977). Crystalline anhydrous Ca-phosphatidylserine bilayers. *Biochemical and Biophysical Research Communications*, 76(2), 267–274. [https://doi.org/10.1016/0006-291X\(77\)90721-5](https://doi.org/10.1016/0006-291X(77)90721-5)

Hossain, Z., Konishi, M., Hosokawa, M., & Takahashi, K. (2006). Effect of polyunsaturated fatty acid-enriched phosphatidylcholine and phosphatidylserine on butyrate-induced growth inhibition, differentiation and apoptosis in Caco-2 cells. *Cell Biochemistry and Function*, 24(2), 159–165. <https://doi.org/10.1002/cbf.1202>

Huang, W., Zhang, Z., Han, X., Tang, J., Wang, J., Dong, S., & Wang, E. (2002). Ion channel behavior of Amphotericin B in sterol-free and cholesterol- or ergosterol-containing supported phosphatidylcholine bilayer model membranes investigated by electrochemistry and spectroscopy. *Biophysical Journal*, 83(6), 3245–3255. [https://doi.org/10.1016/S0006-3495\(02\)75326-5](https://doi.org/10.1016/S0006-3495(02)75326-5)

Hubatsch, I., Ragnarsson, E. G. E., & Artursson, P. (2007). Determination of drug permeability and prediction of drug absorption in Caco-2 monolayers. *Nature Protocols*, 2(9), 2111–2119. <https://doi.org/10.1038/nprot.2007.303>

Hui, S. W., Boni, L. T., Stewart, T. P., & Isac, T. (1983). Identification of phosphatidylserine and phosphatidylcholine in calcium-induced phase separated domains. *Biochemistry*, 22(14), 3511–3516. <https://doi.org/10.1021/bi00283a032>

Ibrahim, F., Sivak, O., Wasan, E. K., Bartlett, K., & Wasan, K. M. (2013). Efficacy of an oral and tropically stable lipid-based formulation of Amphotericin B (iCo-010) in an experimental mouse model of systemic candidiasis. *Lipids in Health and Disease*, 12(1), 158. <https://doi.org/10.1186/1476-511X-12-158>

Jain, S., Yadav, P., Swami, R., Swarnakar, N. K., Kushwah, V., & Katiyar, S. S. (2018). Lyotropic liquid crystalline nanoparticles of Amphotericin B: Implication of phytantriol and glyceryl monooleate on bioavailability enhancement. *AAPS PharmSciTech*, 19(4), 1699–1711. <https://doi.org/10.1208/s12249-018-0986-3>

Jin, T., Mannino, R. & Zarif, L. (2000). Nanocochleate formulations, process of preparation and method of delivery of pharmaceutical agents. US Patent US6153217A <https://patents.google.com/patent/US6153217A/en>.

Kelly, S. M. K. and Price N. C. (2000). The use of circular dichroism in the investigation of protein structure and function. *Current Protein & Peptide Science*, 1. <http://www.eurekaselect.com/81742/article>

Khan, M., Nadhman, A., Shah, W., Khan, I., & Yasinzai, M. (2019). Formulation and characterisation of a self-nanoemulsifying drug delivery system of amphotericin B for the treatment of leishmaniasis. *IET Nanobiotechnology*, 13(5), 477–483. <https://doi.org/10.1049/iet-nbt.2018.5281>

Kowapradit, J., Opanasopit, P., Ngawhirunpat, T., Apirakaramwong, A., Rojanarata, T., Ruktanonchai, U., & Sajomsang, W. (2010). In vitro permeability enhancement in intestinal epithelial cells (Caco-2) monolayer of water soluble quaternary ammonium chitosan derivatives. *AAPS PharmSciTech*, 11(2), 497–508. <https://doi.org/10.1208/s12249-010-9399-7>

Lu, R., Hollingsworth, C., Qiu, J., Wang, A., Hughes, E., Xin, X., Konrath, K. M., Elsegeiny, W., Park, Y.-D., Atakulu, L., Craft, J. C., Tramont, E. C., Mannino, R., & Williamson, P. R. (2019). Efficacy of oral encochleated Amphotericin B in a mouse model of cryptococcal meningoencephalitis. *MBio*, 10(3). <https://doi.org/10.1128/mBio.00724-19>

Mannino, R. & Perlin, D. (2015). Oral dosing of encochleated amphotericin B (CAmB): rapid drug targeting to infected tissues in mice with invasive candidiasis. Scientific Presentations & Publications Matinas Biopharma 2015. Available online: <https://www.matinasbiopharma.com/media/scientific-presentations-publications> (accessed on 21 April 2021).

Ménez, C., Buyse, M., Besnard, M., Farinotti, R., Loiseau, P. M., & Barratt, G. (2006a). Interaction between miltefosine and amphotericin B: consequences for their activities towards intestinal epithelial cells and *Leishmania donovani* promastigotes *in vitro*. *Antimicrobial Agents and Chemotherapy*, 50(11), 3793–3800. <https://doi.org/10.1128/AAC.00837-06>

Ménez, C., Buyse, M., Chacun, H., Farinotti, R., & Barratt, G. (2006b). Modulation of intestinal barrier properties by miltefosine. *Biochemical Pharmacology*, 71(4), 486–496. <https://doi.org/10.1016/j.bcp.2005.11.008>

Menotti, J., Alanio, A., Sturny-Leclere, A., Vitry S., Sauvage, F., Barratt, G. & Bretagne S. (2017). A cell impedance-based real-time *in vitro* assay to assess the toxicity of amphotericin B formulations. *Toxicology and Applied Pharmacology*, 334, 18-23. <https://doi.org/10.1016/j.taap.2017.08.017>

Moulin, M., Solgadi, A., Veksler, V., Garnier, A., Ventura-Clapier, R., & Chaminade, P. (2015). Sex-specific cardiac cardiolipin remodelling after doxorubicin treatment. *Biology of Sex Differences*, 6(1), 20. <https://doi.org/10.1186/s13293-015-0039-5>

Nagarsekar, K., Ashtikar, M., Steiniger, F., Thamm, J., Schacher, F., & Fahr, A. (2016). Understanding cochleate formation: Insights into structural development. *Soft Matter*, 12(16), 3797–3809. <https://doi.org/10.1039/C5SM01469G>

Nagarsekar, K., Ashtikar, M., Steiniger, F., Thamm, J., Schacher, F. H., & Fahr, A. (2017). Micro-spherical cochleate composites: Method development for monodispersed cochleate system. *Journal of Liposome Research*, 27(1), 32–40. <https://doi.org/10.3109/08982104.2016.1149865>

No, J. H. (2016). Visceral leishmaniasis: Revisiting current treatments and approaches for future discoveries. *Acta Tropica*, 155, 113–123. <https://doi.org/10.1016/j.actatropica.2015.12.016>

Rochelle do Vale Morais, A.R., Silva, A. L., Cojean, S., Balaraman, K., Bories, C., Pomel, S., Barratt, G., do Egito, E. S. T., & Loiseau, P. M. (2018a). In-vitro and in-vivo antileishmanial activity of inexpensive Amphotericin B formulations: Heated Amphotericin B and Amphotericin B-loaded microemulsion. *Experimental Parasitology*, 192, 85–92. <https://doi.org/10.1016/j.exppara.2018.07.017>

Pawar, A., Bothiraja, C., Shaikh, K., & Mali, A. (2015). An insight into cochleates, a potential drug delivery system. *RSC Advances*, 5(99), 81188–81202. <https://doi.org/10.1039/C5RA08550K>

Pham, T. T. H., Barratt, G., Michel, J. P., Loiseau, P. M., & Saint-Pierre-Chazalet, M. (2013). Interactions of antileishmanial drugs with monolayers of lipids used in the development of amphotericin B–miltefosine-loaded nanocochleates. *Colloids and Surfaces B: Biointerfaces*, 106, 224–233. <https://doi.org/10.1016/j.colsurfb.2013.01.041>

Pham, T. T. H., Gueutin, C., Cheron, M., Abreu, S., Chaminade, P., Loiseau, P. M., & Barratt, G. (2014). Development of antileishmanial lipid nanocomplexes. *Biochimie*, 107, 143–153. <https://doi.org/10.1016/j.biochi.2014.06.007>

Santangelo, R., Paderu, P., Delmas, G., Chen, Z.-W., Mannino, R., Zarif, L., & Perlin, D. S. (2000). Efficacy of oral cochleate-Amphotericin B in a mouse model of systemic candidiasis. *Antimicrobial Agents and Chemotherapy*, 44(9), 2356–2360. <https://doi.org/10.1128/AAC.44.9.2356-2360.2000>

Serrano, D. R., Lalatsa, A., Dea-Ayuela, M. A., Bilbao-Ramos, P. E., Garrett, N. L., Moger, J., Guarro, J., Capilla, J., Ballesteros, M. P., Schätzlein, A. G., Bolás, F., Torrado, J. J., & Uchegbu, I. F. (2015). Oral particle uptake and organ targeting drives the activity of Amphotericin B nanoparticles. *Molecular Pharmaceutics*, 12(2), 420–431. <https://doi.org/10.1021/mp500527x>

Shervani, Z., Etori, H., Taga, K., Yoshida, T., & Okabayashi, H. (1996). Aggregation of polyene antibiotics as studied by electronic absorption and circular dichroism spectroscopies. *Colloids and Surfaces B: Biointerfaces*, 7(1), 31–38. [https://doi.org/10.1016/0927-7765\(96\)01283-0](https://doi.org/10.1016/0927-7765(96)01283-0)

Thanki, K., Date, T., & Jain, S. (2019). Improved oral bioavailability and gastrointestinal stability of Amphotericin B through fatty acid conjugation approach. *Molecular Pharmaceutics*, 16(11), 4519–4529. <https://doi.org/10.1021/acs.molpharmaceut.9b00662>

Torres-Guerrero, E., Quintanilla-Cedillo, M. R., Ruiz-Esmenjaud, J., & Arenas, R. (2017). Leishmaniasis: A review. *F1000Research*, 6, 750. <https://doi.org/10.12688/f1000research.11120>.

Wasan, K.M., Kennedy, A.L., Cassidy, S.M., Ramaswamy, M., Holtorf, L. Chou, J.W. & Pritchard, P.H. (1998). Pharmacokinetics, distribution in serum lipoproteins and tissues, and renal toxicities of amphotericin B and Amphotericin B Lipid Complex in a hypercholesterolemic rabbit model: single-dose studies. *Antimicrobial Agents and Chemotherapy*, 42(12): 3146–3152. <https://doi.org/10.1128/AAC.42.12.3146>.

Yang, Z., Chen, M., Yang, M., Chen, J., Fang, W., & Xu, P. (2014). Evaluating the potential of cubosomal nanoparticles for oral delivery of amphotericin B in treating fungal infection. *International Journal of Nanomedicine*, 9, 327–336. <https://doi.org/10.2147/IJN.S54967>

Zarif, L., Graybill, J. R., Perlin, D., Najvar, L., Bocanegra, R., & Mannino, R. J. (2000). Antifungal activity of Amphotericin B cochleates against Candida albicans infection in a mouse model. *Antimicrobial Agents and Chemotherapy*, 44(6), 1463–1469. <https://doi.org/10.1128/AAC.44.6.1463-1469.2000>

2.3 Chapitre 3 : Etudes *in vivo* des cochléates à base de phospholipides naturels chargés en AmB (article).

Dans ce chapitre, nous présentons les études de pharmacocinétique et de l'activité *in vivo* d'une des formulations développées à base du phospholipide naturel Lipoid PS P 70 contenant l'AmB. La formulation étudiée correspond aux cochléates avec les proportions LipoidPSP/Cho/AmB/VitE (9:2:2:0.06) préparés par la méthode de l'hydrogel décrite dans le chapitre 2.

Les études de pharmacocinétique ont été réalisées sur un modèle de rat Wistar mâle (Zou et al., 2017) ayant reçu une seule dose d'AmB. Des prélèvements sanguins ont été réalisés pendant 48h et le taux d'AmB dans le plasma a été déterminé par HPLC. Quatre groupes de rat ont été constitués comme suivant :

- Groupe 1 : AmB-Cochléates en gélules gastro-résistantes (7,5 mg AmB/kg) par voie orale.
- Groupe 2 : AmB-Cochléates en suspension tamponnée avec Tris 0,2 M pH 8,4 (7,5 mg AmB/kg) par voie orale.
- Groupe 3 : AmBisome® (7,5 mg AmB/kg) par voie orale.
- Groupe 4 : AmBisome® (1 mg AmB/kg) par voie intraveineuse.

A la fin de l'expérience, des analyses des organes (foie, rate, poumon et rein) ont été réalisées afin de déterminer la biodistribution de la molécule active. L'étude de l'activité *in vivo* a été réalisée à l'aide d'un modèle de leishmaniose viscérale chez la souris Balb/C (Campos Vieira et al., 2011). Des souris ont été infectées et, une semaine plus tard, divisées en 6 groupes de traitement :

- Groupe 1: Témoins, sans traitement.
- Groupe 2: AmBisome® (1 mg/kg) par voie intraveineuse.
- Groupe 3: Cochléates sans principe actif en suspension tamponnée Tris 0,2 M pH 8,4, (masse de cochléates équivalente à 20 mgAmB/kg/jour sous forme de cochléates) par voie orale.
- Groupe 4: Cochléates chargés en AmB en suspension tamponnée avec Tris 0,2 M pH 8,4 (5 mgAmB/kg/jour) par voie orale,

- Groupe 5: Cochléates chargés en AmB en suspension tamponnée Tris 0,2 M pH 8,4 (20 mg/kg/jour) voie orale.
- Groupe 6: Cochléates chargés en AmB dans des gélules gastro-résistantes (5mg/kg/jour) par voie orale.

Trois administrations ont été réalisées à 48h d'intervalle puis quatorze jours après l'infection, les animaux ont été euthanasiés par dislocation cervicale et les foies ont été prélevés. Des frottis ont été effectués et colorés avec du Giemsa afin de compter les parasites et déterminer l'efficacité de chaque traitement.

**PHARMACOKINETIC STUDIES, BIODISTRIBUTION AND EVALUATION
ACTIVITY OF AGAINST LEISHMANIASIS OF AmB-LOADED COCHLEATES
BASED ON NATURALLY OCCURRING PHOSPHOLIPIDS.**

**Antonio LIPA CASTRO¹; Catherine CAILLEAU¹; Sébastien POMEL²; Philippe LOISEAU²;
Indira DENNEMONT²; Gillian BARRATT¹**

¹ Institut Galien Paris-Saclay, UMR CNRS 8612, Faculty of Pharmacy,

Univ. Paris-Saclay, 92296 Chatenay-Malabry Cedex, France

² BioCIS, UMR CNRS 8076, Faculty of Pharmacy,

Univ. Paris-Saclay, 92296 Chatenay-Malabry Cedex, France

Abstract

This study describes the pharmacokinetic profile in rats and the antiparasitic activity in a mouse model of visceral leishmaniasis of a cochleate formulation prepared from naturally occurring phospholipid and loaded with Amphotericin B (AmB). The formulation was administered either as a buffered suspension or in enteric-coated capsules. In both cases, the AmB-loaded cochleates provided lower concentrations of Amphotericin B in the plasma than AmBisome®, when all formulations were administered orally at 7.5mg AmB/kg. However, an accumulation in the organs of interest (liver, spleen) was observed for both presentations of cochleates than AmBisome® after oral administration. Furthermore, slow elimination and higher accumulation of AmB in key organs were observed when AmB-loaded cochleates were administered in enteric-coated capsules. Finally, AmB-loaded cochleates administered as a suspension at a higher dose (20mg/kg) exhibited significant antiparasitic activity while AmB-loaded cochleates in enteric-coated capsules at the lower dose (5mg/kg) presented a slightly higher significant activity. This cochleate formulation of AmB that could be produced at a cost accessible for developing countries shows promise for the treatment of visceral leishmaniasis.

2.3.1 Introduction

Amphotericin B (AmB) is the first choice of drug to treat visceral leishmaniasis due to its very high cure rate and almost complete absence of resistance (Berman, 2005, Serrano et al., 2015). Despite its efficacy, AmB, as its conventional form Fungizone® (micellar dispersion), shows a narrow therapeutic window that can cause several side effects, especially nephrotoxicity (Faustino & Pinheiro, 2020). In addition, all formulations currently available must be administrated by the parenteral route due its low oral bioavailability (0.2–0.9%) (Serrano & Lalatsa, 2017). Liposomes (AmBisome®) have been developed to improve the effectiveness and reduce the toxicity of AmB but this formulation still has to be given by injection and is prohibitively expensive for developing countries (Berman, 2005). In recent years, new oral drug delivery systems for AmB have been developed in order to increase its efficacy and tolerability. Among these are cochleates, which are undergoing clinical trials (Serrano & Lalatsa, 2017). They are biocompatible drug delivery systems formed from negatively charged phospholipids bridged with Ca^{2+} ions (Bozó et al., 2017). Some authors have formulated cochleates from synthetic dioleoylphosphatidylserine and obtained promising results for the encapsulation and release of AmB (Pham et al., 2014; L. Zarif et al., 2000). In this work, we have evaluated the pharmacokinetic profile in rats and the *in-vivo* activity in a mouse model of visceral leishmaniasis of AmB encapsulated in cochleate systems made from a naturally occurring phospholipid. Since it has been observed that the gastric environment can destabilize cochleates (Pham et al., 2014), therefore two administration forms able to protect the cochleates containing AmB from the gastric medium were evaluated: a suspension in concentrated buffer and enteric-coated capsules.

Keywords: naturally occurring phospholipid, cochleates, amphotericin B, pharmacokinetic, biodistribution, antileishmaniasis activity

2.3.2 Material

Lipoid PSP70 was provided by Lipoid (Germany). AmB was purchased from Alfa Aesar™. Cholesterol (Cho) was purchased from Sigma, and α -tocopherol (VitE) from Acros Organics. Dextran (500.000 Da), poly(ethylene glycol) (PEG 8000), tris base, calcium chloride and all other chemical reagents were obtained from Sigma. AmBisome® was purchased from Gilead. Methanol, chloroform and other solvents were purchased from Sigma. HP-50 was obtained from Shin-Etsu Chemical. Explotab® was obtained from JRS PHARMA. Hard gelatin capsules of sizes 9 and M suitable for rats and mice respectively were purchased from Torpac. AMBERLITE™ 200CNa resin was a gift from Dow Water & Process. Water was purified by reverse osmosis (Milli-Q, Millipore).

2.3.3 Method

2.3.3.1 Ion exchange treatment of the Lipoid PSP70

Lipoid PSP70 was supplied as a calcium salt was subjected to an ion exchange treatment to convert it to the sodium salt (Lipa-Castro et al., 2021). Lipoid PSP70 in chloroform/methanol/water (20/10/2) at a concentration of 5mg/ml was treated with 75g of resin (previously dried over 24 hours at 50°C due to its high water content) and stirred for 12 hours followed by filtration (PTFE 0.2 μ m) and drying by vacuum evaporation (Buchi R-210 Rotavapor System). The product was redissolved in chloroform/methanol/water (20/10/2) to obtain a concentration of 5mg/ml. Then a second ion exchange treatment was carried out with 10g of resin and stirring for 2 hours followed by filtration and drying by vacuum evaporation. Finally, the lipid film was recovered in chloroform/methanol (60/40) at 5mg/ml. Phosphatidylserine was quantified by normal phase high-performance liquid chromatography (HPLC) coupled to electrospray tandem mass spectrometry (Moulin et al., 2015).

2.3.3.2 Formulation

2.3.3.2.1 Preparation of AmB-loaded cochleate nanoparticles

Cochleates loaded with AmB were prepared by the hydrogel isolation method (Zarif et al., 2000). Firstly, small unilamellar liposomes were formed by film hydration of a mixture of 9DOPS/2Cho/2AmB/0.06VitE (molar proportions) (Lipa-Castro et al., 2021). Lipoid PSP70, cholesterol and vitamin E dissolved in chloroform/methanol 60/40 and AmB dissolved in

alkaline methanol (sodium hydroxide at 2.5 mM) were mixed, dried by rotary evaporation and hydrated with 0.05 M Tris buffer pH 7.4 (5.6 mM total lipid concentration) to form multilamellar liposomes. Their size was reduced and homogenized by probe sonication followed by sequential extrusion on calibrated membranes with 200 nm (1 pass) and 100 nm (3 pass) pores (Whatman® Nucleopore) to form liposomes with a mean diameter of 100 nm. The sonication (Bioblock Scientific vibracell 72441 ultrasons) used a power level of 2 for 7 x 1 min over ice with 1min intervals. Liposomes were mixed at 1/2 (vol/vol) with dextran 40% (wt/wt) and injected into 15% (wt/wt) polyethylene glycol 8000 with stirring. CaCl₂ solution was added at a final concentration of 50 mM, and stirring was continued for 15 min to form cochleates. The cochleates recovered by filtration were washed with 2mM CaCl₂/10mM NaCl and freeze-dried. Unloaded cochleates were also prepared omitting AmB.

2.3.3.2.2 Preparation of the AmB-loaded cochleate formulations for the pharmacokinetic study in rats

Suspension form: Samples of cochleates were suspended in a solution containing 0.2MolTris/10mMolCaCl₂/20mMolNaCl (adjusted at pH 8.4) at a concentration of 2.25 mgAmB/mL for an oral administration volume of 1mL, providing a dose of 7.5 mg/kg.

Enteric-coated capsule form: 17.3 mg of freeze-dried cochleates (containing 2.25mg AmB to provide a dose of 7.5 mg/kg) were mixed with 8mg Explotab, 3mg CaCl₂ and 1mg NaCl then introduced into size 9 Torpac capsules. Finally, enteric coating was achieved by dipping the capsule 5 times into a solution of hypromellose phthalate (HP-50) for 10 seconds with 10 mins of drying. *In-vitro* tests with gastrointestinal solutions were carried out to demonstrate resistance to the gastric environment for subsequent degradation in the intestinal environment, data not shown.

AmBisome®: For oral administration at 7.5 mg/kg, the liposomes were reconstituted as a suspension containing 4mg AmB/mL for an administration volume of 0.560 mL. For intravenous administration at 1 mg/kg, 1.0 ml of a suspension at 0.3mg AmB/mL was used.

2.3.3.2.3 Preparation AmB-loaded cochleate formulations for antileishmanial activity study in mice

Suspension form: Cochleates were suspended in a solution containing 0.2M Tris / 10mM CaCl₂ / 20mM NaCl (adjusted to pH 8.4) at a concentration of 0.5 mgAmB/mL for the dose of 5 mg/kg and 2mg AmB/mL the dose of 20 mg/kg for an oral administration volume of 0.2 mL.

Enteric-coated capsule form: A mixture of 0.77mg freeze-dried cochleates (0.1mg AmB), 0.45mg Explotab, 0.13mgCaCl₂ and 0.04mg NaCl was introduced into size M Torpac capsules. Enteric coating was achieved by immersing the capsule 3 times in a solution of hypromellose phthalate (HP-50) for 10 seconds with 10 mins of drying. *In-vitro* tests with gastrointestinal solutions were carried out to demonstrate resistance to the gastric environment for subsequent degradation in the intestinal environment, data not shown.

AmBisome®: A suspension of liposomes containing 0.2mg AmB/mL was used for an intravenous administration volume of 0.1mL to provide a dose of 1 mg AmB/kg.

2.3.3.3 Determination of AmB concentration by HPLC

Three different variations of the HPLC method were used to determine AmB in cochleates, plasma and organs. All analyses were carried out with a HPLC system Dionex Thermoline Fisher Scientific equipped with an UltiMate 3000 high pressure pump, an UltiMate 3000 autosampler and an UltiMate 3000DAD detector. The column was a Symmetry® C₁₈ column 150mm x 4.6 cm, 5µm particle size (Waters). The flow rate was 1 mL/min and the injection volume was 100 µL. A calibration curve was constructed from a series of dilutions of an AmB reference standard in MeOH/H₂O (3/1) in the range of 0.1 and 5µg/mL for AmB in the cochleates and a range of 0.01 and 5 µg/mL containing 20 µg/mL of piroxicam (internal standard) for AmB in plasma and organs.

AmB in cochleates

The column was operated with 100% of mobile phase A containing 0.5% aqueous solution of triethylamine (adjusted to pH 5.2 with formic acid), acetonitrile and tetrahydrofuran (1000/385/154 v/v) (Lipa-Castro et al., 2021). AmB was quantified using the peak areas acquired at 408 nm. The correlation coefficient (R^2) was 0.9995 and the limit of quantification was 0.010 µg/mL. Retention time of AmB was 9 min.

AmB in plasma

The column was operated with 90% mobile phase A and 10% mobile phase B containing a mixture of water/acetonitrile (95/5 v/v). AmB was quantified at 408 nm and the internal standard piroxicam was quantified at 360 nm. The correlation coefficient (R^2) was 0.9995 and the limit of quantification was 0.01 μ g/mL. Retention time of AmB was 13 min and for piroxicam was 4 min.

AmB in organs

The column was operated with 86% mobile phase A and 14% mobile phase B. AmB was quantified at 408 nm and the internal standard piroxicam was quantified at 360 nm. The correlation coefficient (R^2) was 0.9988 and the limit of quantification was 0.020 μ g/mL. Retention time of AmB was 18 min and for piroxicam was 4 min.

2.3.3.4 Pharmacokinetic studies

Pharmacokinetic studies were carried out in male Wistar rats weighing 300 g purchased from (Zou et al., 2017). The experimental procedures were authorized by the Ethics Committee for Animal Experimentation, in accordance with European Union regulations. Animals were randomly divided into four groups of 12 rats and each group was divided into 2 subgroups of 6 rats (A and B) to allow alternation of samples. Animals were fasted overnight and treated only with single doses of the AmB formulations, as follows:

- Group 1: AmB-Cochleates in enteric-coated capsules at 7.5mg AmB/kg by oral administration.
- Group 2: AmB-Cochleates in suspension at 7.5mg AmB/kg by oral administration
- Group 3: AmBisome® at 7.5mg AmB/kg by oral administration
- Group 4: AmBisome® at 1mg AmB/kg by intravenous administration into the caudal vein.

Blood samples of 600 μ L of blood were taken from the caudal vein at different time points. For oral administration: sub-group A: 1h, 3h, 6h, 24h followed by euthanasia; sub-group B: 2h, 4h, 8h, 48h followed by euthanasia. For IV administration: sub-group A: 5 min, 10min, 15min, 30min, 1h, 24h followed by euthanasia, sub-group B: 1h, 4h, 8h, 48h followed by euthanasia. The animals were anesthetized with isoflurane during blood sampling. A 23 G

winged needle blood collection set, tubing and pre-assembled Luer adapter were used. The sample was collected in tubes coated with sodium heparin (Vacutest®). The last samples (24h and 48h) were taken by cardiac puncture in order to collect as much blood as possible. The rats were euthanized by an overdose of pentobarbital. Liver, lung, spleen and kidney were removed for the determination of AmB content. Plasma was separated by centrifugation with a VWR Galaxy Mini Centrifuge C1413 8 (2000g) and all tissues were stored at – 25 °C until analysis.

2.3.3.4.1 Treatment of plasma samples

All plasma samples were treated with 3 volumes of acetonitrile containing piroxicam as an internal standard to final concentration of 20 µg/ml, followed by centrifugation with a VWR Galaxy Mini Centrifuge C1413 8 (2000g) for 10 min. The recovered supernatant was evaporated to dryness under a stream of nitrogen. It was then suspended in 0.150 ml of a mixture of water and methanol (1/3) followed by centrifugation (2000g) for 10 min. Finally, the supernatant was taken for analysis by HPLC as described above.

2.3.3.4.2 Treatment of organ sample

Organ samples (liver, lung, spleen and kidney) were added to water at a concentration of 0.5, 0.2, 0.2, 0.2 g tissue / mL respectively and homogenized. All samples were treated with 3 volumes of acetonitrile containing piroxicam as internal standard to a final concentration of 20 µg/mL and centrifuged (2000g) for 10 min. The recovered supernatant was evaporated to dryness under a stream of nitrogen and suspended in 0.150 µl of a mixture of water and methanol (1/3) followed by centrifugation (2000g). Finally, the supernatant was taken for analysis by the HPLC method described above.

2.3.3.5 Evaluation of activity against leishmaniasis

The *in-vivo* anti-parasitic activity was assessed in a model of visceral leishmaniasis in mice (Campos Vieira et al., 2011). The experimental procedures were authorized by the Ethics Committee for Animal Experimentation, in accordance with European Union regulations. Female BALB/c mice weighing 18-20g (7-8 weeks old) supplied by JANVIER LABS were infected intravenously with 10^7 amastigotes of *L. donovani* and randomized into groups of 7-9. Animals were fasted overnight and given three doses of AmB formulations at 48-h intervals. Six experimental groups were used.

- Group 1: control, without any treatment.
- Group 2: intravenous treatment with AmBisome® at a dose of 1 mg AmB/kg/day.
- Group 3: oral treatment with unloaded cochleates at a dose equivalent to Group 5 (AmB-loaded cochleate in suspension at 20mg/kg/day).
- Group 4: oral treatment with AmB-loaded cochleate suspension at a dose of 5mg AmB/kg/day.
- Group 5: oral treatment with AmB-loaded cochleate suspension at a dose of 20 mg AmB/kg/day.
- Group 6: oral treatment with AmB-loaded cochleates in enteric-coated capsules at a dose of 5 mg AmB/kg/day.

The treatments were started 1 week after infection. In day 14 post infection, all mice were euthanized by cervical dislocation and the liver and spleen were removed and weighed. The number of parasites was determined by counting the number of amastigotes per 500 hepatocytes prepared from liver smears stained with Giemsa. Statistical differences between treatment groups were determined by the Kruskal Wallis non parametric test followed by an uncorrected Dunn's test. Significance was established for a P value <0.05.

2.3.3.6 In-vivo toxicity assay

In order to evaluate toxicity of AmB formulations, blood samples taken from the mice and centrifuged with a VWR Galaxy Mini Centrifuge C1413 8 (2000g) for 10 min to separate plasma. Cholesterol, triglycerides, creatinine and urea concentrations were determined on plasma using Beckman Coulter equipment.

2.3.4 Result and discussion

2.3.4.1 Efficiency entrapment

The AmB entrapment efficiency was about 80%, demonstrating the capacity of the cochleates from Lipoid PSP70 to encapsulate AmB in sufficient quantities for *in-vivo* studies.

2.3.4.2 Pharmacokinetic and Biodistribution study

Figure 36 shows that the pharmacokinetic profiles for the AmB-loaded cochleate suspension is almost similar to that observed for AmBisome® by the oral route, with a C_{max} between 2 and 8 hours. It is noteworthy that a double peak of AmB in the blood was observed, which could indicate that AmB entered into an enterohepatic cycle and was excreted in the bile and reabsorbed, as already observed by Fielding et al. (1992). In previous work (Lipa-Castro et al., 2021), results obtained *in vitro* on the release of AmB from cochleates in different gastro-intestinal median indicate a strong influence of bile salts that could cause the disintegration of the cochleates and form micelles with their components. This could promote absorption, as observed for many active molecules (Mikov et al., 2006).

In contrast, the pharmacokinetic profile for the AmB-loaded cochleates enclosed in gastro-resistant capsules was completely different. Very little AmB was detected in the plasma at 8h but it was apparent at 24h. The C_{max} was probably reached between 8h and 24h, so its value could not be determined. The fact that the cochleates were released in the intestine as a compact dry powder probably reduced their sensitivity to disruption by bile salts and allowed them to reach the intestinal cell membrane as intact cochleates. Our studies on Caco2 cell monolayers *in vitro* (Chapter 1) showed that in the absence of bile salts absorption on and fusion with the cell membrane could be observed. However, this was greatly reduced in the presence of bile salts, since the cochleates were transformed into micelles.

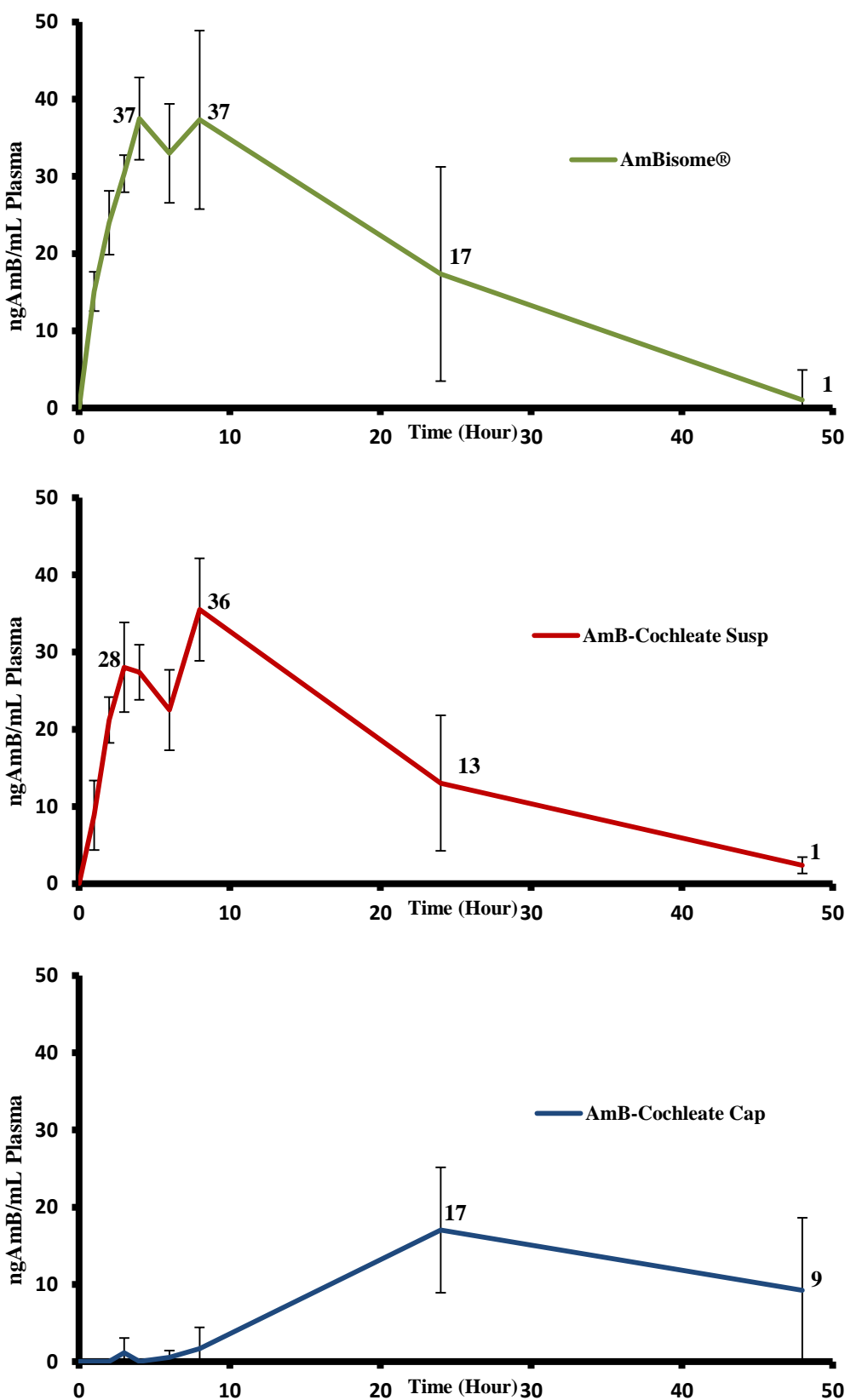


Figure 36. Pharmacokinetic profiles after oral administration of AmB-cochleate formulations and AmBisome® at a dose of 7.5mg/kg (mean \pm S.D. , n=6)

The terminal rate of elimination of AmB from the capsule formulation is clearly slower than that of the suspension, again indicating a different mode of absorption. The pharmacokinetic profile obtained for AmBisome® after intravenous administration is shown in Figure 37. It is clear that the plasma concentrations obtained for all formulations administered orally (at a dose of 7.5 mg/kg) are much lower than those obtained with AmBisome® administered intravenously (at a dose of 1 mg/kg). Previous studies with AmB-loaded cochleates prepared from another source of phospholipid (Pham et al., unpublished results) also showed very low concentrations of AmB in the plasma after oral administration compared with intravenous administration of AmBisome®. In particular, a pharmacokinetic study of AmB-cochleate made for Matinas Biopharma in humans showed a Cmax not higher than 45 ng/mL; however significant activity against fungal diseases like candidiasis was found (Mannino et al., 2015).

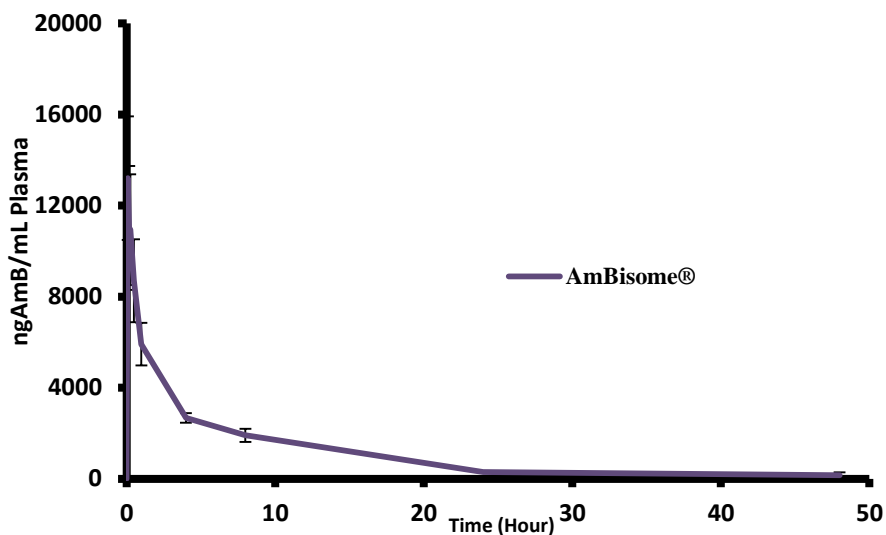


Figure 37. Pharmacokinetic profile of AmBisome® after intravenous administration at a dose of 1mg/kg (mean \pm S.D. , n=6).

The concentrations of AmB recovered in some key organs 24 and 48 hours after administration are showed in Figure 38 for AmBisome® after intravenous administration and in Figure 39 for AmB-cochleate formulations and AmBisome® administered orally. All the formulations administered orally show levels of accumulation of AmB much lower than those from AmBisome® administered intravenously, especially in the organs of interest such as the liver and spleen, demonstrating why the parenteral route is the best form of administration of AmB. However, these results do not differ from the AmB values found in the liver, lung and kidney (<100 ng/ mL) of the AmB-cochleate formulation developed by Matinas Biopharma, from a study also carried out in rats (at a dose of 15 mg/kg). They also point out that in mice

infected with candidiasis, these values were 5 to 10 times higher (Mannino et al., 2015). A better penetration capacity was also observed in a study of fluorescently labeled cochleates administered orally in a mice model of cryptococcal meningoencephalitis (Lu et al., 2019), suggesting that it would be interesting to perform complementary studies in infected models. Therefore, we could expect that in *Leishmania*-treated mice there might also be increased AmB accumulation in these organs.

In Figure 39, the concentrations in the organs are higher than the plasma concentrations for both AmB-cochleate formulations at both timepoints and these values are higher than for AmBisome® administered by oral route. In addition, a clear advantage is observed when AmB-Cochleates enclosed in gastro-resistant capsules were administered; in this case the levels of accumulation of AmB are higher (liver, spleen and kidney) and are maintained 48 hours after administration, compared with AmB-cochleates in suspension and AmBisome® (p.o.), where these values are very low.

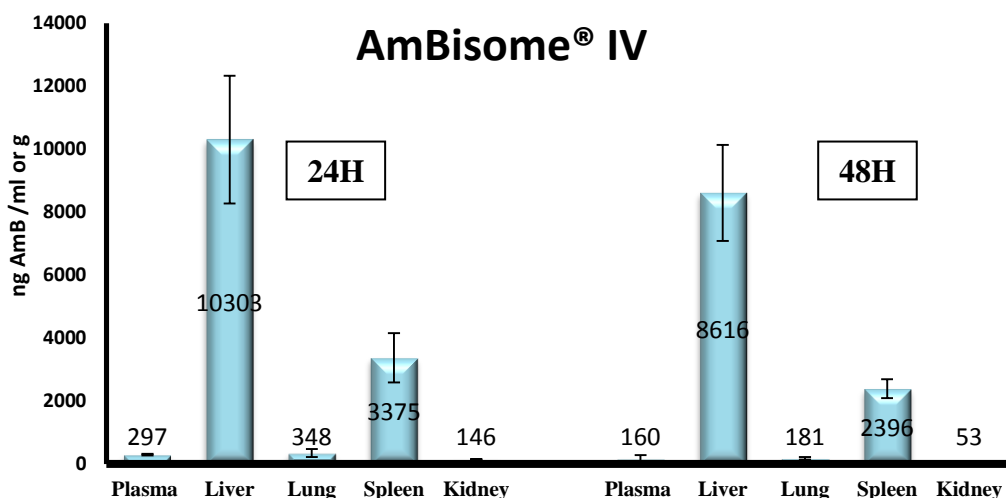


Figure 38. AmB biodistribution after intravenous administration AmBisome® at a dose of 1mg/kg (mean ±S.D. , n=5)

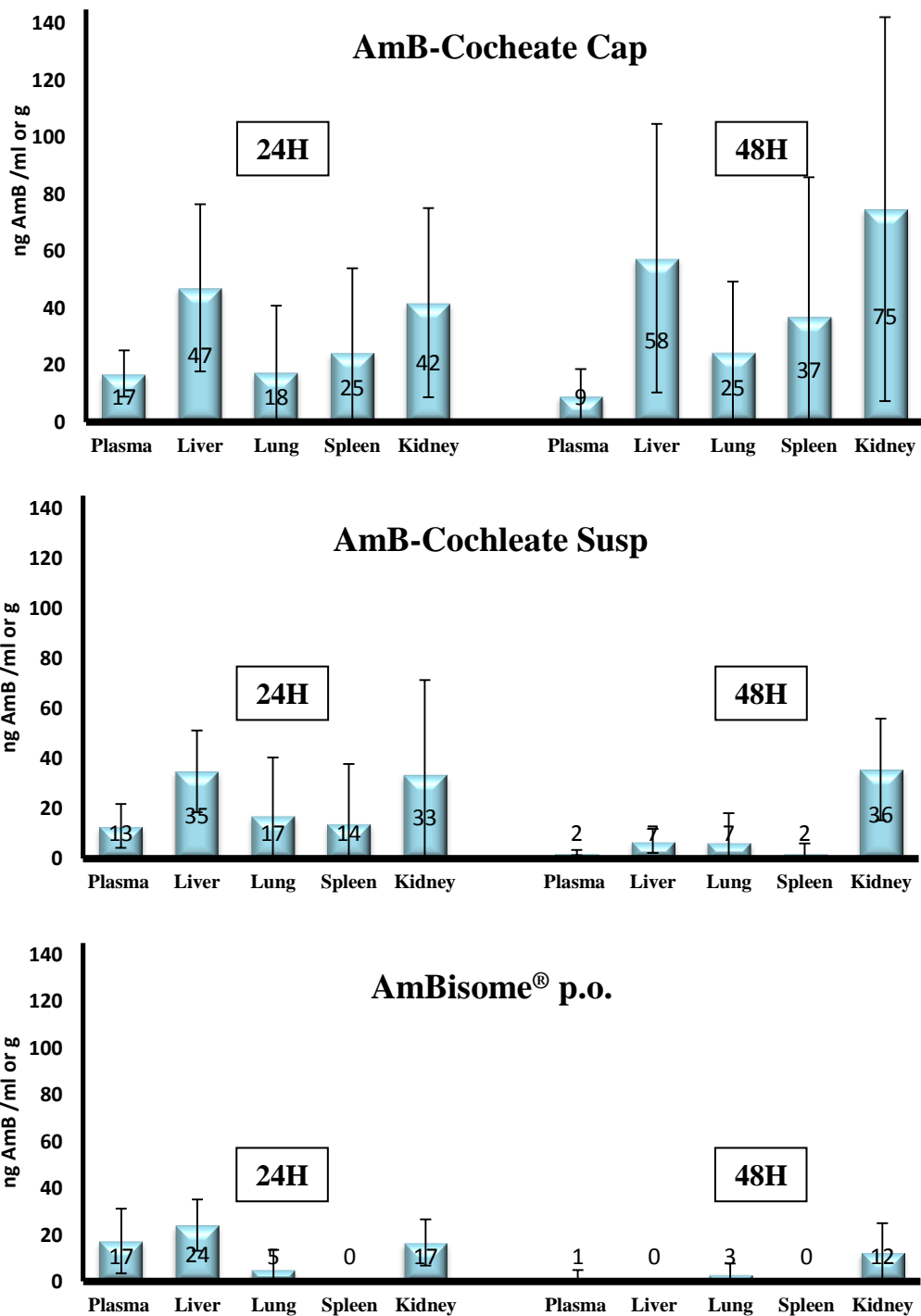


Figure 39. AmB biodistribution after oral administration of AmB-Cochleate formulations and AmBisome® at a dose of 7.5mg/kg (mean \pm S.D. , n=5).

These results indicate the advantage of the oral route for delivering AmB to the organs harbouring *Leishmania* parasites (liver and spleen). Furthermore the differences observed between the suspension and the capsule formulations of AmB-Cochleates may also point to a different mechanism that delivers AmB more efficiently to target organs in the latter case.

However, AmB accumulation is also observed in the kidneys, so, taking into account the nephrotoxicity of AmB, toxicity studies must be done in future studies at higher doses of AmB-Cochleates. Finally, the biodistribution results show that pharmacokinetic profiles do not tell the whole story. As already mentioned by other authors, low levels of AmB in the plasma are not necessarily indicators of low bioavailability because of the tendency of AmB to be highly concentrated in some organs (Serrano & Lalatsa, 2017). This is supported by our results.

2.3.4.3 Evaluation of antileishmanial activity

Figure 40 shows the parasitic load in the different treatment groups. The positive control, intravenous AmBisome®, reduced the parasitic load by 94% compared with the untreated control. The unloaded cochleates and the AmB-loaded cochleates given as a suspension at 5 mg/kg/day did not cause a significant reduction in the number of parasites. However, AmB-loaded cochleates given as a suspension at 20 mg/kg/day produced a significant reduction in the parasitic load of 36%, showing the ability of cochleate prepared from a naturally occurring phospholipid to exert an anti-leishmanial activity by the oral route.

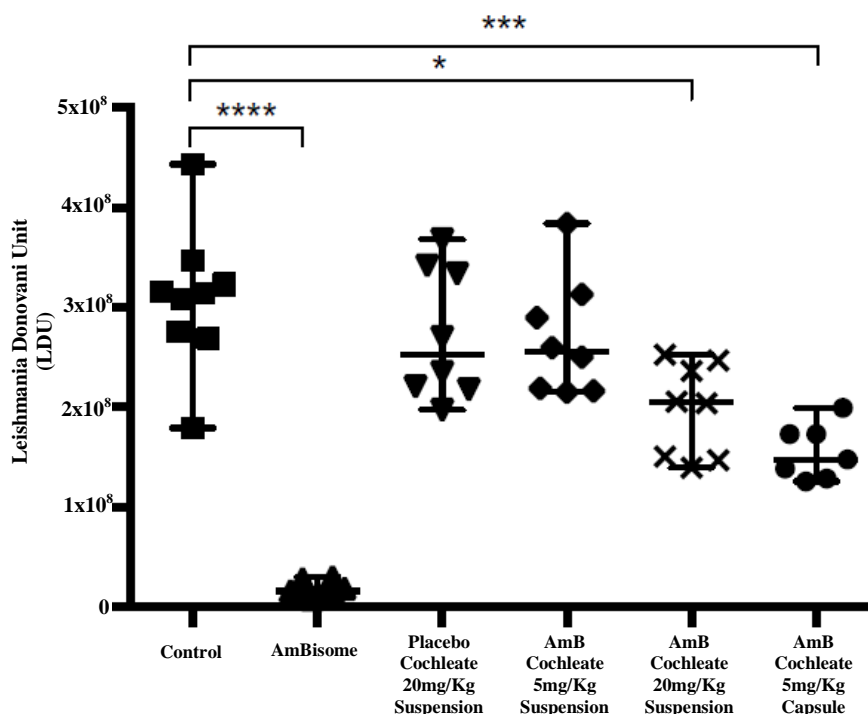


Figure 40. *In-vivo evaluation of AmB formulations against visceral leishmaniasis. There was significant difference in comparison to control *p < 0.05, ***p < 0.001, ****p < 0.0001, n=7).*

The oral activity of AmB-loaded cochleate systems has already been demonstrated in fungal infections: aspergillosis (Delmas et al., 2002) and candidiasis (L. Zarif et al., 2000). Furthermore, treatment with AmB-loaded cochleates enclosed in gastro-resistant capsules at only 5 mg/kg/day led to a significant reduction in the parasite load of 43%. This is consistent with the results of the biodistribution study, showing a better ability to deliver AmB to the liver and the spleen when AmB-loaded cochleates are enclosed in gastro-resistant capsules.

2.3.4.4 Toxicity of the formulation.

Table 12 gives the results of determinations of some key biochemical parameters. In general, there were no significant changes ($p>0.05$) among the treatment groups. In particular, urea and creatinine, indicators of renal toxicity that is dose-limiting for AmB, were not increased in any of the groups. A slight elevation of urea concentration was observed in the AmB-Cochleate capsule group; however it is lower than the values obtained from AmBisome® in other studies (<10.15mM) (Rochelle do Vale Morais et al., 2018), therefore still tolerable. Cholesterol levels seemed to be lower than those reported for uninfected mice, which might be due to an interference of the parasites with liver metabolism.

Table 11. Biochemical parameters in mice infected with *Leishmania* and treated with AmB formulations (n=4).

	UREA mM	CREATININE μM	CHOLESTEROL mM	TRIGLYCERIDES mM
Normal Value (Rochelle do Vale Morais et al., 2018)	7.4	<18	3.5	-----
Untreated	6.6	15.3	2.0	0.6
AmBisome® 1mg/kg	6.8	16.5	1.9	0.8
Placebo-Cochleate susp 5mg/kg	6.8	14.5	2.2	0.7
AmB-cochleate susp 5mg/kg	6.1	14.2	1.9	0.7
AmB-cochleate susp 20mg/kg	6.4	15.2	1.9	0.6
AmB-cochleate capsule 5mg/kg	8.4	16.4	2.1	0.5

2.3.5 Conclusion and perspectives

The administration of AmB encapsulated in cochleate systems prepared from a naturally occurring phospholipid have been shown to deliver AmB to the organs harbouring parasites in visceral leishmaniasis; that is, the liver and the spleen and the accumulation in these organs is greatly increased by loading the cochleates into a gastro-resistant capsule. The higher dose of the drug-loaded cochleate suspension showed a significant activity against the disease, and a better effect was obtained with cochleates administered in gastro-resistant capsules although the dose was four times lower. This is the first time that therapeutic activity of AmB-loaded cochleates against *Leishmania* has been demonstrated, although several studies have demonstrated antifungal activity (Delmas et al., 2002; Santangelo et al., 2000). The increased efficiency of the capsule formulations can be attributed both to the protection of the AmB molecule from degradation in the stomach and also to protection of the cochleate structure against disintegration in the presence of bile salts that has already been noted in several studies.

These experiments have shown that AmB associated with cochleates can treat visceral leishmaniasis orally, even when the cochleates are obtained from a naturally occurring phospholipid. For a total eradication of the parasite, new dosage regimes are required; that is, increasing the dose and/or the frequency of administration. At the same time, toxicity studies must be carried out to ensure the safety of the treatment. In addition, cochleates have already been indicated to improve cutaneous administration, being an alternative vehicle for certain drugs (Landge et al., 2013). Taking into account that cutaneous leishmaniasis is the most abundant form of leishmaniasis worldwide, including in Andean countries as Venezuela, Colombia, Ecuador, Peru, and Bolivia (Davies et al., 2000), it would be very useful to evaluate AmB-Cochleates by the topical route in *in-vivo* models of this disease.

REFERENCES

- Berman, J. (2005). Recent Developments in Leishmaniasis: Epidemiology, Diagnosis, and Treatment. *Current Infectious Disease Reports*, 7(1), 33–38. <https://doi.org/10.1007/s11908-005-0021-1>
- Bozó, T., Wacha, A., Mihály, J., Bóta, A., & Kellermayer, M. S. Z. (2017). Dispersion and stabilization of cochleate nanoparticles. *European Journal of Pharmaceutics and Biopharmaceutics*, 117, 270–275. <https://doi.org/10.1016/j.ejpb.2017.04.030>
- Campos Vieira, N., Vacus, J., Fournet, A., Baudouin, R., Bories, C., Séon-Méniel, B., Figadère, B., & Loiseau, P. M. (2011). Antileishmanial activity of a formulation of 2-n-propylquinoline by oral route in mice model. *Parasite*, 18(4), 333–336. <https://doi.org/10.1051/parasite/2011184333>
- Davies, C. R., Reithinger, R., Campbell-Lendrum, D., Feliciangeli, D., Borges, R., & Rodriguez, N. (2000). The epidemiology and control of leishmaniasis in Andean countries. *Cadernos de Saúde Pública*, 16(4), 925–950. <https://doi.org/10.1590/S0102-311X2000000400013>
- Delmas, G., Park, S., Chen, Z. W., Tan, F., Kashiwazaki, R., Zarif, L., & Perlin, D. S. (2002). Efficacy of Orally Delivered Cochleates Containing Amphotericin B in a Murine Model of Aspergillosis. *Antimicrobial Agents and Chemotherapy*, 46(8), 2704–2707. <https://doi.org/10.1128/AAC.46.8.2704-2707.2002>
- Faustino, & Pinheiro. (2020). Lipid Systems for the Delivery of Amphotericin B in Antifungal Therapy. *Pharmaceutics*, 12(1), 29. <https://doi.org/10.3390/pharmaceutics12010029>
- Fielding, R. M., Singer, A. W., Wang, L. H., Babbar, S., & Guo, L. S. (1992). Relationship of pharmacokinetics and drug distribution in tissue to increased safety of amphotericin B colloidal dispersion in dogs. *Antimicrobial Agents and Chemotherapy*, 36(2), 299–307. <https://doi.org/10.1128/AAC.36.2.299>
- Landge, A., Pawar, A., Shaikh K. (2013). Investigation of cochleates as carriers for topical drug delivery. *International Journal of Pharmacy and Pharmaceutical Sciences*, 5(2), 314-320.
- Lipa-Castro, A., Nicolas, V., Angelova, A., Mekhloufi, G., Prost, B., Chéron, M., Faivre, V., & Barratt, G. (2021). Cochleate formulations of Amphotericin b designed for oral administration using a naturally occurring phospholipid. *International Journal of Pharmaceutics*, 603, 120688. <https://doi.org/10.1016/j.ijpharm.2021.120688>
- Lu, R., Hollingsworth, C., Qiu, J., Wang, A., Hughes, E., Xin, X., Konrath, K. M., Elsegeiny, W., Park, Y.-D., Atakulu, L., Craft, J. C., Tramont, E. C., Mannino, R., & Williamson, P. R. (2019). Efficacy of Oral Encocochleated Amphotericin B in a Mouse Model of Cryptococcal Meningoencephalitis. *MBio*, 10(3). <https://doi.org/10.1128/mBio.00724-19>
- Mannino R, Perlin D. (2015). Oral dosing of encochleated amphotericin B (CAmB): rapid drug targeting to infected tissues in mice with invasive candidiasis. *Scientific Presentations & Publications* Matinas Biopharma. Available online:

https://d1io3yog0oux5.cloudfront.net/_d38280067c63da37f40edbd3b0afe24f/matinasbiopharma/db/284/2323/pdf/Oral_Dosing_of_Encocleated_Amphotericin_B_%28CAmB%29_Rapid_Drug_Targeting_to_Infected_Tissues_in_Mice_with_Invasive_Candidiasis.pdf (Accessed 11 june 2021)

Mikov, M., Fawcett, J. P., Kuhajda, K., & Kevresan, S. (2006). Pharmacology of bile acids and their derivatives: Absorption promoters and therapeutic agents. European Journal of Drug Metabolism and Pharmacokinetics, 31(3), 237–251. <https://doi.org/10.1007/BF03190714>

Moulin, M., Solgadi, A., Veksler, V., Garnier, A., Ventura-Clapier, R., & Chaminade, P. (2015). Sex-specific cardiac cardiolipin remodelling after doxorubicin treatment. Biology of Sex Differences, 6(1), 20. <https://doi.org/10.1186/s13293-015-0039-5>

Pham, T. T. H., Gueutin, C., Cheron, M., Abreu, S., Chaminade, P., Loiseau, P. M., & Barratt, G. (2014). Development of antileishmanial lipid nanocomplexes. Biochimie, 107, 143–153. <https://doi.org/10.1016/j.biochi.2014.06.007>

Rochelle do Vale Moraes, A., Silva, A. L., Cojean, S., Balaraman, K., Bories, C., Pomel, S., Barratt, G., do Egito, E. S. T., & Loiseau, P. M. (2018). In-vitro and in-vivo antileishmanial activity of inexpensive Amphotericin B formulations: Heated Amphotericin B and Amphotericin B-loaded microemulsion. Experimental Parasitology, 192, 85–92. <https://doi.org/10.1016/j.exppara.2018.07.017>

Santangelo, R., Paderu, P., Delmas, G., Chen, Z.-W., Mannino, R., Zarif, L., & Perlin, D. S. (2000). Efficacy of Oral Cochleate-Amphotericin B in a Mouse Model of Systemic Candidiasis. Antimicrobial Agents and Chemotherapy, 44(9), 2356–2360. <https://doi.org/10.1128/AAC.44.9.2356-2360.2000>

Serrano, D. R., & Lalatsa, A. (2017). Oral amphotericin B: The journey from bench to market. Journal of Drug Delivery Science and Technology, 42, 75–83. <https://doi.org/10.1016/j.jddst.2017.04.017>

Serrano, D. R., Lalatsa, A., Dea-Ayuela, M. A., Bilbao-Ramos, P. E., Garrett, N. L., Moger, J., Guarro, J., Capilla, J., Ballesteros, M. P., Schätzlein, A. G., Bolás, F., Torrado, J. J., & Uchegbu, I. F. (2015). Oral Particle Uptake and Organ Targeting Drives the Activity of Amphotericin B Nanoparticles. Molecular Pharmaceutics, 12(2), 420–431. <https://doi.org/10.1021/mp500527x>

Zarif, L., Graybill, J. R., Perlin, D., Najvar, L., Bocanegra, R., & Mannino, R. J. (2000). Antifungal Activity of Amphotericin B Cochleates against *Candida albicans* Infection in a Mouse Model. Antimicrobial Agents and Chemotherapy, 44(6), 1463–1469. <https://doi.org/10.1128/AAC.44.6.1463-1469.2000>

Zarif, Leila, Graybill, J. R., Perlin, D., & Mannino, R. J. (2000). Cochleates: New Lipid-Based Drug Delivery System. Journal of Liposome Research, 10(4), 523–538. <https://doi.org/10.3109/08982100009031116>

Zou, W., Yang, Y., Gu, Y., Zhu, P., Zhang, M., Cheng, Z., Liu, X., Yu, Y., & Peng, X. (2017). Repeated Blood Collection from Tail Vein of Non-Anesthetized Rats with a Vacuum Blood Collection System. Journal of Visualized Experiments, 130, 55852. <https://doi.org/10.3791/55852>

3. DISCUSION

En raison de son efficacité pour traiter des maladies graves comme les infections fongiques disséminées et la leishmaniose résistante, l'AmB a attiré l'attention de la recherche et du développement galénique. Cette attention cherche surtout à pallier ses propriétés physicochimiques désavantageuses comme sa faible solubilité, sa faible perméabilité à travers les barrières biologiques, son instabilité en milieu gastrique, sa sensibilité à la lumière et surtout sa faible biodisponibilité orale qui nécessite une administration parentérale avec des effets secondaires sévères (Faustino & Pinheiro, 2020). Malgré tous ces désavantages, l'AmB est considérée comme la molécule antileishmanienne la plus prometteuse ; mais son utilisation reste à optimiser (Singh et al., 2012). Actuellement, de nombreuses recherches se focalisent sur le développement de systèmes de délivrance de l'AmB par voie orale, à cause des avantages que l'absorption gastro-intestinale présente pour cibler des médicaments vers des organes comme le foie et la rate (Serrano & Lalatsa, 2017), qui sont les organes les plus touchés par la leishmaniose viscérale. Parmi ces systèmes, nous avons étudié les cochléates, qui sont des précipités de phospholipides chargés négativement obtenus à la suite de l'ajout de cations divalents. Nous avons développé ces systèmes pour encapsuler l'AmB (AmB-Cochléates) en utilisant la méthode de l'hydrogel pour leur préparation, une méthode citée dans la littérature pour obtenir des systèmes à l'échelle nanométrique (Zarif et al., 2003).

Formulation du système AmB-Cochléates

En guise de travaux préliminaires, nous avons formulé un système AmB-Cochléates à partir de DOPS (un phospholipide synthétique) prenant comme référence une formulation optimisée auparavant avec une composition en ratio molaire de DOPS/Cho/AmB/VitE (9:1:0,5:0,06) (Pham et al., 2014). Nous avons obtenu des nanocochléates contenant l'AmB avec un rendement d'encapsulation satisfaisant. Malgré les résultats prometteurs obtenus avec le système AmB-Cochléates à base de DOPS, cette formulation s'avère très coûteuse pour une éventuelle transposition d'échelle et reste inaccessible pour une utilisation dans les pays en voie de développement.

Pour cette raison, la suite du projet a porté sur le développement d'AmB-Cochléates à base d'un phospholipide d'origine naturelle (Lipoid PS P 70). Pham et al., (2013) ont optimisé les ratios de composants (phospholipide, cholestérol, AmB et vitamine E) en utilisant la méthode

de la balance de Langmuir. Cet outil permet d'étudier l'interaction, l'insertion, la stabilité et l'orientation des principes actifs dans un film lipidique à l'interface air-eau (Pham et al., 2013). Cette méthodologie convient pour étudier les liposomes, formulation intermédiaire dans la fabrication des cochléates. Cependant, elle n'était pas adaptée au phospholipide d'origine naturelle Lipoid PS P 70, qui est un mélange de phospholipides à chaînes acyles différentes, donnant de courbes via la balance de Langmuir non répétables donc non exploitables pour trouver le meilleur ratio de composés. En outre, les résultats de taille par DLS, de la morphologie par microscopie optique et électronique et du taux d'encapsulation par HPLC n'ont pas permis de trancher entre les différents ratios de composants.

Afin d'optimiser la composition nous avons utilisé la méthodologie SAXS ainsi qu'une étude de stabilité de l'AmB dans le milieu gastrique comme critères. En effet la méthodologie SAXS est actuellement très utilisée pour l'étude de la structure interne des cochléates mais est également très utile pour étudier les états intermédiaires, des liposomes multilamellaires jusqu'à la structure cochléaire (Bozó et al., 2017; Nagarsekar et al., 2017). Ainsi, nos résultats ont montré qu'au fur et à mesure que le ratio de cholestérol augmentait dans la formulation, la stabilité de l'AmB dans le milieu acide était améliorée. Un ratio de 9LipoidPSP/2Cho est optimal pour stabiliser l'AmB dans le milieu gastrique, quelle que soit la proportion d'AmB (ratios 0,5, 1, 2 ou 3). Cette proportion en cholestérol est différente de celle de 9DOPS/1Cho trouvé par Pham et al. (2013), proportion établie à l'aide de la balance de Langmuir pour encapsuler l'AmB à un ratio de 0,5. Ces résultats ont été confortés par les résultats de SAXS qui ont montré le profil d'une structure multicouche déshydratée typique des cochléates à la proportion de 9LipoidPSP/2Cho/0,5AmB. Cependant, quand la quantité d'AmB a été augmentée à 1, 2 ou 3, le profil SAXS a montré l'apparition d'un nouveau signal, indiquant probablement la formation de complexes de l'AmB avec le phospholipide ou le cholestérol. Pourtant, ces différences de structures ne semblent pas avoir d'impact sur la stabilité de l'AmB dans le milieu gastrique, qui était protégée même en forte proportion. Ce comportement a déjà été signalé dans des travaux précédents où l'AmB interagit avec le cholestérol et les phospholipides pour former des complexes dans la bicouche (Bolard et al., 1980). De plus, les études de dichroïsme circulaire ont également mis en évidence qu'aux ratios 1, 2 et 3, des pics dans le spectre UV-Vis typique de la formation de complexes d'AmB avec le phospholipide ou le cholestérol, augmentent proportionnellement avec la quantité d'AmB. La question que l'on peut se poser est si ces complexes se trouvent à l'intérieur ou

l'extérieur de la structure cochléaire et si ceux-ci peuvent influencer la vitesse de libération de l'AmB des cochléates.

D'ailleurs, malgré la taille nanométrique obtenue pour toutes les formulions par DLS et par microscopie électronique, des études par microscopie optique ont mis en évidence qu'une proportion de cochléates avait une taille à l'échelle micrométrique. En effet, cet inconvénient de distribution hétérogène de taille et la probable agglomération des cochléates ont déjà été décrits par plusieurs auteurs (Asprea et al., 2019; Bozó et al., 2017). Cette agrégation peut être évitée par l'ajout de certains excipients comme la caséïne, la méthylcellulose ou l'albumine qui inhibent les interactions entre cochléates (Lu, 2018). Nagarsekar et al., (2017) ont proposé une méthodologie à l'aide d'un appareil microfluidique ainsi que l'utilisation d'un mélange hydroalcoolique pour obtenir une population de cochléates homogènes.

Etudes de libération *in vitro* et interaction avec les cellules Caco2

Les résultats de Pham et al. (2014) ont démontré la sensibilité des cochléates aux milieux gastro-intestinaux ; et plus précisément la sensibilité de leur structure enroulée à l'acidité et la dissolution des cochléates en présence de sels biliaires. Leur conclusion a été qu'il fallait les protéger du milieu gastrique mais, par contre, favoriser leur interaction avec les sels biliaires pour promouvoir la libération et l'absorption de l'AmB (Pham et al., 2014). Cependant, Asprea et al. (2019) recommandent d'assurer la stabilité de la formulation dans le milieu gastrique et plutôt d'éviter la dissolution des cochléates par les sels biliaires en ajoutant un excès de calcium (Asprea et al., 2019). Nos formulations obtenues à base 9LipoidPSP/2Cho avec les différents ratios AmB (0.5, 1, 2, 3) ont toutes montré la capacité à protéger l'AmB de la dégradation en milieu acide et en présence d'un excès de calcium les formulations ont été stables dans les conditions intestinales FASSIF (sels biliaires à faible concentration) mais dans les conditions FESSIF (sels biliaires à haute concentration), les cochléates ont été dissous au cours de temps.

Les résultats obtenus sur le modèle cellulaire Caco2 ont montré la capacité des formulations à adhérer à la membrane cellulaire, conduisant à obtenir des quantités importantes d'AmB dans la monocouche cellulaire, quantités croissantes avec les ratios 0,5, 1 et 2. Cependant, à partir du ratio égal à 3, une diminution de la quantité d'AmB dans la monocouche a été observée, probablement à cause de la diminution de la quantité de PS disponible pour interagir avec la membrane cellulaire. Compte tenu de tous ces résultats, la composition 9LipoidPSP70/2Cho/2AmB/0,06VitamineE a été choisie pour la suite des expériences.

L'adsorption et la fusion des structures cochléaires avec la membrane cellulaire conduisant ensuite à la libération postérieure à l'intérieur des cellules des molécules encapsulées sont évoquées par de nombreux auteurs comme étant le mécanisme par lequel les cochléates améliorent la biodisponibilité orale des médicaments (Syed et al., 2008; Zarif et al., 2000). Des autres études soulignent la capacité des cochléates à traverser la membrane cellulaire (Vijeta & Vivek, 2011). Nos résultats en microscopie confocale sur le modèle cellulaire Caco2 avec les cochléates à base de Lipoid PS P 70 marqués par un phospholipide porteur de rhodamine n'ont pas démontré ce mécanisme mais indiquent plutôt la capacité des cochléates à adhérer à la surface de la membrane et d'y fusionner, soutenant le premier mécanisme proposé (adsorption, fusion et libération de la molécule à l'intérieur des cellules). Cependant, des études préliminaires réalisées avec les cochléates à base de DOPS sur le modèle Caco2 ont montré que cette adhérence était réduite quand des sels biliaires (milieu FASSIF) sont présents. Ceci démontre encore un fois la sensibilité des cochéates aux sels biliaires décrite par Pham et al. (2014) qui propose comme mécanisme un probable déroulement des cochléates avec formation de micelles mixtes composés des sels biliaires et des composants des cochléates, micelles mixtes qui peuvent être absorbées par la suite.

Evaluation *in vivo* de la formulation LipoidPSP 9/2Cho/2AmB/0,06VitE

Lors de l'étude pharmacocinétique, pour le système AmB-Cochléates administré sous forme de suspension, le profil obtenu a montré un double pic qui pourrait indiquer une absorption, sécrétion et réabsorption d'AmB suivant une circulation entéro-hépatique comme pour les sels biliaires. Ceci pourrait être une preuve d'un mécanisme d'absorption impliquant la formation des micelles mixtes avec les sels biliaires. Toutefois, un comportement différent a été observé quand les AmB-Cochléates ont été administrés dans les gélules gastro-résistantes. Très peu d'AmB a été trouvé dans le plasma pendant les 8 premières heures et la pente d'élimination lente indique un temps de résidence de l'AmB plus long. Le mécanisme d'absorption est probablement très différent dans ce cas. L'explication pourrait être basée sur le fait que la formulation arrive dans l'intestin sous forme de poudre déshydratée, ce qui permet aux cochléates de résister aux sels biliaires, d'adhérer à la membrane cellulaire pour fusionner et ensuite de libérer l'AmB au niveau intracellulaire. Dans ce cas, il y aurait également la possibilité de phagocytose par les cellules M comme cela a déjà été observé pour plusieurs types de nanoparticules (Khan et al., 2013) suivi par une absorption lymphatique.

La faible concentration d'AmB plasmatique suite à l'administration orale de systèmes contenant l'AmB comparée à celle obtenue après l'administration de l'AmBisome par voie intraveineuse a déjà été observée, mais n'est pas forcément à prendre comme évidence du système (Serrano & Lalatsa, 2017). Ces auteurs ont souligné l'importance de prendre en compte la concentration d'AmB dans les organes, à cause de la propriété de l'AmB de se cumuler dans différents organes comme le poumon, le foie et la rate. Ces études sont nécessaires pour évaluer une possible vectorisation de la molécule. Nos résultats de biodistribution montrent des concentrations plus élevées dans le foie et la rate par rapport à la concentration d'AmB dans le plasma. Ceux-ci représentent des résultats prometteurs pour le traitement de la leishmaniose viscérale. Des études sur un modèle *ex vivo* comme les chambres de Ussing qui simulent plus précisément les conditions intestinales (Mendes et al., 2018) pourraient être très utiles pour élucider le mécanisme d'action des cochléates.

Bien que la formulation proposée AmB-Cochleates, que ce soit sous forme de suspension ou en gélules gastro-résistantes, n'a pas donné des concentrations d'AmB plasmatiques plus importantes que celles obtenue avec l'AmBisome administré aussi par voie orale, des activités significatives dans le modèle de leishmaniose viscérale ont été observées pour la suspension à une dose de 20 mg AmB/kg et pour les gélules à une dose moindre de 5 mg/kg. Un système AmB-Cochléates a déjà été évalué par voie orale sur un modèle de candidose (Santangelo et al., 2000). En plus de constater une activité significative, ils ont comparé la concentration d'AmB dans le plasma et dans les organes des animaux sains et des animaux infectés. Tandis que la concentration d'AmB dans le plasma des animaux infectés n'était pas très différente de celle des animaux sains, la concentration d'AmB dans les organes (poumon, rate, foie) était plus importante dans les animaux infectés. Ce résultat est très encourageant pour cibler l'AmB vers les organes impliqués dans la leishmaniose viscérale (foie et rate). Ainsi, des études de pharmacocinétique et de biodistribution dans le modèle animal infecté par la leishmaniose doivent être réalisées pour essayer d'expliquer l'activité, significative, du traitement observé. Par ailleurs, l'activité supérieure des AmB-Cochléates en gélules à faible concentration (5 mg AmB/kg) par rapport à l'AmB-Cochléates en suspension à plus haute concentration (20 mg AmB/kg) reste encore à étudier afin d'optimiser le traitement pour le rendre plus accessible et plus efficace.

Enfin, en mettant ensemble les résultats obtenus dans les différentes études, nous pouvons proposer trois mécanismes d'action (figure 41) selon l'interaction et la stabilité des cochléates dans les milieux intestinaux. Les cochléates en présence de sels biliaires seront dissous sous

formes de micelles pour être postérieurement absorbés par le cycle entéro-hépatique (41A). Cependant en l'absence ou en présence de faibles concentrations de sels biliaires, les cochléates interagissent directement avec la membrane cellulaire par adsorption, fusion et libération de la drogue (41B) pour arriver à la voie sanguine et/ou par phagocytose par les cellules M pour arriver à la voie lymphatique (41C).

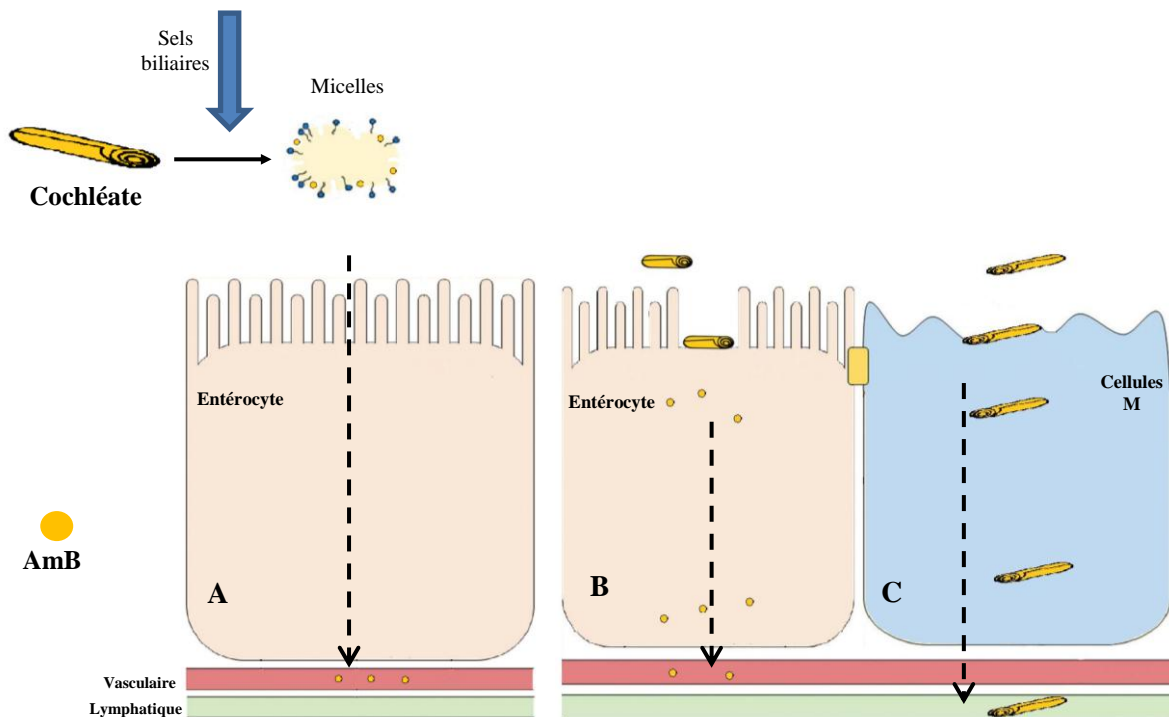


Figure 41. Schéma de mécanismes d'absorption proposés

4. CONCLUSION ET PERSPECTIVE

À la suite de nos études de formulation et de caractérisation physicochimique, des cochléates contenant l'AmB à base d'un phospholipide d'origine naturelle, Lipoid PS P 70, peuvent être obtenus avec une taille nanométrique, une structure multilamellaire déshydratée et un bon taux d'encapsulation avec le ratio molaire 9LipoidPSP70/2Cho/2AmB/0,06VitamineE. De plus, cette formulation est capable d'améliorer la stabilité de l'AmB dans le milieu gastrique. Ces cochléates conservent aussi des propriétés similaires aux cochléates à base de phospholipide d'origine synthétique comme la DOPS, c'est-à-dire de pouvoir interagir avec les cellules intestinales et libérer leur contenu, soit par interaction avec les sels biliaires ou par un mécanisme de fusion avec la membrane cellulaire.

Deuxièmement, lors de l'étude pharmacocinétique, ce système a montré un profil prometteur pour cibler l'AmB vers le foie et le rate, organes impliqués dans la leishmaniose viscérale. Des études supplémentaires de pharmacocinétique dans des animaux porteurs de la pathologie doivent être réalisées par la suite pour déterminer si l'infection favorise le ciblage de la molécule vers les organes d'intérêt.

Troisièmement, le traitement avec AmB-Cochléates soit en suspension soit en gélules gastro-résistantes démontre une activité significative pour réduire la charge parasitaire sans avoir d'indices de néphrotoxicité, effet secondaire notoire de l'AmB. Par ailleurs, une autre posologie de traitement pourrait être proposée pour une éradication complète du parasite, en augmentant la dose, la fréquence des administrations et la durée du traitement. Ainsi la formulation AmB-Cochléates dans des gélules gastro-résistantes doit être prise comme la forme de référence pour continuer les essais *in vivo* (pharmacocinétique et activité).

Enfin l'élucidation du mécanisme par lequel les cochléates peuvent améliorer la biodisponibilité semble indispensable pour la suite, non seulement pour la connaissance scientifique mais aussi pour trouver les meilleures conditions (à jeun ou nourri) et la forme (gélules, suspension, autre.) d'administration des cochléates pour maximiser leur efficacité. Pour ceci l'étude *ex vivo* à l'aide des chambres d'Ussing semble être la méthodologie la plus pertinente.

5. REFERENCES

- Aigner, M., & Lass-Flörl, C. (2020). Encocleated Amphotericin B: Is the Oral Availability of Amphotericin B Finally Reached? *Journal of Fungi*, 6(2), 66. <https://doi.org/10.3390/jof6020066>
- Alexander, B., & Maroli, M. (2003). Control of phlebotomine sandflies. *Medical and Veterinary Entomology*, 17(1), 1–18. <https://doi.org/10.1046/j.1365-2915.2003.00420.x>
- Aronson, N., Herwaldt, B. L., Libman, M., Pearson, R., Lopez-Velez, R., Weintraub, P., Carvalho, E., Ephros, M., Jeronimo, S., & Magill, A. (2017). Diagnosis and Treatment of Leishmaniasis: Clinical Practice Guidelines by the Infectious Diseases Society of America (IDSA) and the American Society of Tropical Medicine and Hygiene (ASTMH). *The American Journal of Tropical Medicine and Hygiene*, 96(1), 24–45. <https://doi.org/10.4269/ajtmh.16-84256>
- Asprea, M., Tatini, F., Piazzini, V., Rossi, F., Bergonzi, M. C., & Bilia, A. R. (2019). Stable, Monodisperse, and Highly Cell-Permeating Nanocoachleates from Natural Soy Lecithin Liposomes. *Pharmaceutics*, 11(1), 34. <https://doi.org/10.3390/pharmaceutics11010034>
- Bañuls, A.-L., Hide, M., & Prugnolle, F. (2007). Leishmania and the Leishmaniases: A Parasite Genetic Update and Advances in Taxonomy, Epidemiology and Pathogenicity in Humans. In *Advances in Parasitology* (Vol. 64, pp. 1–458). Elsevier. [https://doi.org/10.1016/S0065-308X\(06\)64001-3](https://doi.org/10.1016/S0065-308X(06)64001-3)
- Bhosale, R. R., Ghodake, P. P., Nandkumar, A., & Ghadge, A. A. (2013). Nanocoachleates: A novel carrier for drug transfer. 6.
- Bolard, J., Seigneuret, M., & Boudet, G. (1980). Interaction between phospholipid bilayer membranes and the polyene antibiotic amphotericin B: Lipid state and cholesterol content dependence. *Biochimica et Biophysica Acta (BBA) - Biomembranes*, 599(1), 280–293. [https://doi.org/10.1016/0005-2736\(80\)90074-7](https://doi.org/10.1016/0005-2736(80)90074-7)
- Borowski, E., Salewska, N., Boros-Majewska, J., Serocki, M., Chabowska, I., Milewska, M. J., Ziętkowski, D., & Milewski, S. (2020). The Substantial Improvement of Amphotericin B Selective Toxicity Upon Modification of Mycosamine with Bulky Substituents. *Medicinal Chemistry*, 16(1), 128–139. <https://doi.org/10.2174/1573406415666181203114629>
- Bozó, T., Wacha, A., Mihály, J., Bóta, A., & Kellermayer, M. S. Z. (2017). Dispersion and stabilization of cochleate nanoparticles. *European Journal of Pharmaceutics and Biopharmaceutics*, 117, 270–275. <https://doi.org/10.1016/j.ejpb.2017.04.030>
- Campos Vieira, N., Vacus, J., Fournet, A., Baudouin, R., Bories, C., Séon-Méniel, B., Figadère, B., & Loiseau, P. M. (2011). Antileishmanial activity of a formulation of 2-n-propylquinoline by oral route in mice model. *Parasite*, 18(4), 333–336. <https://doi.org/10.1051/parasite/2011184333>
- Cavassin, F. B., Baú-Carneiro, J. L., Vilas-Boas, R. R., & Queiroz-Telles, F. (2021). Sixty years of Amphotericin B: An Overview of the Main Antifungal Agent Used to Treat Invasive

Fungal Infections. Infectious Diseases and Therapy, 10(1), 115–147.
<https://doi.org/10.1007/s40121-020-00382-7>

CDC. (2020, February 18). CDC - Leishmaniasis—Epidemiology & Risk Factors.
<https://www.cdc.gov/parasites/leishmaniasis/epi.html>

Chappuis, F., Sundar, S., Hailu, A., Ghalib, H., Rijal, S., Peeling, R. W., Alvar, J., & Boelaert, M. (2007). Visceral leishmaniasis: What are the needs for diagnosis, treatment and control? *Nature Reviews Microbiology*, 5(11), 873–882. <https://doi.org/10.1038/nrmicro1748>

Chen, Y.-C., Su, C.-Y., Jhan, H.-J., Ho, H.-O., & Sheu, M.-T. (2015). Physical characterization and in vivo pharmacokinetic study of self-assembling amphotericin B-loaded lecithin-based mixed polymeric micelles. *International Journal of Nanomedicine*, 10, 7265–7274. <https://doi.org/10.2147/IJN.S95194>

Croft, S. L., Seifert, K., & Yardley, V. (2006). Current scenario of drug development for leishmaniasis. *The Indian Journal of Medical Research*, 123, 399-410.

Croft, S. L., Sundar, S., & Fairlamb, A. H. (2006). Drug Resistance in Leishmaniasis. *Clinical Microbiology Review*, 19, 16.

Delmas, G., Park, S., Chen, Z. W., Tan, F., Kashiwazaki, R., Zarif, L., & Perlin, D. S. (2002). Efficacy of Orally Delivered Cochleates Containing Amphotericin B in a Murine Model of Aspergillosis. *Antimicrobial Agents and Chemotherapy*, 46(8), 2704–2707. <https://doi.org/10.1128/AAC.46.8.2704-2707.2002>

Faustino, & Pinheiro. (2020). Lipid Systems for the Delivery of Amphotericin B in Antifungal Therapy. *Pharmaceutics*, 12(1), 29. <https://doi.org/10.3390/pharmaceutics12010029>

Georgiadou, S. P., Makaritsis, K. P., & Dalekos, G. N. (2015). Leishmaniasis revisited: Current aspects on epidemiology, diagnosis and treatment. *Journal of Translational Internal Medicine*, 3(2), 43–50. <https://doi.org/10.1515/jtim-2015-0002>

Gershkovich, P., Sivak, O., Wasan, E. K., Magil, A. B., Owen, D., Clement, J. G., & Wasan, K. M. (2010). Biodistribution and tissue toxicity of amphotericin B in mice following multiple dose administration of a novel oral lipid-based formulation (iCo-009). *The Journal of Antimicrobial Chemotherapy*, 65(12), 2610–2613. <https://doi.org/10.1093/jac/dkq358>

Goto, H. (2012). Review of the current treatments for leishmaniases. *Research and Reports in Tropical Medicine*, 69. <https://doi.org/10.2147/RRTM.S24764>

Harkare, B., Kulkarni, A., Aloorkar, N., Suryawanshi, J., Wazarkar, A., & Osmani, R. (2013). Nanocochleate: a new cornucopia in oral drug delivery. *International Journal of Innovations in Pharmaceutical Sciences*, 2, 1–9.

Hirano, M., Takeuchi, Y., Matsumori, N., Murata, M., & Ide, T. (2011). Channels Formed by Amphotericin B Covalent Dimers Exhibit Rectification. *The Journal of Membrane Biology*, 240(3), 159–164. <https://doi.org/10.1007/s00232-011-9354-x>

Hubatsch, I., Ragnarsson, E. G. E., & Artursson, P. (2007). Determination of drug permeability and prediction of drug absorption in Caco-2 monolayers. *Nature Protocols*, 2(9), 2111–2119. <https://doi.org/10.1038/nprot.2007.303>

Ismail, N., Kaul, A., Bhattacharya, P., Gannavaram, S., & Nakhasi, H. L. (2017). Immunization with Live Attenuated Leishmania donovani Centrin-/- Parasites Is Efficacious in Asymptomatic Infection. *Frontiers in Immunology*, 8. <https://doi.org/10.3389/fimmu.2017.01788>

Jain, S., Yadav, P., Swami, R., Swarnakar, N. K., Kushwah, V., & Katiyar, S. S. (2018). Lyotropic Liquid Crystalline Nanoparticles of Amphotericin B: Implication of Phytantriol and Glyceryl Monooleate on Bioavailability Enhancement. *AAPS PharmSciTech*, 19(4), 1699–1711. <https://doi.org/10.1208/s12249-018-0986-3>

Jin, T., Mannino, R., Zarif, L., & Zarif, L. (2001). Novel hydrogel isolated cochleate formulations, process of preparation and their use for the delivery of biologically relevant molecules. Google Patents. 24.

Joshi, H. A., & Gawade, P. S. (2016). Self emulsifying drug delivery system for improved oral delivery of lipophilic drug, *Pharmacophore*, Vol. 7 (6), 613-624.

Kay, J. G., & Grinstein, S. (2011). Sensing Phosphatidylserine in Cellular Membranes. *Sensors* (Basel, Switzerland), 11(2), 1744–1755. <https://doi.org/10.3390/s110201744>

Ketllyn, S. V., Baracat, L. F., Nath, C. S. C., Raissa, H. de M., Eliz, C. P. P., Jheneffer, D. I., Emerson, C., Guilherme, B. L. de F., Weber, C. F. N. da S., & Juliana, S. B. (2016). Difficulties in antifungal therapy with amphotericin B and the continuous search for new formulations: A literature review. *African Journal of Pharmacy and Pharmacology*, 10(24), 512–520. <https://doi.org/10.5897/AJPP2015.4280>

Khan, A. A., Mudassir, J., Mohtar, N., & Darwis, Y. (2013). Advanced drug delivery to the lymphatic system: Lipid-based nanoformulations. *International Journal of Nanomedicine*, 8, 2733–2744. <https://doi.org/10.2147/IJN.S41521>

Kumar, A. (2013). *Leishmania and Leishmaniasis*. Springer Science & Business Media.

Ling Tan, J. S., Roberts, C. J., & Billa, N. (2019). Mucoadhesive chitosan-coated nanostructured lipid carriers for oral delivery of amphotericin B. *Pharmaceutical Development and Technology*, 24(4), 504–512. <https://doi.org/10.1080/10837450.2018.1515225>

Mekarnia, N. (2020). Étude des paramètres biologiques de la chimiorésistance aux antimoniés dans un modèle de cycle naturel expérimental de leishmaniose cutanée zoonotique à Leishmania major. Paris-Saclay.

Mendes, C., Meirelles, G. C., Silva, M. A. S., & Ponchel, G. (2018). Intestinal permeability determinants of norfloxacin in Ussing chamber model. *European Journal of Pharmaceutical Sciences*, 121, 236–242. <https://doi.org/10.1016/j.ejps.2018.05.030>

Menez, C., Buyse, M., Chacun, H., Farinotti, R., & Barratt, G. (2006). Modulation of intestinal barrier properties by miltefosine. *Biochemical Pharmacology*, 71(4), 486–496. <https://doi.org/10.1016/j.bcp.2005.11.008>

Mikov, M., Fawcett, J. P., Kuhajda, K., & Kevresan, S. (2006). Pharmacology of bile acids and their derivatives: Absorption promoters and therapeutic agents. European Journal of Drug Metabolism and Pharmacokinetics, 31(3), 237–251. <https://doi.org/10.1007/BF03190714>

Mischler, B. (2017). Prise en charge de la leishmaniose cutanée: Intérêt de nouvelles formulations de paromomycine topique [Université de Rouen]. <https://dumas.ccsd.cnrs.fr/dumas-01643492/document>

Monzote, L. (2009). Current Treatment of Leishmaniasis: A Review. Open Antimicrobial Agents Journal, 1. <https://doi.org/10.2174/1876518100901010009>

Nagarsekar, K., Ashtikar, M., Steiniger, F., Thamm, J., Schacher, F., & Fahr, A. (2016). Understanding cochleate formation: Insights into structural development. Soft Matter, 12(16), 3797–3809. <https://doi.org/10.1039/C5SM01469G>

Nagarsekar, K., Ashtikar, M., Steiniger, F., Thamm, J., Schacher, F. H., & Fahr, A. (2017). Micro-spherical cochleate composites: Method development for monodispersed cochleate system. Journal of Liposome Research, 27(1), 32–40. <https://doi.org/10.3109/08982104.2016.1149865>

Otte, A., Soh, B.-K., Yoon, G., & Park, K. (2018). Liquid crystalline drug delivery vehicles for oral and IV/subcutaneous administration of poorly soluble (and soluble) drugs. International Journal of Pharmaceutics, 539(1–2), 175–183. <https://doi.org/10.1016/j.ijpharm.2018.01.037>

Padilla, C. A., Álvarez, M. J., Combariza, A. F (2019). Leishmania Proteomics: An in Silico Perspective. Preprints 2019, 2019020122. <https://doi.org/10.20944/preprints201902.0122.v3>.

Palatnik-de-Sousa, C. B. (2008). Vaccines for leishmaniasis in the fore coming 25 years. Vaccine, 26(14), 1709–1724. <https://doi.org/10.1016/j.vaccine.2008.01.023>

Pathak, Y., & Thassu, D. (2016). Drug Delivery Nanoparticles Formulation and Characterization. CRC Press.

Pham, T. T. H., Barratt, G., Michel, J. P., Loiseau, P. M., & Saint-Pierre-Chazalet, M. (2013). Interactions of antileishmanial drugs with monolayers of lipids used in the development of amphotericin B–miltefosine-loaded nanocochleates. Colloids and Surfaces B: Biointerfaces, 106, 224–233. <https://doi.org/10.1016/j.colsurfb.2013.01.041>

Pham, T. T. H., Gueutin, C., Cheron, M., Abreu, S., Chaminade, P., Loiseau, P. M., & Barratt, G. (2014). Development of antileishmanial lipid nanocomplexes. Biochimie, 107, 143–153. <https://doi.org/10.1016/j.biochi.2014.06.007>

Ponte-Sucre, A., Gamarro, F., Dujardin, J.-C., Barrett, M. P., López-Vélez, R., García-Hernández, R., Pountain, A. W., Mwenechanya, R., & Papadopoulou, B. (2017). Drug resistance and treatment failure in leishmaniasis: A 21st century challenge. PLOS Neglected Tropical Diseases, 11(12), e0006052. <https://doi.org/10.1371/journal.pntd.0006052>

Rao, R., Squillante, E., & Kim, K. H. (2007). Lipid-based cochleates: A promising formulation platform for oral and parenteral delivery of therapeutic agents. Critical Reviews

in Therapeutic Drug Carrier Systems, 24(1), 41–61.
<https://doi.org/10.1615/critrevtherdrugcarriersyst.v24.i1.20>

Santangelo, R., Paderu, P., Delmas, G., Chen, Z.-W., Mannino, R., Zarif, L., & Perlin, D. S. (2000). Efficacy of Oral Cochleate-Amphotericin B in a Mouse Model of Systemic Candidiasis. *Antimicrobial Agents and Chemotherapy*, 44(9), 2356–2360.
<https://doi.org/10.1128/AAC.44.9.2356-2360.2000>

Scorza, B., Carvalho, E., & Wilson, M. (2017). Cutaneous Manifestations of Human and Murine Leishmaniasis. *International Journal of Molecular Sciences*, 18(6), 1296.
<https://doi.org/10.3390/ijms18061296>

Serrano, D. R., & Lalatsa, A. (2017). Oral amphotericin B: The journey from bench to market. *Journal of Drug Delivery Science and Technology*, 42, 75–83.
<https://doi.org/10.1016/j.jddst.2017.04.017>

Serrano, D. R., Lalatsa, A., Dea-Ayuela, M. A., Bilbao-Ramos, P. E., Garrett, N. L., Moger, J., Guarro, J., Capilla, J., Ballesteros, M. P., Schätzlein, A. G., Bolás, F., Torrado, J. J., & Uchegbu, I. F. (2015). Oral Particle Uptake and Organ Targeting Drives the Activity of Amphotericin B Nanoparticles. *Molecular Pharmaceutics*, 12(2), 420–431.
<https://doi.org/10.1021/mp500527x>

Sesana, A. M., Monti-Rocha, R., Vinhas, S. A., Moraes, C. G., Dietze, R., & Lemos, E. M. (2011). In vitro activity of amphotericin B cochleates against Leishmania chagasi. *Memórias Do Instituto Oswaldo Cruz*, 106(2), 251–253. <https://doi.org/10.1590/S0074-02762011000200022>

Shuddhodana, Nagarsekar, K., & Judeh, Z. (2016). Recent Advances and Developments in Cochleate Technology. *Nanomedicine & Nanotechnology Open Access*.
<https://doi.org/10.23880/NNOA-16000119>

Singh, N., Kumar, M., & Singh, R. K. (2012). Leishmaniasis: Current status of available drugs and new potential drug targets. *Asian Pacific Journal of Tropical Medicine*, 5(6), 485–497. [https://doi.org/10.1016/S1995-7645\(12\)60084-4](https://doi.org/10.1016/S1995-7645(12)60084-4)

Syed, U. M., Woo, A. F., Plakogiannis, F., Jin, T., & Zhu, H. (2008). Cochleates bridged by drug molecules. *International Journal of Pharmaceutics*, 363(1–2), 118–125.
<https://doi.org/10.1016/j.ijpharm.2008.06.026>

Taheri, A. R., Rad, S. S., & Molkara, S. (2019). Systemic Treatments of Leishmaniasis: A Narrative Review. 6(3), 7.

Thakur, S., Joshi, J., & Kaur, S. (2020). Leishmaniasis diagnosis: An update on the use of parasitological, immunological and molecular methods. *Journal of Parasitic Diseases*, 44(2), 253–272. <https://doi.org/10.1007/s12639-020-01212-w>

Thanki, K., Prajapati, R., Sangamwar, A. T., & Jain, S. (2018). Long chain fatty acid conjugation remarkably decreases the aggregation induced toxicity of Amphotericin B. *International Journal of Pharmaceutics*, 544(1), 1–13.
<https://doi.org/10.1016/j.ijpharm.2018.04.009>

Torres-Guerrero, E., Quintanilla-Cedillo, M. R., Ruiz-Esmenjaud, J., & Arenas, R. (2017). Leishmaniasis: A review. F1000Research, 6, 750. <https://doi.org/10.12688/f1000research.11120.1>

Vijeta, P., & Vivek, M. (2011). Nanocochleate: as drug delivery vehicle. International Journal of Pharmacy and Biological Sciences, 1(1), 8.

Wasan, E. K., Gershkovich, P., Zhao, J., Zhu, X., Werbovetz, K., Tidwell, R. R., Clement, J. G., Thornton, S. J., & Wasan, K. M. (2010). A Novel Tropically Stable Oral Amphotericin B Formulation (iCo-010) Exhibits Efficacy against Visceral Leishmaniasis in a Murine Model. PLoS Neglected Tropical Diseases, 4(12). <https://doi.org/10.1371/journal.pntd.0000913>

Zarif, L., Graybill, J. R., Perlin, D., Najvar, L., Bocanegra, R., & Mannino, R. J. (2000). Antifungal Activity of Amphotericin B Cochleates against *Candida albicans* Infection in a Mouse Model. Antimicrobial Agents and Chemotherapy, 44(6), 1463–1469. <https://doi.org/10.1128/AAC.44.6.1463-1469.2000>

Zarif, Leila, Graybill, J. R., Perlin, D., & Mannino, R. J. (2000). Cochleates: New Lipid-Based Drug Delivery System. Journal of Liposome Research, 10(4), 523–538. <https://doi.org/10.3109/08982100009031116>

Zarif, Leila, Jin, T., Segarra, I., & Mannino, R. J. (2003). Hydrogel-isolated cochleate formulations, process of preparation and their use for the delivery of biologically relevant molecules (United States Patent No. US6592894B1). <https://patents.google.com/patent/US6592894B1/en>

Zhou, L., Zhang, P., Chen, Z., Cai, S., Jing, T., Fan, H., Mo, F., Zhang, J., & Lin, R. (2017, June 6). Preparation, characterization, and evaluation of amphotericin B-loaded MPEG-PCL-g-PEI micelles for local treatment of oral *Candida albicans*. International Journal of Nanomedicine. <https://www.dovepress.com/preparation-characterization-and-evaluation-of-amphotericin-b-loaded-m-peer-reviewed-fulltext-article-IJN>

6. ANNEXES

Table S1. Quaternary gradient programme for HPLC separation of phosphatidylserine species. A: heptane/ Isopropanol 98/2; B: chloroform/ Isopropanol 65/35; C: methanol/water 95/5; D: Isopropanol. A, B and C contained 1% acetic acid and 0.08% triethylamine.

Time (min)	A	B	C	D
0	98	2	0	0
2	98	2	0	0
8	12	88	0	0
22	0	60	40	0
26	0	60	40	0
27	0	0	0	100
29	0	0	0	100
30	98	2	0	0
44	98	2	0	0

Table S2. Stability study of AmB in different formulation after 1 hour of incubation in synthetic gastric medium at 37°C. Values are the percentage of intact AmB remaining, expressed as mean ± SD (n=3).

Formulation	AmB after 1h (%)
AmB in DMSO	37 ± 3
9 Lipoid PSP70 /0 Cholesterol /0.5 AmB	60 ± 3
9 Lipoid PSP70 /1 Cholesterol /0.5 AmB	67 ± 2
9 Lipoid PSP70 /2 Cholesterol /0.5 AmB	86 ± 4
9 Lipoid PSP70 /4 Cholesterol /0.5 AmB	84 ± 2
9 Lipoid PSP70 /6 Cholesterol /0.5 AmB	86 ± 4

Table S3. Composition of modified SGF, FaSSIF and FeSSIF media

Component/medium	SGF	FaSSIF	FeSSIF
Pepsin	0.32% (w/v)	---	---
Sodium taurocholate	---	3 mM	15 mM
Lecithin	---	0.8 mM	3.8 mM
Tween 80	0.1% (w/v)	0.1% (w/v)	0.1% (w/v)
Sodium monobasic phosphate (anhydrous)	---	28.7 mM	-
Sodium hydroxide	---	8.7 mM	101.0 mM
Sodium chloride	34.2 mM	105.9 mM	203.2 mM
Calcium chloride	50 mM	50 mM	750 mM
Acetic acid	---	-	144.0 mM
Hydrochloric acid	0.7% (v/v)	-	-
pH	1.2	6.5	5

Table S4. Summary of SAXS data showing the lamellar distances observed in the MLV and cochleate samples shown in Chapter 2 figure 30.

Formulation	q (Å⁻¹)	Distance (Å)
Lipoid PSP70 (as MLV)	0.1098	57.2
	0.1645	38.2
Lipoid PSP70 (as cochleates)	0.1281	49.1
	0.2559	24.6
	0.3843	16.4
9 Lipoid PSP70 /2 Cholesterol /0.5 AmB (as cochleates, F0.5)	0.1274	49.3
	0.2545	24.7
	0.3831	16.4
9 Lipoid PSP70 /2 Cholesterol /1 AmB (as cochleates, F1)	0.1281	49.1
	0.2557	24.6
	0.3818	16.5
9 Lipoid PSP70 /2 Cholesterol /2 AmB (as cochleates, F2)	0.1281	49.1
	0.2560	24.6
	0.3834	16.4
9 Lipoid PSP70 /2 Cholesterol /3 AmB (as cochleates, F3)	0.1263	49.8
	0.2529	24.9
	0.3790	16.6

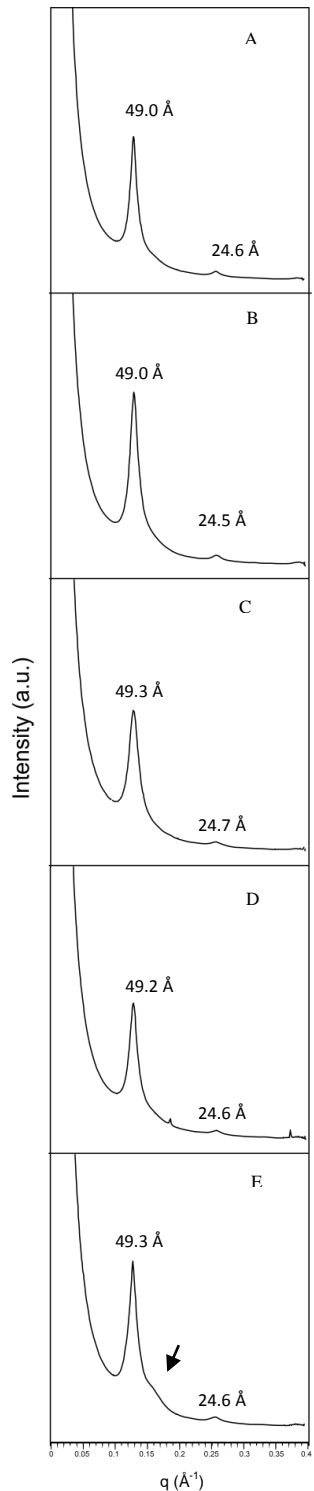


Figure S1. SAXS patterns for AmB-loaded cochleates with increasing molar proportions of cholesterol. A: 9 LipoidPSP70 /0 cholesterol /0.5 AmB; B: 9 LipoidPSP70/ 1 cholesterol /0.5 AmB; C: 9 LipoidPSP70 /2 cholesterol /0.5 AmB; D: 9 LipoidPSP70 /4 cholesterol /0.5 AmB; E: 9 LipoidPSP70 /6 cholesterol /0.5 AmB

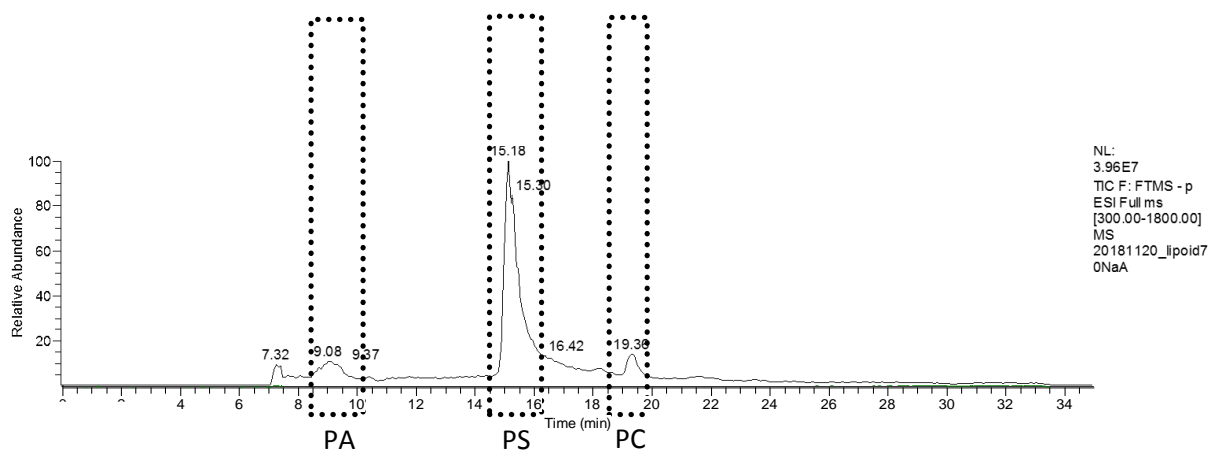


Figure S2. Mass spectrometry profile of LipoidPSP70 in negative mode ESI-HRMS after normal phase HPLC. PA: phosphatidic acid , PS: phosphatidylserine, PC: phosphatidylcholine

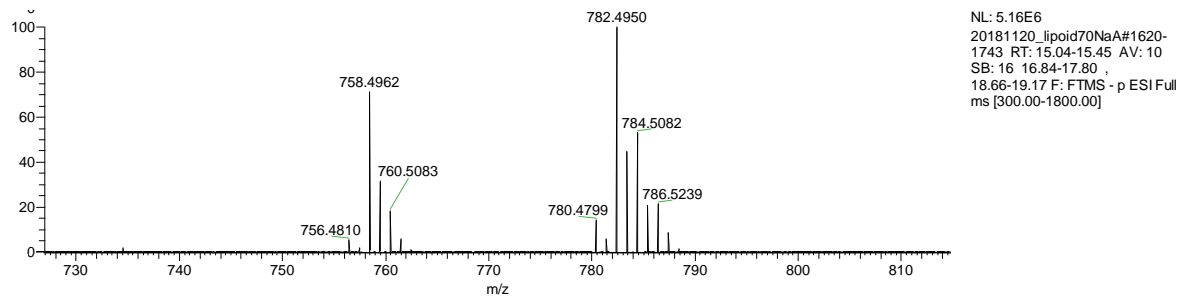


Figure S3. Phosphatidylserine composition of Lipoid PSP70 observed by mass spectrometry in negative ESI-HRMS fullscan mode

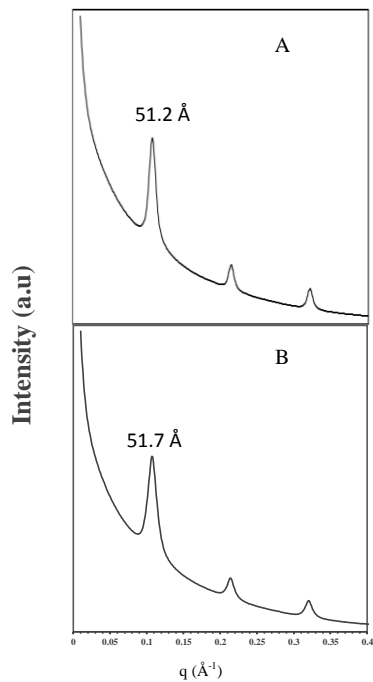


Figure S4. SAXS patterns for cochleates formed from pure DOPS with and without AmB.
A: 9 DOPS /1 Cholesterol; B: 9 DOPS /1 Cholesterol /0.5 AmB (molar proportions)

Titre : Nanoparticules pour l'administration orale de l'amphotéricine B pour le traitement de la leishmaniose

Mots clés : Leishmaniose, amphotericine B, cochléates, voie orale, vectorisation

Résumé : La leishmaniose est une maladie très répandue dans le monde dont, malgré les mesures de prévention et les traitements existants, le nombre de cas reste en augmentation. L'amphotericine B (AmB), antifongique et antileishmanien, est la molécule de référence à cause de sa bonne efficacité et de l'absence de résistance. Cependant sa faible biodisponibilité orale et son étroite fenêtre thérapeutique limitent son utilisation.

Dans ce travail, un système de délivrance de l'AmB, les cochléates, a été développé afin de proposer un traitement efficace par voie orale. Les cochléates sont des assemblages de bicouches de phospholipide enroulées et stabilisées par des cations divalents. Afin de faciliter l'accès aux pays en voie de

de développement, un phospholipide d'origine naturelle a été utilisé. La composition a été optimisée pour le taux d'encapsulation de l'AmB et sa protection dans les milieux gastro-intestinaux. Les cochléates ont été caractérisés par diverses techniques physico-chimiques telles que les microscopies optique et électronique, la diffraction des rayons X aux petits angles et le dichroïsme circulaire.

Après une étude d'interaction avec les cellules Caco2, le profil pharmacocinétique et la biodistribution chez le rat ainsi que l'efficacité sur *Leishmania donovani* chez la souris ont été déterminés. Les résultats sont prometteurs pour le développement d'une nouvelle thérapie anti-leishmanienne.

Title: Nanoparticles for oral administration of amphotericin B for the leishmaniasis treatment

Keywords: Leishmaniasis, amphotericin B, cochleate, oral administration, drug delivery

Summary: Leishmaniasis is a wide-spread tropical disease with an increasing number of cases despite preventive and therapeutic intervention. The treatment of choice is the antifungal Amphotericin B (AmB) that shows food efficacy and low resistance, but has low oral bioavailability and a small therapeutic window.

In this work, a drug delivery system for AmB, cochléates, was developed as an oral treatment. Cochléates are assemblies of phospholipid bilayers rolled into cylinders bridged by divalent cations. In order to provide an affordable product for developing countries, a phospholipid of natural

origin was used. The composition was optimized in terms of AmB encapsulation and protection in gastro-intestinal conditions. The cochléates were characterized by various physico-chemical techniques such as optical and electron microscopy, small-angle X-ray diffraction and circular dichroism. After a study of their interactions with Caco2 cells, pharmacokinetics and biodistribution in rats and efficacy against *Leishmania donovani* in mice were determined. The results are promising for the development of new therapy for Leishmaniasis.